**Doctoral Dissertation**

# Synthesis and Properties of Fluorene Based Anion Conducting Membranes for Fuel Cells

**Umme Salma**

**Supervisor: Yuki NAGAO**

**Graduate School of Advanced Science and Technology**

**Japan Advanced Institute of Science and Technology**

**Doctor of Science (Material Science)**

**March 2020**

# TABLE OF CONTENTS

**Page**

## Chapter 3

Ether Bond Free Anion Exchange Membrane Containing Cycloaliphatic Quaternary Ammonium Groups for Fuel Cells

## Chapter 4

# LIST OF FIGURES

Figure Page

## LIST OF TABLES

Table Page

## LIST OF SCHEMES

Scheme Page

# LIST OF ABBREVIATIONS

| | |
|---|---|
| AEMs | Anion Exchange Membranes |
| PEMFCs | Proton Exchange Membrane Fuel Cells |
| AEMFCs | Anion Exchange Membrane Fuel Cells |
| QA | Quaternary Ammonium |
| PPO | Polyphenylene Oxide |
| PF | Polyfluorene |
| IMI | 1-Isopropyl-2-Methylimidazole |
| Pip | N-Methyl Piperidine |
| DMF | N,N-dimethylformamide |
| THF | Tetrahydrofuran |
| IEC | Ion Exchange Capacity |
| NMR | Nuclear Magnetic Resonance |
| FTIR | Fourier Transform Infrared |
| SEM | Scanning Electron Microscope |
| EDX | Energy Dispersive X-ray |
| TGA | Thermogravimetric Analyzer |
| DSC | Differential Scanning Calorimetry |
| WU | Water Uptake |
| SR | Swelling Ratio |

# Abstract

**Part 1: Research content**

**Background**

Alkaline anion exchange membrane fuel cells (AEMFCs) are recognized as one of the most efficient power sources for portable electronics, stationary power generation, and transportation. AEMFCs offer higher reaction kinetics for oxygen reduction, lower fuel crossover, fuel flexibility, and independence on noble metal electrocatalyst than proton exchange membrane fuel cells (PEMFCs). The key component of AEMFCs is the anion exchange membranes (AEMs) that act as a separator between anode and cathode and migrate the ions. One of the key challenges is finding durable AEM that combines a long time alkaline stability and high ionic conductivity.

In recent years, many research groups have effort significantly to improve the AEMs; their focusing points involved molecular engineering of functional groups and polymer backbones. Different backbones including polyphenylene oxide, polyphenylene, polyarylene ether ketone, polyarylene ether sulfone, polyetherimide, polystyrene, and polyethylenes have been extensively studied. Among these, polymers containing arylene ether, arylene ketone, and arylene sulfone bonds in their backbones, activate hydroxide ion attack and chain scission. As a result, the chemical stability of the corresponding AEMs decreased.

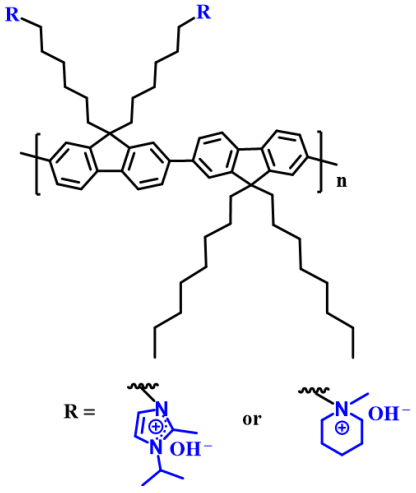


**Fig. 1 Structure of the synthesized polymers.**

On the other hand, the fluorenyl group containing polymers have attracted much attention due to high chemical stability in alkaline condition. It was reported that alkyl quaternary ammonium (QA) functionalized polyfluorene AEMs were stable in alkaline condition for a long time. There is no literature for imidazolium containing AEM with

the same fluorene backbone. In this study, I have synthesized fluorene based polymer by using Pd catalyzed Suzuki cross-coupling reaction which is free from arylene ether, arylene ketone, and arylene sulfone bond and newly incorporated 1-isopropyl-2-methylimidazolium as a cationic group. I also investigated the effect of the N-methyl piperidinium cationic group on the same polyfluorene backbone (Fig. 1).

**Objective**

In this research, the design and synthesis of new polyfluorene AEMs containing 1-isopropyl-2-methylimidazolium and N-methyl piperidinium were demonstrated. The effect of two different functional groups on the membrane properties including hydroxide conductivity, ion exchange capacity, water uptake and swelling behaviour, thermal and chemical stability were systematically investigated. The chemical structure of synthesized monomers and polymers were confirmed by Nuclear magnetic resonance (NMR) spectroscopy, Fourier transform infrared (FTIR) spectroscopy and mass spectrometry. The AEMs were characterized using scanning electron microscope (SEM) and energy dispersive X-ray (EDX) spectroscopy, thermogravimetric analyser, and impedance analyser.

**Summary of Results**

In **Chapter 2** of this dissertation, poly[(9,9-bis(6′-bromohexyl)-9H-fluorene)-co-(9,9-bis(6′-octyl)fluorene)] denoted as PF-IMIBr was synthesized from 2,7-dibromo-9,9-dioctyl fluorene and 2,7-bis(4,4,5,5-tetramethyl-1,3,2-dioxaborolan -2-yl)-9,9-bis(6′-bromohexyl)fluorene by using Suzuki cross-coupling reaction. 1-Isopropyl-2-methylimidazolium was incorporated as a functional group. The membrane was casted from a 4 wt% dimethylformamide (DMF) solution of the polymer. The $OH^-$ containing membranes (PF-IMI) were obtained by immersing the PF-IMIBr polymer in argon saturated 1M NaOH solution. Thermogravimetric analyser studies suggest that the synthesized polymer maintain high thermal stability up to 200 °C as shown in Fig. 2a, which is far beyond the desired temperature range for fuel cell applications. The water uptake and swelling behaviour studies unveiled that the dimensional stability of the resultant membranes was high and adsorbed a sufficient

amount of water for ionic migration. The AEM exhibited an in-plane linear expansion ratio of 7% and $OH^-$ conductivity of 46 mS $cm^{-1}$ at 80 °C in liquid water, as shown in Fig. 2b & c.

The alkaline stability of AEM in argon-saturated 1 M NaOH (aq.) solution was investigated by FT-IR spectra and demonstrated that imidazolium cationic groups were degraded upon exposure to 1 M NaOH solution at room temperature and 80 °C though the backbone was chemically stable (Fig. 2d).

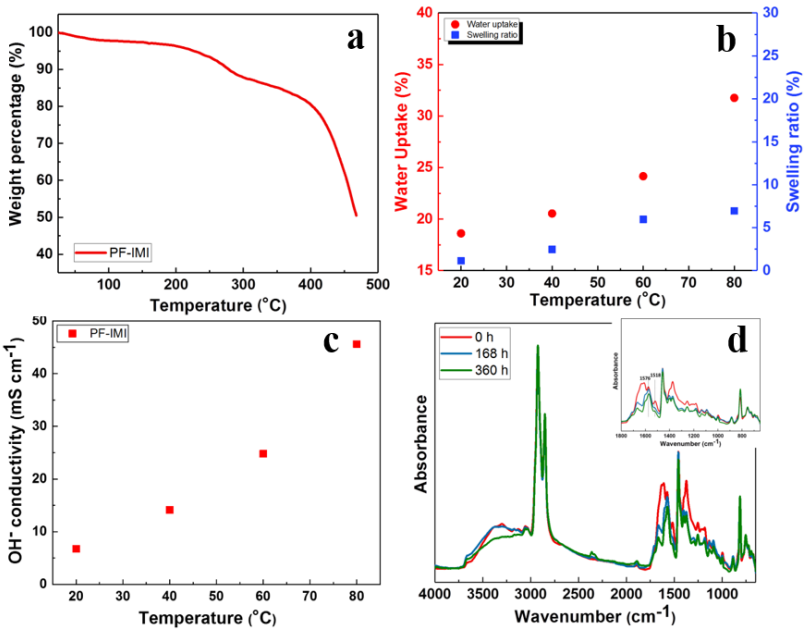


**Fig. 2. a) TGA curve, b) water uptake & swelling ratio, c) hydroxide conductivity, d) alkaline stability at 80 °C of the PF-IMI membrane.**

In **Chapter 3,** N-methylpiperidinium was attached to the PFBr polymer and membrane properties of as-synthesized AEM were systematically investigated including water uptake, swelling ratio, ion exchange capacity, thermal stability, hydroxide conductivity, and chemical stability. By introducing the piperidinium functional group, the properties of the membrane denoted as PF-Pip were much improved. For example, the water uptake of PF-Pip increased to 81% and conductivity reached up to 58 mS $cm^{-1}$ at 80 °C in liquid water as shown in Fig. 3a & b. The water uptake and ionic conductivity of the PF-Pip membrane were higher than that of imidazolium functionalized $OH^-$ form (PF-IMI) membrane; this may happen, due to the higher free space or cavities of piperidinium containing AEM than that of imidazolium functionalized AEM. I have observed only 13% of the cationic loss by $^1H$ NMR spectra after storage in 1 M NaOH solution for 168 h at 80 °C.

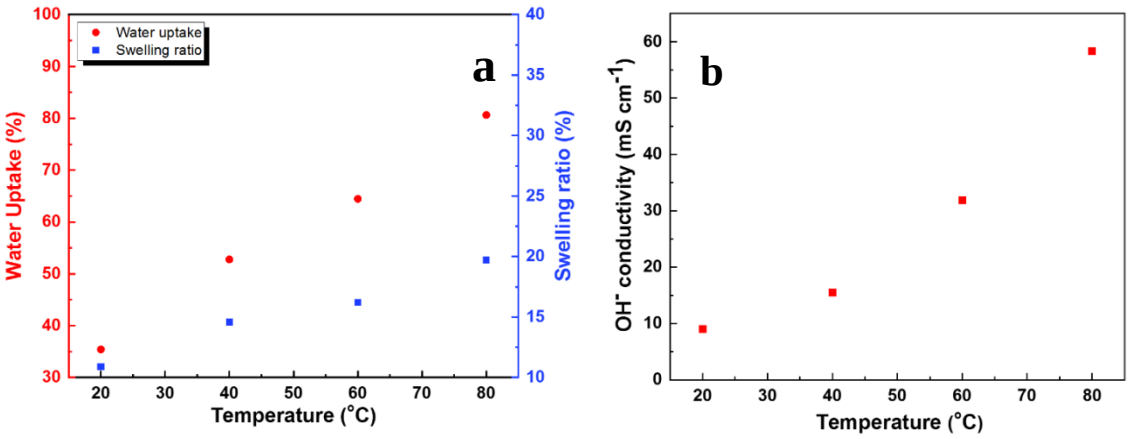


**Fig. 3. a) Water uptake and swelling behaviour b) hydroxide conductivity of the PF-Pip membrane.**

**Chapter 4** highlighted the effect of functional groups e.g., imidazolium and piperidinium on the performances of the AEMs. In comparison to the imidazolium group containing AEM, the piperidinium functionalized AEM showed better membrane properties.

**Part 2: Research Purpose**

The design, synthesis, and findings of this thesis provide an opportunity of designing novel AEMs based on alkaline stable ether free polyfluorene polymer by using different functional groups that will enrich the diversity of the polymeric AEMs′ structure. As some literature has revealed that imidazolium functional groups are chemically stable, but some other literature has suggested the less chemical stability of imidazolium groups. The investigated results of alkaline stability of imidazolium containing AEM can conclude this discrepancy state. Some researchers reported that alkyl tethered N-methyl piperidinium cationic groups were quite stable in alkaline condition. However, I have observed 13% cationic group was lost after 168 h of the alkaline test though it was alkyl substituted. So, from this study, I have outlined the challenge of chemical stability of imidazolium cationic groups on the polyfluorene backbone. Sufficient hydroxide conductivity and good chemical stability was observed in case of piperidinium containing membrane as only 13% cationic group was lost. The findings

of this study will provide significant directions and insights for choosing functional groups for the development of AEMs for practical applications. The results of this study can benefit a broad audience of fuel cells.

## Part 3: Research Accomplishments

### Publications

(i) **Umme Salma**, Dishen Zhang and Yuki Nagao "Imidazolium Functionalized Fluorene based Anion Exchange Membrane (AEM) for Fuel Cell Applications." *ChemistrySelect* **2020**, *5,* 1255-1263. (Peer-reviewed)

(ii) **Umme Salma** and Yuki Nagao "Alkaline stability of ether bond free fluorene based anion exchange polymer containing cycloaliphatic quaternary ammonium groups." (*Submitted*)

### Conferences

(i) Umme Salma and Yuki Nagao "A polyfluorene polymer containing imidazolium cationic groups for anion exchange membrane fuel cells" 68th Polymer Symposium, September 25-27, 2019, Fukui, Japan. Style of presentation: Poster.

(ii) Umme Salma, Dishen Zhang, Yuki Nagao "Hydroxide ion conducting fluorene based polymers for fuel cell applications" 2019 年度北陸地区講演会と研究発表会, 29 November 2019, Kanazawa, Japan. Style of presentation: Poster.

**Keywords:** Anion exchange membrane, 1-isopropyl-2-methylimidazole, N-methyl piperidine, alkyl side chains, polyfluorene

# General Introduction

## 1.1. Introduction of Fuel Cells

Fuel cells are recognized as highly efficient energy devices that can meet energy demand for transportation, portable equipment, and stationary power generations [1-3]. The key component of a fuel cell is the solid polymeric membrane that separates electrodes and helps to transport ions. The properties of the membrane influence the performances of a fuel cell. For the functional life of a fuel cell, the durability of the solid polymeric membrane is the most important point.

Among the fuel cells, proton exchange membrane fuel cells (PEMFCs) use polymeric membranes for proton conduction, most extensively explored, as they are highly efficient for energy conversion, have high power density, low operating temperature and no emission for environmental pollution [4]. However, the commercialization of PEMFCs is limited due to the use of Pt catalyst and perfluorosulfonate as an electrolyte.

The alkaline anion exchange membrane fuel cells (AEMFCs) use solid membranes as electrolytes for conducting hydroxide, bicarbonate, chloride, or bromide ions as charge carriers and can be the alternative of PEMFCs. The electrolytes have positively charged cationic groups that are covalently attached to the polymer backbones. The polymer

electroneutrality is preserved due to the presence of mobile counterions. AEMFCs offer some advantages over PEMFCs such as low fuel crossover, fuel flexibility, faster oxygen reduction, and non-noble metal electrocatalysts, for example, iron, silver, nickel, or cobalt can be used in AEMFCs [5-7]. An ideal polymeric anion exchange membrane (AEM) for the practical use in AEMFCs should have moderate water swelling, chemical and thermal stability, robust mechanical properties, low fuel permeation and adequate ionic conductivity [8, 9]. In the development of AEMFCs, one of the major challenges is the synthesis of AEMs having longtime chemical stability and high ionic conductivity [10]. Therefore, researchers are focusing on the development of AEMs to build high-performance AEMFCs.

## 1.2. Alkaline Anion Exchange Membrane Fuel Cells

Alkaline AEMFCs as shown in Fig. 1.1 generate electricity from fuel such as hydrogen by the following reactions [11]. At the cathode, hydroxide ion ($OH^-$) is produced by an oxygen reduction reaction (ORR) in the presence of $H_2O$.

Cathode reaction: $O_2 + 2\ H_2O + 4e^- \rightarrow 4\ OH^-$

Anode reaction: $2\ H_2 + 4\ OH^- \rightarrow 4\ H_2O + 4\ e^-$

Overall reaction: $2\ H_2 + O_2 \rightarrow 2\ H_2O$

The produced 4 $OH^-$ in cathode side then transports through AEM to the anode side of the cell. Then $H_2$ is oxidized and produce $H_2O$ by the reaction with $OH^-$ [11]. The overall reaction is the generation of $H_2O$, heat, and electricity by the reaction of $H_2$ and $O_2$. $H_2O$ is produced at the anode side of AEMFC, whereas simultaneously at the cathode side $H_2O$ acts as a reactant. The unique feature of AEMFCs is the water transport mechanism and high alkaline medium.

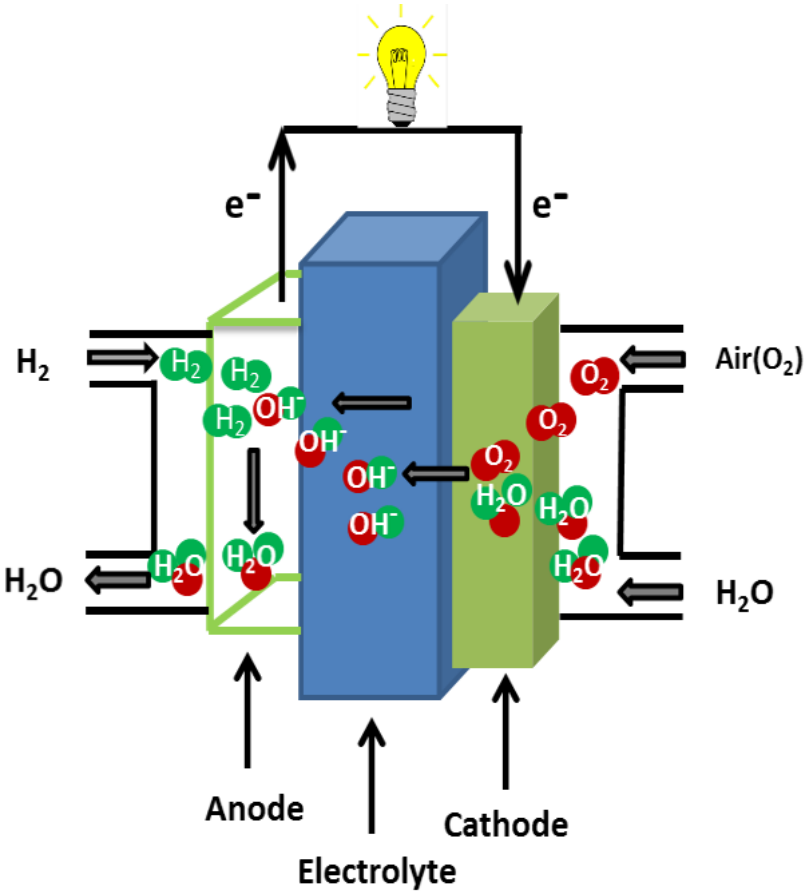


Fig. 1.2. Schematic diagram of an AEMFC.

## 1.3. AEMs Based on Different Backbones

The alkaline fuel cells (AFCs) was first invented by Reid in 1902 [12]. During the time of 1960s and 1970s, NASA space flights used the AFCs [13]. At that time the aqueous KOH was chosen as an electrolyte. The main disadvantages of KOH as electrolyte were the formation of $K_2CO_3$ by the reaction with $CO_2$ and electrode flooding. Due to these drawbacks, the performance of AFCs decreased. By using solid polymer electrolyte (SPE), these problems were solved. The development of SPEs for AFCs was extensively started since 1970 [14]. Nowadays the SPEs are known as AEMs.

In early studies, polystyrene (PS) was the most commonly used polymeric material for AEMs because of low-cost starting materials and easy synthetic procedure [15]. But polystyrene is naturally brittle, therefore, divinylbenzene containing benzylmethylammonium group is cross-linked with polystyrene. However, the application of PS as AEMs is limited due to the inadequate processability, poor chemical and thermal stability [15]. In view of this, several forms of AEMs have been developed based on polyphenylenes [16, 17], polyphenylene oxides [18-21], polyarylene sulfones [22-31], polyether imides [32], polyether oxadiazoles [33-35], polybenzimidazole [36, 37], perfluorinated types [38-43], polyether ether ketone [44,

45], polyepichlorohydrins [14, 46-50], unsaturated polyolefins [51-53], polypropylene [54], polyphosphazenes [55], and the polymers based on polyvinyl alcohol [50, 56-58]. The classification of polymer backbones used for the synthesis of AEMs is shown in Scheme 1.1.

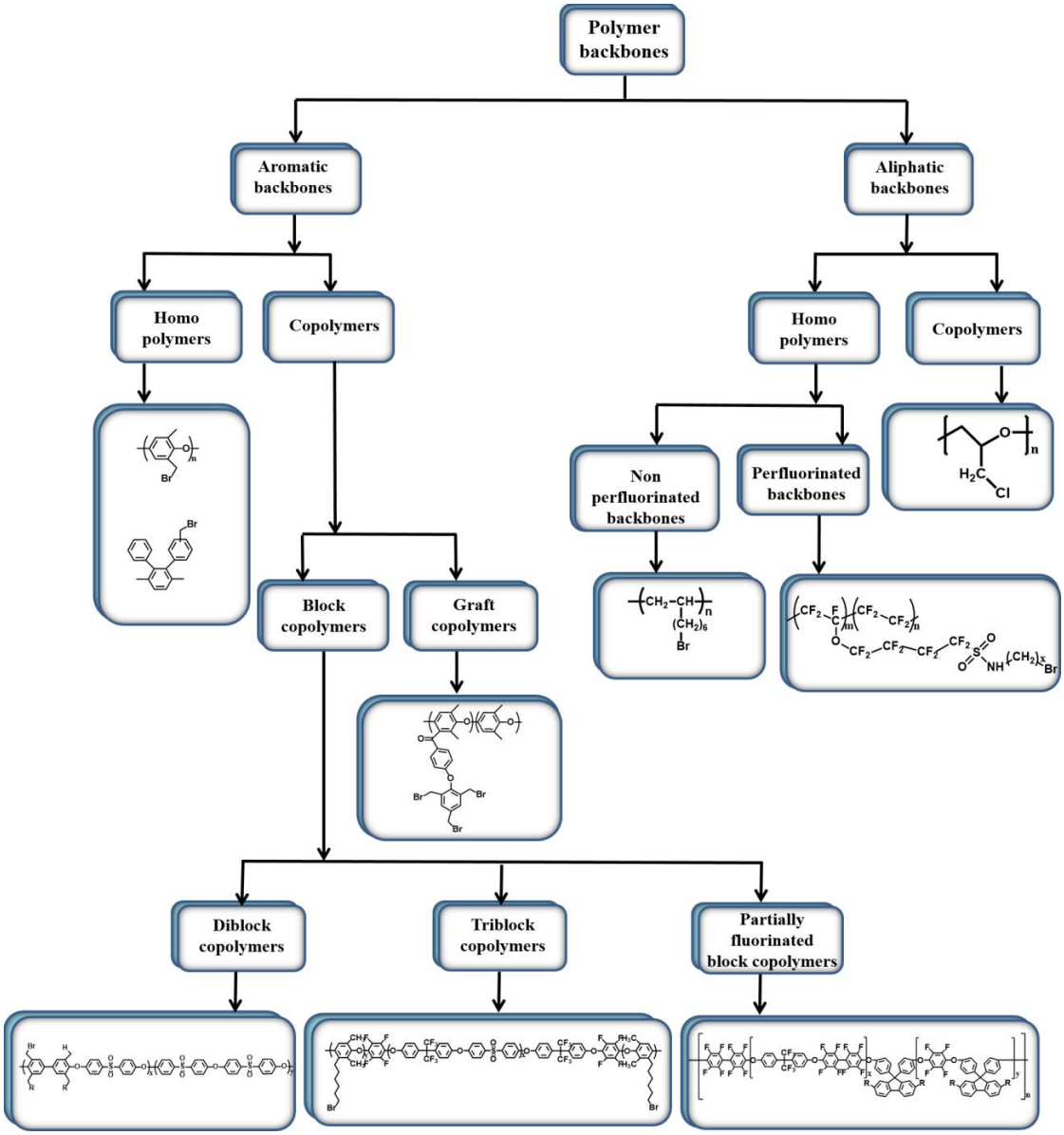


Scheme 1.1. Schematic illustration of the various polymer backbones used to synthesize the AEMs.

Among the polymeric materials, the AEMs containing fluorenyl groups on their backbone have attracted considerable attention due to the possibility of diverse chemical modifications. Alkyl or dialkyl groups can be introduced on the fluorene ring to increase the molecular weight and solubility of the polymer. Fluorenyl group containing AEMs reported to have high thermal and chemical stability and provide high hydroxide conductivity [59, 60]. Bae and coworkers [17] reported that polyfluorene based AEMs containing alkyl QAs cationic groups were stable in NaOH (1 M) aqueous solution at 80 °C for one month. In this study, as the polymer backbone, I have synthesized similar type of aryl-ether-bond free polyfluorene since in basic media it can provide high alkaline stability.

## 1.4. AEMs with Single Cation and Multication at Side Chains

Quaternary ammonium (QA) functionalized polymeric AEMs based on different backbones have been studied extensively [61, 62]. These AEMs are typically synthesized via chloromethylation reaction of benzylic carbons followed by quaternization of benzyl halide and formed ammonium salts by a Menshutkin reaction. However, chloromethyl methyl ether is poisonous and difficult to control functionalization processes precisely [60]. Therefore, researchers are trying to synthesis AEMs by using simple synthetic procedures without using any toxic reagents. Additionally, to synthesize highly conductive and alkaline stable AEMs, quaternary ammonium cations [63, 64] and functionalization processes [65, 66] are continuously developed. Many functional groups other than QA such as guanidinium [67], phosphonium [68], sulfonium [69], imidazolium [60, 70, 71], benzimidazolium [72] have been used as cationic groups. Scheme 1.2 shows different cationic groups used in AEMs. In recent studies, heterocyclic aliphatic QA cationic groups, for example, piperidinium [20, 73, 74] and pyrrolidinium [75] exhibit higher chemical stability. Morpholinium group containing AEMs also show higher dimensional stability and better phase separation [20, 76, 77]. Triazolium, a cationic group, can form the hydrogen bond with water and enhance the hydroxide conductivity [78].

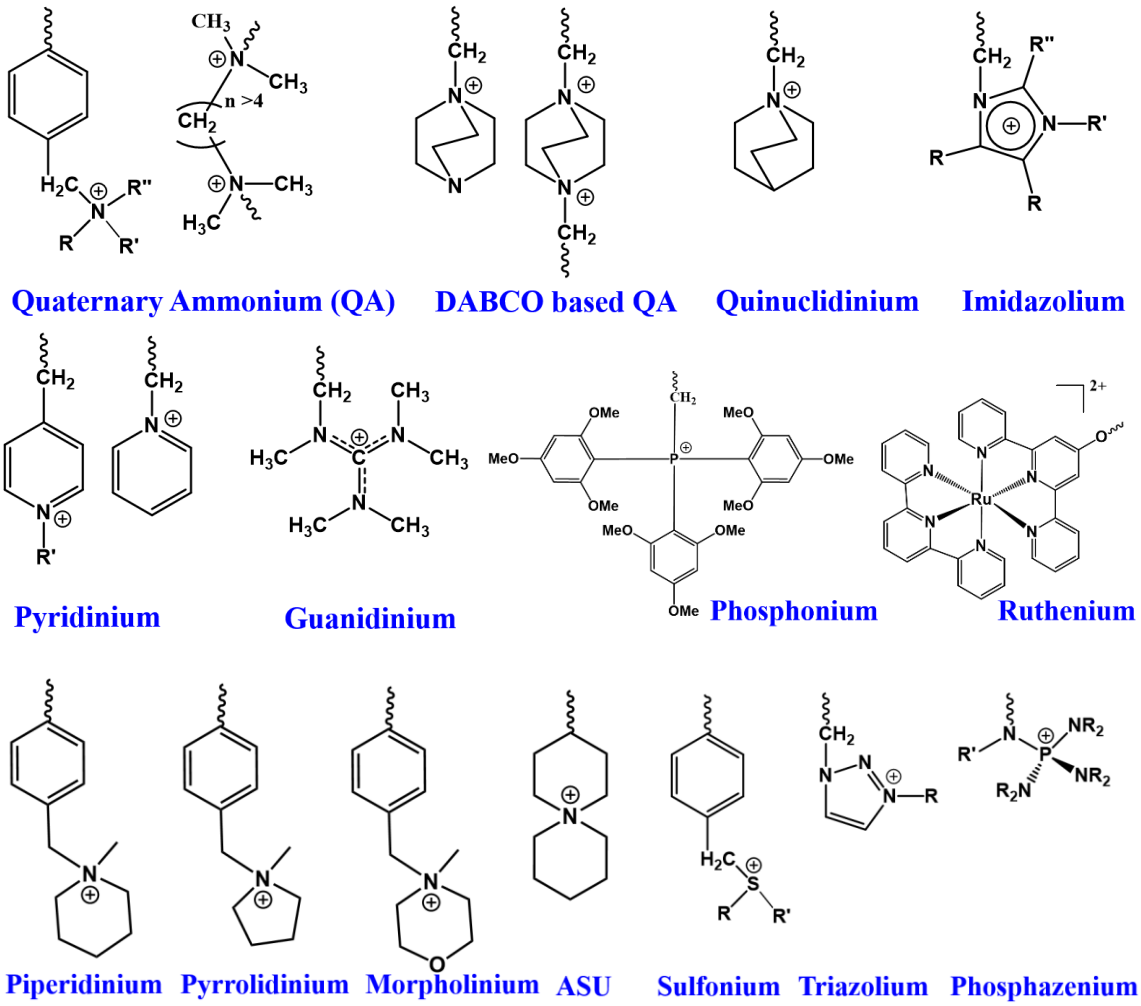


Scheme. 1.2. Chemical structure of different cationic groups in AEM.

High hydroxide conductivity is required for practical application of a high-performance AEM. The conductivity can increase by grafting more cationic groups to the backbone of the polymer, as a result, increases the ion exchange capacity (IEC). Although the high IEC facilitates the high ionic conductivity, the AEMs become

more swollen and show poor mechanical properties [79, 80]. Many research groups have tried to solve these problems by increasing tethered cationic groups on the polymer backbone [64, 81], whereas incorporating multiple cationic groups on the same side chain [21, 82, 83], or multiple cationic groups are incorporated to the backbone of the polymer by crosslinking [84-86]. Fig. 1.2 represents the strategies to synthesize AEMs with multication at the side chain.

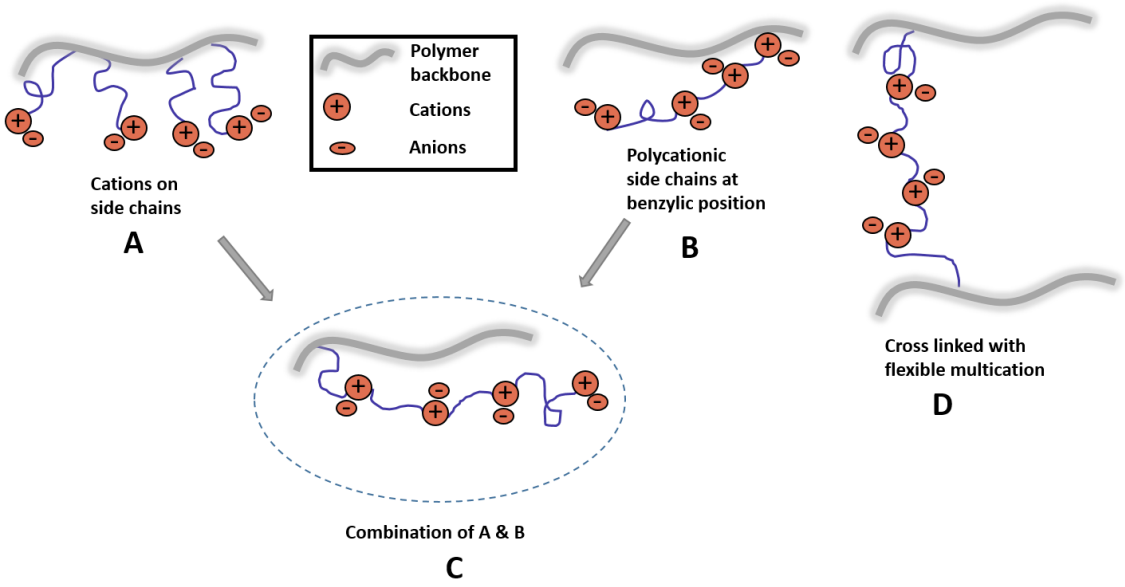


Fig. 1.2. Different strategies to synthesize multication AEMs.

## 1.5. Chemical Degradation of AEMs

The major concern of AEMs in electrochemical devices is long-term alkaline stability. Among the different cationic groups, tetraalkyl quaternary ammonium is used commonly to synthesize the AEMs. Some literature is available where researchers reported that QA cationic groups are quite stable for long time in alkaline condition [17, 87] but some other literature [20, 86] revealed that QA salts are susceptible to $OH^-$ attack and alkaline stability is decreased due to a variety of chemical degradation including elimination [88], substitution [89], N-ylide formation and rearrangement reactions [89, 90] as shown in Fig. 1.3.

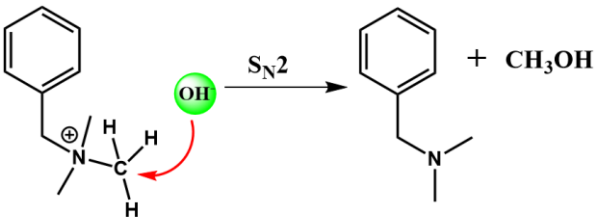


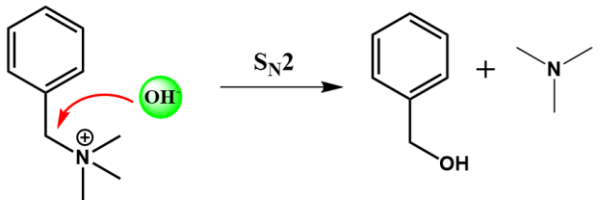


(A) Nucleophilic substitution

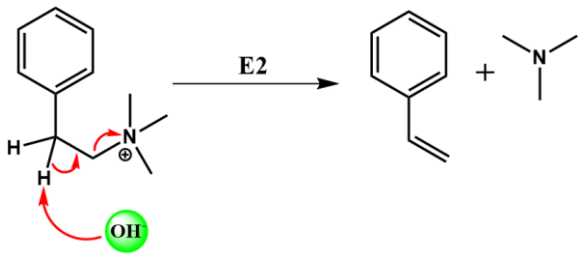


(B) Hofmann elimination

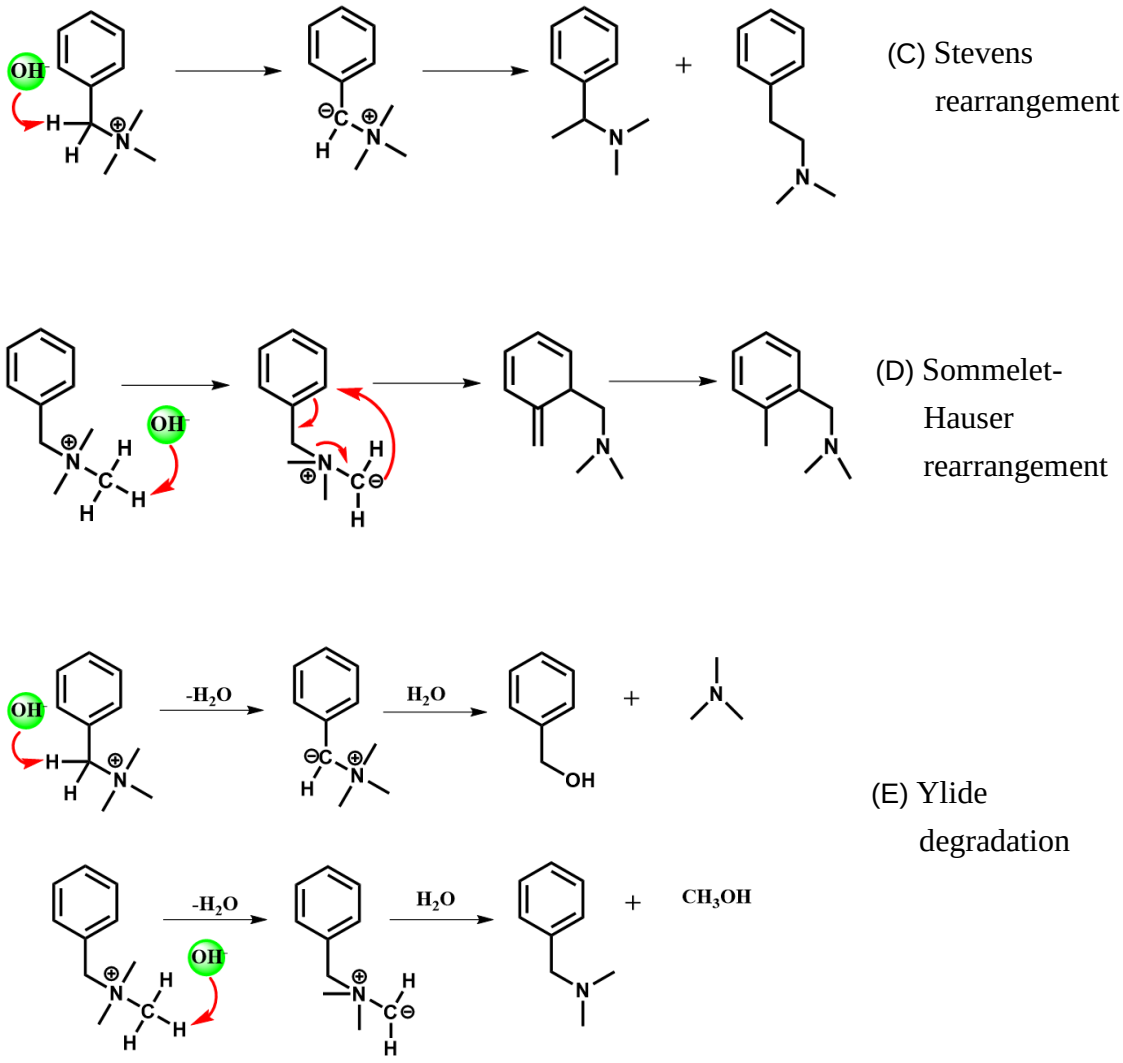


Fig. 1.3. Different chemical degradation mechanisms of QA [90].

To enhance the chemical stability of AEMs, various types of imidazolium salt have incorporated to side chains of polymeric materials. C2 substituted imidazolium cations are found to be more alkaline stable than the unsubstituted one. C2 unsubstituted imidazolium cationic groups are more easily degraded by the nucleophilic attack of $OH^-$ ion at the high alkaline condition [91] shown in Fig. 1.4

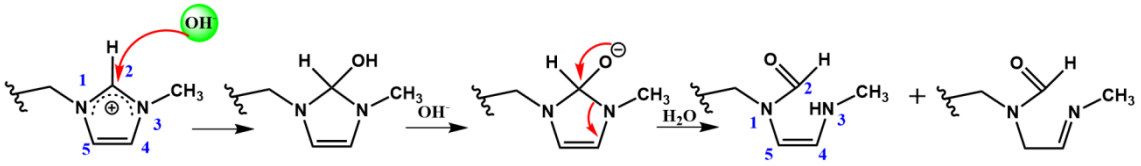


Fig. 1.4. Degradation of imidazolium cationic group by ring opening mechanism.

Similar to QA cationic group some researchers [60, 92-94] found that imidazolium cationic groups are stable in highly basic condition; however, some other researchers [16, 95] have revealed that in highly alkaline media, the imidazolium cations are less stable. To conclude this discrepancy of imidazolium alkaline stability I have chosen imidazolium as cationic groups to synthesize hydroxide ion conducting AEM.

The chemical stability of functional groups and the polymer backbones are important for alkaline AEMFCs application. A variety of AEMs based on different polymer backbones has been synthesized. Polyvinylidene fluoride is partially fluorinated and known to degrade in the high alkaline environment by dehydrofluorination. The degradation occurs due to the attack of $OH^-$ ions leading to the formation of carbon carbon double bond (C═C), hence chain scission occurred. [30, 96]. Another polymeric material such as polysulfone (PSF) is also used as a backbone for synthesizing AEMs. The polymers containing aryl ether bonds and electron-withdrawing groups such as aryl ketone, aryl sulfone, in their backbone, causes chain scission hence alkaline stability

decreases [97, 98]. Ramani *et al.* [99] pointed out that the polymer backbone of polysulfone is degraded in high alkaline condition by the attack of nucleophilic $OH^-$ ion (Fig. 1.5). The degradation rate can be reduced by separating the cation from the polymer backbone by an alkyl spacer. Highly alkaline stable AEMs can be synthesized by removing fluorine, sulfone, ketone, and aryl ether bond from the polymer backbone.

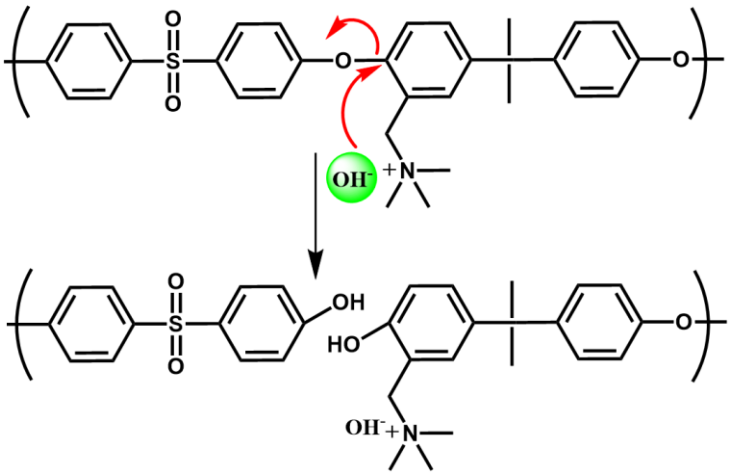


Fig. 1.5. The degradation pathways of polysulfone backbone [99].

In this study, to avoid the degradation I have synthesized polyfluorene as polymer backbone which is free from aryl ether, aryl ketone or, aryl sulfone bonds. In addition, I have separated the cationic group by a long alkyl side chain. To conclude the inconsistency of imidazolium alkaline stability I have chosen imidazolium cationic group and membrane properties such as hydroxide conductivity, IEC, chemical and

thermal stability, water uptake and swelling behavior were systematically investigated. I also have incorporated the piperidinium cationic group to observe the effect on the membrane properties.

## 1.6. Outline of this Thesis

Investigation of the chemical stability of fluorene based anion exchange membranes containing imidazolium and piperidinium cationic groups is the objective of this study. Fluorene-based $OH^-$ ion conducting polymers were synthesized and the membrane properties including hydroxide conductivity, water uptake, swelling behavior, thermal and chemical stabilities were fully assessed as shown in scheme 1.3.

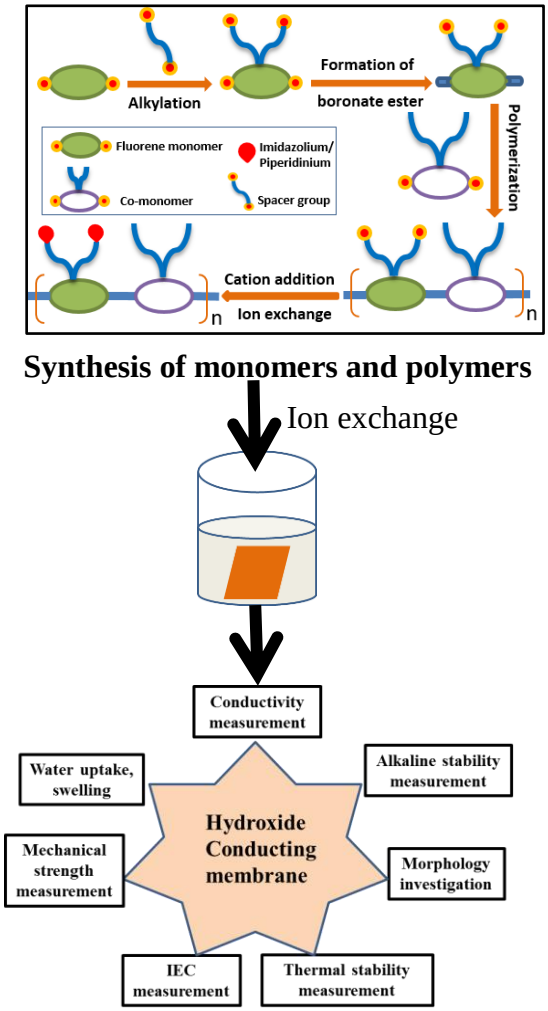


Scheme 1.3. Schematic diagram of research objectives.

Chapter 1 is the general introduction of AEMFCs and provides background on the major issues of AEMs and general design approaches to mitigate these challenges.

In chapter 2, poly[(9,9-bis(6′-(1-isopropyl-2-methylimidazolium)hexyl)fluorene)-co-(9,9-bis(6′-octyl)fluorene)]bromide (PF-IMIBr) was successfully synthesized, and membrane properties were measured. The membrane showed high dimensional stability with adequate hydroxide conductivity.

In chapter 3 piperidinium functionalized fluorene-based anion exchange membrane (PF-PipBr) was synthesized and membrane properties including hydroxide conductivity, thermal and alkaline stability, ion exchange capacity, water uptake, and the swelling ratio were assessed. This study revealed that the piperidinium cationic group has significantly influenced the membrane properties.

Chapter 4 presents the general conclusion of this study. All the results of this study will provide significant directions and insights for the synthesis of AEMs for practical applications in AEMFCs.

## References

[1] L. Carrette, K. Friedrich, U. Stimming, Fuel cells–fundamentals and applications, Fuel cells 1 (2001) 5-39.

[2] S. Mekhilef, R. Saidur, A. Safari, Comparative study of different fuel cell technologies, Renewable and Sustainable Energy Reviews 16 (2012) 981-989.

[3] M. Winter, R.J. Brodd, What Are Batteries, Fuel Cells, and Supercapacitors?, Chemical Reviews 104 (2004) 4245-4269.

[4] M.A. Hickner, H. Ghassemi, Y.S. Kim, B.R. Einsla, J.E. McGrath, Alternative polymer systems for proton exchange membranes (PEMs), Chemical Reviews 104 (2004) 4587-4612.

[5] M.M. Hossen, K. Artyushkova, P. Atanassov, A. Serov, Synthesis and characterization of high performing Fe-NC catalyst for oxygen reduction reaction (ORR) in Alkaline Exchange Membrane Fuel Cells, Journal of Power Sources 375 (2018) 214-221.

[6] L. Zeng, T. Zhao, L. An, A high-performance supportless silver nanowire catalyst for anion exchange membrane fuel cells, Journal of Materials Chemistry A 3 (2015) 1410-1416.

[7] Z. Zhuang, S.A. Giles, J. Zheng, G.R. Jenness, S. Caratzoulas, D.G. Vlachos, Y. Yan,

Nickel supported on nitrogen-doped carbon nanotubes as hydrogen oxidation reaction catalyst in alkaline electrolyte, Nature Communications 7 (2016) 10141.

[8] R. Borup, J. Meyers, B. Pivovar, Y.S. Kim, R. Mukundan, N. Garland, D. Myers, M. Wilson, F. Garzon, D. Wood, Scientific aspects of polymer electrolyte fuel cell durability and degradation, Chemical Reviews 107 (2007) 3904-3951.

[9] O. Diat, G. Gebel, Fuel cells: Proton channels, Nature Materials 7 (2008) 13.

[10] M.A. Hickner, Strategies for developing new anion exchange membranes and electrode ionomers, The Electrochemical Society Interface 26 (2017) 69-73.

[11] S. Lu, J. Pan, A. Huang, L. Zhuang, J. Lu, Alkaline polymer electrolyte fuel cells completely free from noble metal catalysts, Proceedings of the National Academy of Sciences 105 (2008) 20611-20614.

[12] J.H. Reid, Gas-battery, US Patents, 757637, 1904.

[13] K.V. Kordesch, G.R. Simader, Environmental impact of fuel cell technology, Chemical Reviews 95 (1995) 191-207.

[14] E. Agel, J. Bouet, J. Fauvarque, Characterization and use of anionic membranes for alkaline fuel cells, Journal of Power Sources 101 (2001) 267-274.

[15] S. Maurya, S.-H. Shin, Y. Kim, S.-H. Moon, A review on recent developments of anion exchange membranes for fuel cells and redox flow batteries, Rsc Advances 5

(2015) 37206-37230.

[16] M.R. Hibbs, Alkaline stability of poly(phenylene) based anion exchange membranes with various cations, Journal of Polymer Science Part B: Polymer Physics 51 (2013) 1736-1742.

[17] W.-H. Lee, A.D. Mohanty, C. Bae, Fluorene-based hydroxide ion conducting polymers for chemically stable anion exchange membrane fuel cells, ACS Macro Letters 4 (2015) 453-457.

[18] N. Chen, C. Long, Y. Li, C. Lu, H. Zhu, Ultrastable and High Ion-Conducting Polyelectrolyte Based on Six-Membered N-Spirocyclic Ammonium for Hydroxide Exchange Membrane Fuel Cell Applications, ACS Applied Materials & Interfaces 10 (2018) 15720-15732.

[19] S. He, L. Liu, X. Wang, S. Zhang, M.D. Guiver, N. Li, Azide-assisted self-crosslinking of highly ion conductive anion exchange membranes, Journal of Membrane Science 509 (2016) 48-56.

[20] H. Lim, B. Lee, D. Yun, A.Z. Al Munsur, J.E. Chae, S.Y. Lee, H.-J. Kim, S.Y. Nam, C.H. Park, T.-H. Kim, Poly(2, 6-dimethyl-1, 4-phenylene oxide)s with various head groups: effect of head groups on the properties of anion exchange membranes, ACS Applied Materials & Interfaces 10 (2018) 41279-41292.

[21] H.-S. Dang, P. Jannasch, High-performing hydroxide exchange membranes with flexible tetra-piperidinium side chains linked by alkyl spacers, ACS Applied Energy Materials 1 (2018) 2222-2231.

[22] N. Li, Q. Zhang, C. Wang, Y.M. Lee, M.D. Guiver, Phenyltrimethylammonium functionalized polysulfone anion exchange membranes, Macromolecules 45 (2012) 2411-2419.

[23] Z. Zhao, J. Wang, S. Li, S. Zhang, Synthesis of multi-block poly(arylene ether sulfone) copolymer membrane with pendant quaternary ammonium groups for alkaline fuel cell, Journal of Power Sources 196 (2011) 4445-4450.

[24] J. Kerres, A. Ullrich, M. Hein, Preparation and characterization of novel basic polysulfone polymers, Journal of Polymer Science Part A: Polymer Chemistry 39 (2001) 2874-2888.

[25] L. Li, Y. Wang, Quaternized polyethersulfone Cardo anion exchange membranes for direct methanol alkaline fuel cells, Journal of Membrane Science 262 (2005) 1-4.

[26] X. Li, Y. Yu, Y. Meng, Novel quaternized poly(arylene ether sulfone)/nano-ZrO2 composite anion exchange membranes for alkaline fuel cells, ACS Applied Materials & Interfaces 5 (2013) 1414-1422.

[27] D.W. Seo, M.A. Hossain, D.H. Lee, Y.D. Lim, S.H. Lee, H.C. Lee, T.W. Hong,

W.G. Kim, Anion conductive poly(arylene ether sulfone)s containing tetra-quaternary ammonium hydroxide on fluorenyl group for alkaline fuel cell application, Electrochimica Acta 86 (2012) 360-365.

[28] D.W. Seo, Y.D. Lim, M.A. Hossain, S.H. Lee, H.C. Lee, H.H. Jang, S.Y. Choi, W.G. Kim, Anion conductive poly(tetraphenyl phthalazine ether sulfone) containing tetra quaternary ammonium hydroxide for alkaline fuel cell application, International Journal of Hydrogen Energy 38 (2013) 579-587.

[29] D. Xing, S. Zhang, C. Yin, C. Yan, X. Jian, Preparation and characterization of chloromethylated/quanternized poly(phthalazinone ether sulfone) anion exchange membrane, Materials Science and Engineering: B 157 (2009) 1-5.

[30] Q. Zhang, Q. Zhang, J. Wang, S. Zhang, S. Li, Synthesis and alkaline stability of novel cardo poly(aryl ether sulfone)s with pendent quaternary ammonium aliphatic side chains for anion exchange membranes, Polymer 51 (2010) 5407-5416.

[31] J. Zhou, M. Unlu, J.A. Vega, P.A. Kohl, Anionic polysulfone ionomers and membranes containing fluorenyl groups for anionic fuel cells, Journal of Power Sources 190 (2009) 285-292.

[32] G. Wang, Y. Weng, D. Chu, D. Xie, R. Chen, Preparation of alkaline anion exchange membranes based on functional poly(ether-imide) polymers for potential fuel

cell applications, Journal of Membrane Science 326 (2009) 4-8.

[33] Q. Hu, Y. Shang, Y. Wang, M. Xu, S. Wang, X. Xie, Y. Liu, H. Zhang, J. Wang, Z. Mao, Preparation and characterization of fluorinated poly(aryl ether oxadiazole)s anion exchange membranes based on imidazolium salts, International Journal of Hydrogen Energy 37 (2012) 12659-12665.

[34] C. Li, S. Wang, W. Wang, X. Xie, Y. Lv, C. Deng, A cross-linked fluorinated poly (aryl ether oxadiazole)s using a thermal cross-linking for anion exchange membranes, International Journal of Hydrogen Energy 38 (2013) 11038-11044.

[35] W. Wang, S. Wang, W. Li, X. Xie, Synthesis and characterization of a fluorinated cross-linked anion exchange membrane, International Journal of Hydrogen Energy 38 (2013) 11045-11052.

[36] H. Hou, S. Wang, H. Liu, L. Sun, W. Jin, M. Jing, L. Jiang, G. Sun, Synthesis and characterization of a new anion exchange membrane by a green and facile route, International Journal of Hydrogen Energy 36 (2011) 11955-11960.

[37] L.-c. Jheng, S.L.-c. Hsu, B.-y. Lin, Y.-l. Hsu, Quaternized polybenzimidazoles with imidazolium cation moieties for anion exchange membrane fuel cells, Journal of Membrane Science 460 (2014) 160-170.

[38] J. Hu, D. Wan, W. Zhu, L. Huang, S. Tan, X. Cai, X. Zhang, Fabrication of a

high-stability cross-linked quaternized poly(epichlorolydrin)/PTFE composite membrane via a facile route, ACS Applied Materials & Interfaces 6 (2014) 4720-4730.

[39] J.R. Varcoe, R.C. Slade, E. Lam How Yee, S.D. Poynton, D.J. Driscoll, D.C. Apperley, Poly(ethylene-co-tetrafluoroethylene)-derived radiation-grafted anion exchange membrane with properties specifically tailored for application in metal-cation-free alkaline polymer electrolyte fuel cells, Chemistry of Materials 19 (2007) 2686-2693.

[40] A. Bosnjakovic, M. Danilczuk, S. Schlick, P.N. Xiong, G.M. Haugen, S.J. Hamrock, An attempt to generate anion exchange membranes by amination of the perfluorinated 3M precursor leads to the hydrolysis of the precursor, Journal of Membrane Science 467 (2014) 136-141.

[41] D.S. Kim, C.H. Fujimoto, M.R. Hibbs, A. Labouriau, Y.-K. Choe, Y.S. Kim, Resonance stabilized perfluorinated ionomers for alkaline membrane fuel cells, Macromolecules 46 (2013) 7826-7833.

[42] X. Kong, K. Wadhwa, J.G. Verkade, K. Schmidt-Rohr, Determination of the structure of a novel anion exchange fuel cell membrane by solid-state nuclear magnetic resonance spectroscopy, Macromolecules 42 (2009) 1659-1664.

[43] M.A. Vandiver, J.L. Horan, Y. Yang, E.T. Tansey, S. Seifert, M.W. Liberatore, A.M.

Herring, Synthesis and characterization of perfluoro quaternary ammonium anion exchange membranes, Journal of Polymer Science Part B: Polymer Physics 51 (2013) 1761-1769.

[44] T. Li, X. Wu, W. Chen, X. Yan, D. Zhen, X. Gong, J. Liu, S. Zhang, G. He, Poly (ether ether ketone ketone) based Imidazolium as anion exchange membranes for alkaline fuel cells, Chinese Journal of Chemical Engineering 26 (2018) 2130-2138.

[45] X. Yan, G. He, S. Gu, X. Wu, L. Du, H. Zhang, Quaternized poly(ether ether ketone) hydroxide exchange membranes for fuel cells, Journal of Membrane Science 375 (2011) 204-211.

[46] T.Y. Guo, Q.H. Zeng, C.H. Zhao, Q.L. Liu, A.M. Zhu, I. Broadwell, Quaternized polyepichlorohydrin/PTFE composite anion exchange membranes for direct methanol alkaline fuel cells, Journal of membrane science 371 (2011) 268-275.

[47] C. Sollogoub, A. Guinault, C. Bonnebat, M. Bennjima, L. Akrour, J. Fauvarque, L. Ogier, Formation and characterization of crosslinked membranes for alkaline fuel cells, Journal of Membrane Science 335 (2009) 37-42.

[48] D. Stoica, F. Alloin, S. Marais, D. Langevin, C. Chappey, P. Judeinstein, Polyepichlorhydrin membranes for alkaline fuel cells: sorption and conduction properties, The Journal of Physical Chemistry B 112 (2008) 12338-12346.

[49] D. Stoica, L. Ogier, L. Akrour, F. Alloin, J.-F. Fauvarque, Anionic membrane based on polyepichlorhydrin matrix for alkaline fuel cell: Synthesis, physical and electrochemical properties, Electrochimica Acta 53 (2007) 1596-1603.

[50] C.-C. Yang, Alkaline direct methanol fuel cell based on a novel anion-exchange composite polymer membrane, Journal of Applied Electrochemistry 42 (2012) 305-317.

[51] A.N. Lai, K. Zhou, Y.Z. Zhuo, Q.G. Zhang, A.M. Zhu, M.L. Ye, Q.L. Liu, Anion exchange membranes based on carbazole-containing polyolefin for direct methanol fuel cells, Journal of Membrane Science 497 (2016) 99-107.

[52] M. Zhang, C. Shan, L. Liu, J. Liao, Q. Chen, M. Zhu, Y. Wang, L. An, N. Li, Facilitating anion transport in polyolefin-based anion exchange membranes via bulky side chains, ACS Applied Materials & Interfaces 8 (2016) 23321-23330.

[53] T.J. Clark, N.J. Robertson, H.A. Kostalik IV, E.B. Lobkovsky, P.F. Mutolo, H.D. Abruna, G.W. Coates, A ring-opening metathesis polymerization route to alkaline anion exchange membranes: development of hydroxide-conducting thin films from an ammonium-functionalized monomer, Journal of the American Chemical Society 131 (2009) 12888-12889.

[54] A.M. Maes, T.P. Pandey, M.A. Vandiver, L.K. Lundquist, Y. Yang, J.L. Horan, A. Krosovsky, M.W. Liberatore, S. Seifert, A.M. Herring, Preparation and characterization

of an alkaline anion exchange membrane from chlorinated poly(propylene) aminated with branched poly(ethyleneimine), Electrochimica Acta 110 (2013) 260-266.

[55] C. Chen, A.R. Hess, A.R. Jones, X. Liu, G.D. Barber, T.E. Mallouk, H.R. Allcock, Synthesis of new polyelectrolytes via backbone quaternization of poly(aryloxy-and alkoxyphosphazenes) and their small molecule counterparts, Macromolecules 45 (2012) 1182-1189.

[56] G. Merle, S.S. Hosseiny, M. Wessling, K. Nijmeijer, New cross-linked PVA based polymer electrolyte membranes for alkaline fuel cells, Journal of membrane science 409 (2012) 191-199.

[57] L. Zeng, T. Zhao, Y. Li, Synthesis and characterization of crosslinked poly(vinyl alcohol)/layered double hydroxide composite polymer membranes for alkaline direct ethanol fuel cells, International journal of hydrogen energy 37 (2012) 18425-18432.

[58] T. Zhou, J. Zhang, J. Jingfu, G. Jiang, J. Zhang, J. Qiao, Poly(ethylene glycol) plasticized poly(vinyl alcohol)/poly(acrylamide-co-diallyldimethylammonium chloride) as alkaline anion-exchange membrane for potential fuel cell applications, Synthetic Metals 167 (2013) 43-50.

[59] R. Ren, S. Zhang, H.A. Miller, F. Vizza, J.R. Varcoe, Q. He, Facile Preparation of an Ether-free Anion Exchange Membrane with Pendant Cyclic Quaternary Ammonium

Groups, ACS Applied Energy Materials 2 (2019) 4576-4581.

[60] B. Lin, L. Qiu, B. Qiu, Y. Peng, F. Yan, A soluble and conductive polyfluorene ionomer with pendant imidazolium groups for alkaline fuel cell applications, Macromolecules 44 (2011) 9642-9649.

[61] M. Tanaka, K. Fukasawa, E. Nishino, S. Yamaguchi, K. Yamada, H. Tanaka, B. Bae, K. Miyatake, M. Watanabe, Anion conductive block poly(arylene ether)s: synthesis, properties, and application in alkaline fuel cells, Journal of the American Chemical Society 133 (2011) 10646-10654.

[62] F. Zhang, H. Zhang, C. Qu, Imidazolium functionalized polysulfone anion exchange membrane for fuel cell application, Journal of Materials Chemistry 21 (2011) 12744-12752.

[63] J. Pan, J. Han, L. Zhu, M.A. Hickner, Cationic side-chain attachment to poly (phenylene oxide) backbones for chemically stable and conductive anion exchange membranes, Chemistry of Materials 29 (2017) 5321-5330.

[64] L. Zhu, J. Pan, C.M. Christensen, B. Lin, M.A. Hickner, Functionalization of poly(2,6-dimethyl-1,4-phenylene oxide)s with hindered fluorene side chains for anion exchange membranes, Macromolecules 49 (2016) 3300-3309.

[65] R. Akiyama, N. Yokota, E. Nishino, K. Asazawa, K. Miyatake, Anion conductive

aromatic copolymers from dimethylaminomethylated monomers: synthesis, properties, and applications in alkaline fuel cells, Macromolecules 49 (2016) 4480-4489.

[66] A.D. Mohanty, Y.-B. Lee, L. Zhu, M.A. Hickner, C. Bae, Anion exchange fuel cell membranes prepared from C–H borylation and Suzuki coupling reactions, Macromolecules 47 (2014) 1973-1980.

[67] X. Lin, L. Wu, Y. Liu, A.L. Ong, S.D. Poynton, J.R. Varcoe, T. Xu, Alkali resistant and conductive guanidinium-based anion-exchange membranes for alkaline polymer electrolyte fuel cells, Journal of Power Sources 217 (2012) 373-380.

[68] K.J. Noonan, K.M. Hugar, H.A. Kostalik IV, E.B. Lobkovsky, H.c.D. Abruña, G.W. Coates, Phosphonium-functionalized polyethylene: a new class of base-stable alkaline anion exchange membranes, Journal of the American Chemical Society 134 (2012) 18161-18164.

[69] B. Zhang, S. Gu, J. Wang, Y. Liu, A.M. Herring, Y. Yan, Tertiary sulfonium as a cationic functional group for hydroxide exchange membranes, RSC Advances 2 (2012) 12683-12685.

[70] B. Lin, L. Qiu, J. Lu, F. Yan, Cross-linked alkaline ionic liquid-based polymer electrolytes for alkaline fuel cell applications, Chemistry of Materials 22 (2010) 6718-6725.

[71] Y. Song, C. Liu, J. Zhao, J. Luo, Imidazolium-functionalized anion exchange polymer containing fluorine group for fuel cell application, International Journal of Hydrogen Energy 41 (2016) 10446-10457.

[72] X. Lin, X. Liang, S.D. Poynton, J.R. Varcoe, A.L. Ong, J. Ran, Y. Li, Q. Li, T. Xu, Novel alkaline anion exchange membranes containing pendant benzimidazolium groups for alkaline fuel cells, Journal of Membrane Science 443 (2013) 193-200.

[73] J.S. Olsson, T.H. Pham, P. Jannasch, Poly(arylene piperidinium) Hydroxide Ion Exchange Membranes: Synthesis, Alkaline Stability, and Conductivity, Advanced Functional Materials 28 (2018) 1702758.

[74] J. Ponce-González, D.K. Whelligan, L. Wang, R. Bance-Soualhi, Y. Wang, Y. Peng, H. Peng, D.C. Apperley, H.N. Sarode, T.P. Pandey, High performance aliphatic-heterocyclic benzyl-quaternary ammonium radiation-grafted anion-exchange membranes, Energy & Environmental Science 9 (2016) 3724-3735.

[75] K.M. Meek, J.R. Nykaza, Y.A. Elabd, Alkaline chemical stability and ion transport in polymerized ionic liquids with various backbones and cations, Macromolecules 49 (2016) 3382-3394.

[76] F. Gong, R. Wang, X. Chen, P. Chen, Z. An, S. Zhang, Facile synthesis and the properties of novel cardo poly(arylene ether sulfone)s with pendent cycloaminium side

chains as anion exchange membranes, Polymer Chemistry 8 (2017) 4207-4219.

[77] X. Yan, R. Deng, Y. Pan, X. Xu, I. El Hamouti, X. Ruan, X. Wu, C. Hao, G. He, Improvement of alkaline stability for hydroxide exchange membranes by the interactions between strongly polar nitrile groups and functional cations, Journal of Membrane Science 533 (2017) 121-129.

[78] N. Li, M.D. Guiver, W.H. Binder, Towards High Conductivity in Anion‐Exchange Membranes for Alkaline Fuel Cells, ChemSusChem 6 (2013) 1376-1383.

[79] J. Pan, Y. Li, J. Han, G. Li, L. Tan, C. Chen, J. Lu, L. Zhuang, A strategy for disentangling the conductivity–stability dilemma in alkaline polymer electrolytes, Energy & Environmental Science 6 (2013) 2912-2915.

[80] J. Si, S. Lu, X. Xu, S. Peng, R. Xiu, Y. Xiang, A Gemini Quaternary Ammonium Poly(ether ether ketone) Anion‐Exchange Membrane for Alkaline Fuel Cell: Design, Synthesis, and Properties, ChemSusChem 7 (2014) 3389-3395.

[81] D. Guo, A.N. Lai, C.X. Lin, Q.G. Zhang, A.M. Zhu, Q.L. Liu, Imidazolium-functionalized poly(arylene ether sulfone) anion-exchange membranes densely grafted with flexible side chains for fuel cells, ACS Applied Materials & Interfaces 8 (2016) 25279-25288.

[82] C.X. Lin, H.Y. Wu, L. Li, X.Q. Wang, Q.G. Zhang, A.M. Zhu, Q.L. Liu, Anion

Conductive Triblock Copolymer Membranes with Flexible Multication Side Chain, ACS Applied Materials & Interfaces 10 (2018) 18327-18337.

[83] D. Guo, C.X. Lin, E.N. Hu, L. Shi, F. Soyekwo, Q.G. Zhang, A.M. Zhu, Q.L. Liu, Clustered multi-imidazolium side chains functionalized alkaline anion exchange membranes for fuel cells, Journal of Membrane Science 541 (2017) 214-223.

[84] K.H. Lee, D.H. Cho, Y.M. Kim, S.J. Moon, J.G. Seong, D.W. Shin, J.-Y. Sohn, J.F. Kim, Y.M. Lee, Highly conductive and durable poly(arylene ether sulfone) anion exchange membrane with end-group cross-linking, Energy & Environmental Science 10 (2017) 275-285.

[85] J. Pan, L. Zhu, J. Han, M.A. Hickner, Mechanically tough and chemically stable anion exchange membranes from rigid-flexible semi-interpenetrating networks, Chemistry of Materials 27 (2015) 6689-6698.

[86] E.N. Hu, C.X. Lin, F.H. Liu, Q. Yang, L. Li, Q.G. Zhang, A.M. Zhu, Q.L. Liu, Cross-linked poly(vinylbenzyl chloride) anion exchange membranes with long flexible multihead for fuel cells, ACS Applied Energy Materials 1 (2018) 3479-3487.

[87] H. Ono, T. Kimura, A. Takano, K. Asazawa, J. Miyake, J. Inukai, K. Miyatake, Robust anion conductive polymers containing perfluoroalkylene and pendant ammonium groups for high performance fuel cells, Journal of Materials Chemistry A 5

(2017) 24804-24812.

[88] J.R. Varcoe, P. Atanassov, D.R. Dekel, A.M. Herring, M.A. Hickner, P.A. Kohl, A.R. Kucernak, W.E. Mustain, K. Nijmeijer, K. Scott, Anion-exchange membranes in electrochemical energy systems, Energy & Environmental Science 7 (2014) 3135-3191.

[89] A.D. Mohanty, C. Bae, Mechanistic analysis of ammonium cation stability for alkaline exchange membrane fuel cells, Journal of Materials Chemistry A 2 (2014) 17314-17320.

[90] Y. Ye, Y.A. Elabd, Chemical stability of anion exchange membranes for alkaline fuel cells, Polymers for Energy Storage and Delivery: Polyelectrolytes for Batteries and Fuel Cells, ACS Publications2012, pp. 233-251.

[91] S. Gottesfeld, D.R. Dekel, M. Page, C. Bae, Y. Yan, P. Zelenay, Y.S. Kim, Anion exchange membrane fuel cells: Current status and remaining challenges, Journal of Power Sources 375 (2018) 170-184.

[92] W. Li, J. Fang, M. Lv, C. Chen, X. Chi, Y. Yang, Y. Zhang, Novel anion exchange membranes based on polymerizable imidazolium salt for alkaline fuel cell applications, Journal of Materials Chemistry 21 (2011) 11340-11346.

[93] B. Qiu, B. Lin, L. Qiu, F. Yan, Alkaline imidazolium-and quaternary ammonium-functionalized anion exchange membranes for alkaline fuel cell applications,

Journal of Materials Chemistry 22 (2012) 1040-1045.

[94] Z. Sun, B. Lin, F. Yan, Anion‐Exchange Membranes for Alkaline Fuel‐Cell Applications: The Effects of Cations, ChemSusChem 11 (2018) 58-70.

[95] O.I. Deavin, S. Murphy, A.L. Ong, S.D. Poynton, R. Zeng, H. Herman, J.R. Varcoe, Anion-exchange membranes for alkaline polymer electrolyte fuel cells: comparison of pendent benzyltrimethylammonium and benzylmethylimidazolium head groups, Energy & Environmental Science 5 (2012) 8584-8597.

[96] B. Ameduri, From vinylidene fluoride (VDF) to the applications of VDF-containing polymers and copolymers: recent developments and future trends, Chemical Reviews 109 (2009) 6632-6686.

[97] J.S. Olsson, T.H. Pham, P. Jannasch, Poly(N, N-diallylazacycloalkane)s for anion-exchange membranes functionalized with n-spirocyclic quaternary ammonium cations, Macromolecules 50 (2017) 2784-2793.

[98] E.J. Park, Y.S. Kim, Quaternized aryl ether-free polyaromatics for alkaline membrane fuel cells: synthesis, properties, and performance–a topical review, Journal of Materials Chemistry A 6 (2018) 15456-15477.

[99] C.G. Arges, V. Ramani, Two-dimensional NMR spectroscopy reveals cation-triggered backbone degradation in polysulfone-based anion exchange membranes,

Proceedings of the National Academy of Sciences 110 (2013) 2490-2495.

# Synthesis and Characterization of 1-Isopropyl-2-Methylimidazolium Containing Hydroxide Ion Conducting Polymer


## Abstract

An anion exchange membrane (AEM) based on fluorene containing 1-isopropyl-2-methylimidazolium with flexible alkyl side chains was newly prepared by using the Suzuki coupling reaction. The structures of the synthesized monomers and polymers were characterized by $^{1}H$ NMR, $^{13}C$ NMR, FTIR spectroscopies and Mass spectrometry. The properties of the membrane including $OH^-$ conductivities, ion exchange capacity (IEC), chemical stabilities, thermal stabilities, mechanical properties, water uptake, and swelling behavior were assessed. The synthesized membrane exhibited low water uptake and high dimensional stability, adequate hydroxide conductivities and good physical stability. With a swelling ratio of 7%, the hydroxide conductivity of the obtained membrane reached up to 46 mS $cm^{-1}$ at 80 °C in liquid water. The chemical stability of the membrane was investigated in 1 M NaOH solution at room temperature and 80 °C. In both cases, I have observed the degradation of the imidazolium cationic groups though the main chain was chemically stable. Some

literature has suggested that imidazolium cationic groups are chemically stable, but some other reports have revealed the less chemical stability of imidazolium groups. From the results of alkaline stability, this discrepancy can be concluded. All the obtained results of this research will provide significant directions and insights for the synthesis of AEMs for practical applications in anion exchange membrane fuel cells (AEMFCs).

## 2.1. Introduction

Fuel cells are highly efficient and clean energy devices [1-4]. In comparison to AEMFCs, proton exchange membrane fuel cells (PEMFCs) are more developed. However, in the past decades, AEMFCs have become the focusing topic. The shift of attention to AEMFCs from PEMFCs has been mostly because of the use of high-cost platinum (Pt) catalyst in PEMFCs. By using AEMFCs, the cost can be reduced potentially as basic conditions allow using non-noble metal electrocatalysts such as nickel, silver or cobalt. Another advantage is the enhanced oxygen reduction at the cathode side [3, 5-7].

One of the major challenges is finding an AEM which has adequate alkaline stability for long time operation, moderate water uptake, low water swelling, robust mechanical properties, and providing high ionic conductivity [8, 9]. Aromatic polymers are desirable as a backbone of AEMs due to having high chemical and thermal stability [10]. A number of polymeric AEMs based on different backbones including polyarylene ether sulfones [11, 12], polyphenylenes [13, 14], polyphenylene oxides (PPO) [15, 16], polystyrenes (PS) [17, 18], polyarylene ether ketones (PAEK) [19] and polyolefins [20, 21] have been extensively studied as AEM materials as shown in Scheme 2.1. Among the prepared AEMs, polymer backbones containing aryl ketone, aryl sulfone, and aryl

ether bonds are very vulnerable to nucleophilic attack by $OH^-$ ions. Therefore, at the high alkaline condition, the chemical stability decreases due to the degradation of backbones [22-24].

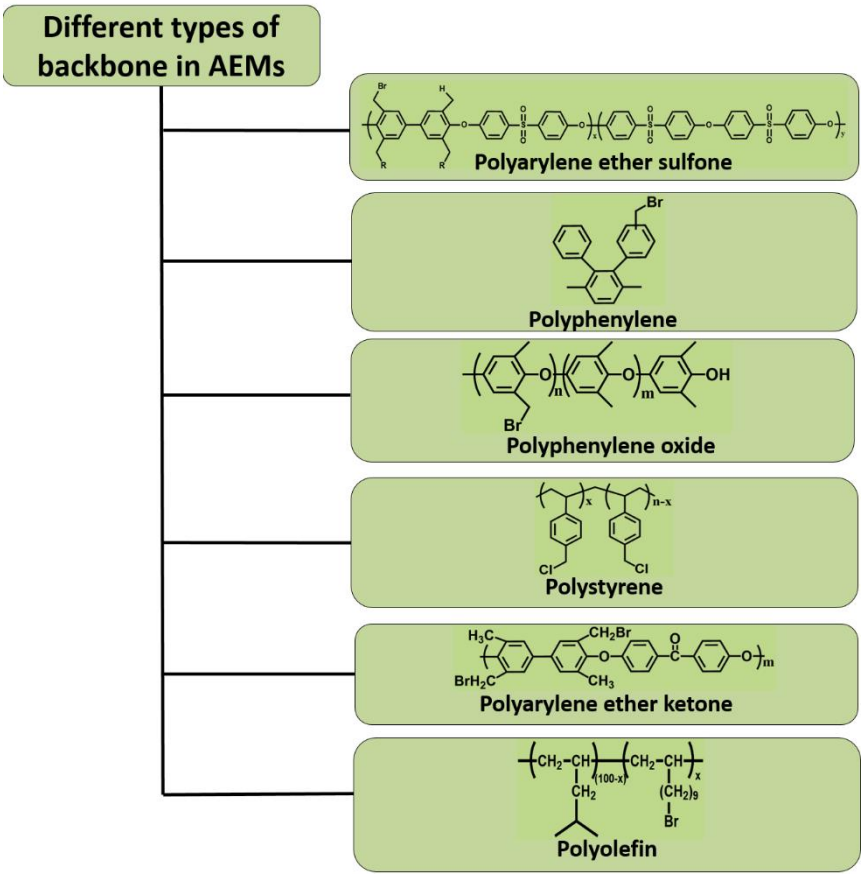


Scheme 2.1. Chemical structure of the different types of backbone used in AEMs.

Among the synthesized AEMs, polymer backbones containing fluorenyl groups are in great attention as it has classic structure and diverse chemical changes are possible [25,

26]. The molecular weights and the solubility of polymers can be enhanced by adding long alkyl or dialkyl groups at the C9-position of fluorene ring [14] as shown in Fig. 2.1. AEMs containing fluorene groups on their backbone were found to have good thermal, alkaline stability, and high $OH^-$ conductivity [14]. The rigid and bulky fluorene groups on the backbone could form large interchain separations or free volumes by forcing each polymer chain apart, and in the free volumes, water molecules might be confined [27]. In a high pH environment, the long alkyl tethered cationic groups show more thermal stability than the benzyl substituted one [14]. Microphase separation is developed by the introduction of flexible side chains. The long alkyl side chain leads to strong self-assembly [28].

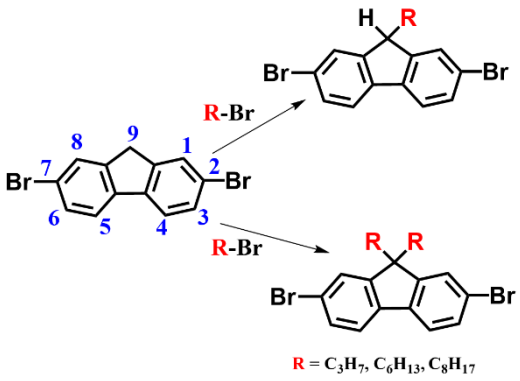


Fig. 2.1. Alkylation or dialkylation at the C9 position of fluorene ring.

Numerous functional groups including quaternary ammonium (QA) [29],

phosphonium [30], sulfonium [31], guanidinium [32], imidazolium [17, 33], piperidinium [16] morpholinium [16] have been widely used to synthesize polymeric membranes for AEMFCs (Scheme 2.2). Among the different cationic groups tetraalkyl quaternary ammonium salts are most commonly used as cationic groups because of the easy synthetic procedure and inexpensive starting materials. Most of the AEMs were prepared by the addition of chloromethyl groups to the backbone of the polymer then QA salts obtained via quaternization reaction. But, chloromethyl methyl ether is very harmful to human health because it′s a carcinogenic reagent [34]. Another serious problem is the efficient degradation of QA cations by a number of different pathways that includes Hofmann (β-hydrogen) or E2 elimination, ylide formation and at the α-carbon direct nucleophilic substitution ($S_N2$) as shown in Fig. 1.3 (Chapter 1) [35, 36]. The ion exchange capacity (IEC) and ionic conductivity of AEMs, rapidly decreases because of the degradation of QA salts.

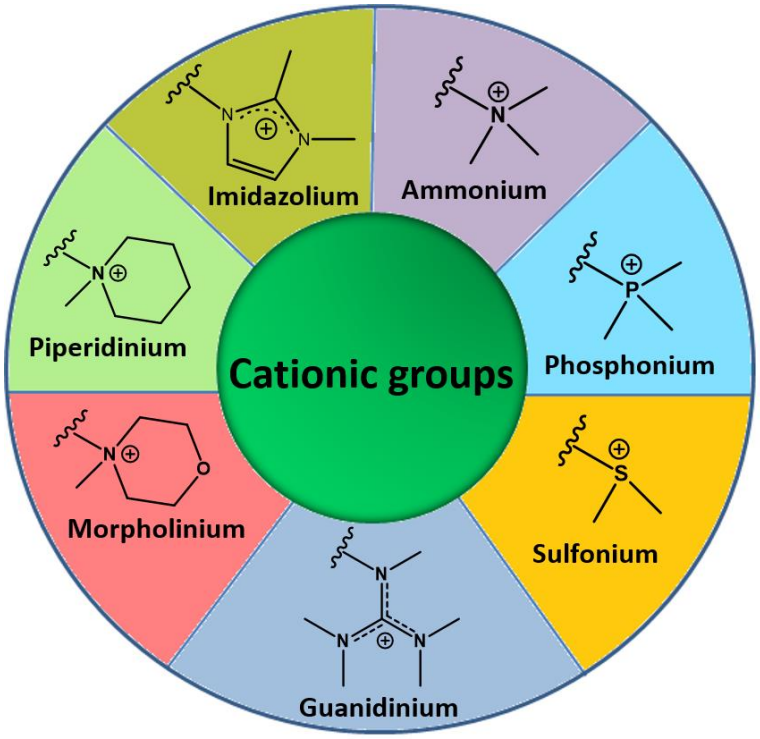


Scheme 2.2. Commonly used cationic groups in AEM.

Imidazolium functionalized AEMs showed enhanced chemical stability in a high alkaline environment with comparable ionic conductivity [37]. Researchers supposed that a π conjugated structure is formed in heterocyclic five-membered imidazolium salts [33, 38]. The delocalization of positive charge in the π-conjugated system hindered the nucleophilic attack of hydroxyl groups (Fig 2.2).

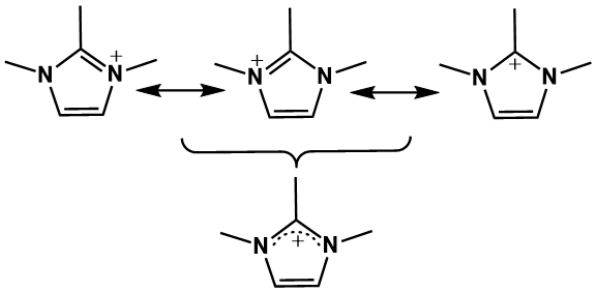

Fig. 2.2. Delocalization of positive charge in the imidazolium salts.

However, imidazolium salts degrade by ring-opening reaction as the nucleophilic attack of $OH^-$ ions [39, 40] takes place at the C2 position. Therefore, C2 substituted imidazolium cations are more stable in high alkaline condition. As an example, Yan *et al.* [33] found that the C2-substituted (methyl, isopropyl or phenyl groups) imidazolium salts were more alkaline stable than the C2-unsubstituted one shown in Fig. 2.3. This research group also compared the chemical stability of some N3 substituted imidazolium and QA cations. The chemical stability was determined from the LUMO energy that was simulated by using density functional theory (DFT). High LUMO energy indicates high chemical stability. Among them, the imidazolium cation substituted by the isopropyl group showed the highest LUMO energy, which facilitates it to be the most stable imidazolium salt (Fig 2.4). The electron density of alkyl-substituted imidazolium salts increased due to the electron donating effect and the hyperconjugation effect between the CH bonds of substituents and the imidazole ring

(π-conjugated) hence, the attack of nucleophilic $OH^-$ ion was decreased. The chemical stability of imidazolium salts also increased because of the steric hindrance of substituents. They also confirmed the chemical stability of the imidazolium salts experimentally by using model compounds [41].

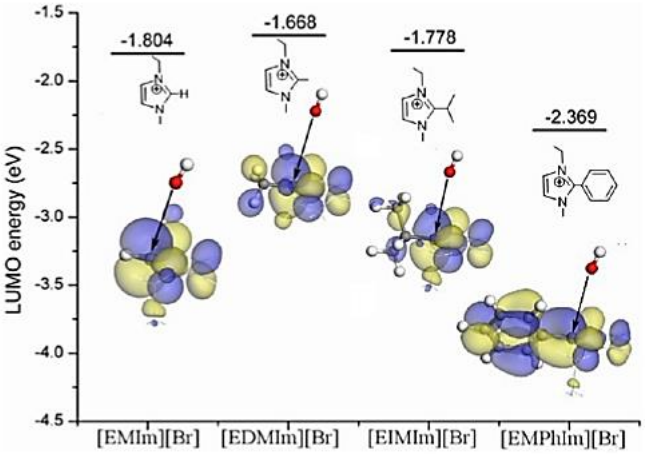


Fig. 2.3. LUMO energy of C2 substituted imidazolium salts. The white, gray, blue, and red colors stand for H, C, N, O atoms, respectively. The nucleophilic attacks of $OH^-$ are indicated by the black arrows [33].

In another research, they used DFT calculations to investigate the effect of C2 substitution on LUMO energy by electron withdrawing and electron donating groups. In their research, the amino substituted imidazolium group showed the highest LUMO energy and alkaline stability. Cycloalkyl substitution at the N3 position could also

significantly increase the LUMO energy. They observed the LUMO energy of cycloheptyl and cyclooctyl substituted imidazolium salt is higher than that of isopropyl

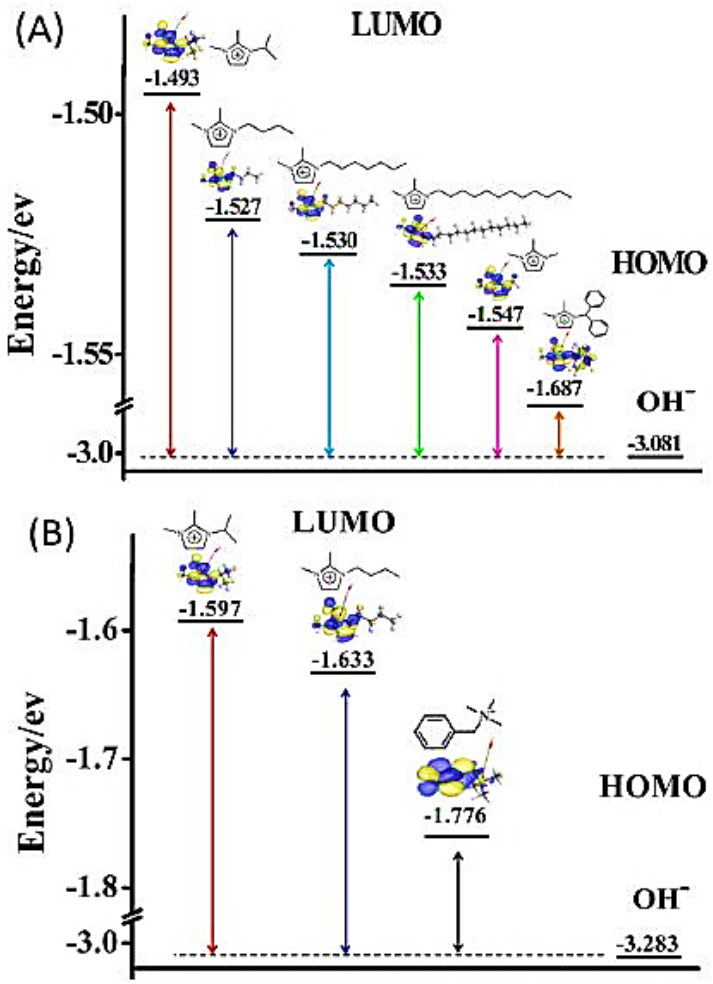


Fig. 2.4. LUMO energy of substituted imidazolium cations and QA cation in (A) water and (B) methanol solution [41].

substituted imidazolium salt [42]. Therefore, they proposed amino and cyclooctyl are

the most suitable substituents for C2 and N3 substitution of the imidazolium group. However, the procedure for the synthesis of this imidazolium salt is not practically revealed yet. Yan *et al.* [43] and Coates *et al.* [44] reported that not only the bulky groups at C2 position but also the substitution of C4 and C5 position by methyl or phenyl groups dramatically suppressed the degradation of imidazolium group in alkaline condition. In alkaline condition, only steric hindrance is not sufficient to stabilize imidazolium cationic groups. The electron donating effect of substituents also important. Yan and coworkers [43] reported PPO based AEM containing 1,4,5-trimethyl-2-(2,4,6-trimethoxyphenyl)imidazolium. Due to high electron density and steric bulk, the 2,4,6-trimethoxyphenyl at C2 position stabilizes the imidazolium group. The additional electron density was donated by the methyl groups at C4 and C5 positions. They observed only 5% conductivity lost in 1 M KOH solution, at 80 °C for 48 h. In addition, 17% conductivity was lost in 1 M KOH solution at 60 °C for the 600 h chemical stability test. However, the synthetic procedure of C2-, C4- and C5-substituted imidazolium groups are much more complex than N-substitutions [45]. N-substituted imidazolium salt can easily be synthesized by the nucleophilic substitution reaction between alkylhalide and lone pair electron of N atom. Consequently, N3-substituted imidazolium salts have drawn significant attention as a cationic group in AEM.

The reduced thermochemical stability of AEMs hindered the practical use of AEMs in alkaline fuel cells. Many research groups have made significant efforts to solve these problems. Such as, by introducing long alkyl groups between cationic groups and polymer backbones [46], by forming different morphologies of polymer including graft [47], block [48], comb-shaped [49] or cluster-type [27] architectures and high concentration of functional groups are introduced to polymer by crosslinking [50, 51] and these proposed ways enhance the hydroxide conductivity in AEMs. Although these investigated materials showed to have a wider conductivity range, the molecular design strategies of high performing AEMs for practical application are not fully revealed yet.

The ion exchange capacity (IEC) value can increase by introducing more cationic groups, hence increase the ion conductivity. Even though the high IEC enhances the conductivity, the mechanical behavior of the resultant AEMs is also affected very badly. Most synthesized AEMs with high IECs display chemical and physical instability and due to high IECs, these membranes are comparatively unstable under the fuel cell operating condition (i.e., at 80 $^{o}$C, and high alkaline medium) [52]. Consequently, researchers significantly motivated to develop the chemical stability of polymer backbones and functional groups.

To determine the synthetic strategy I have summarized hydroxide conductivity, water uptake and ion exchange capacity of some reported AEMs based on different polymer backbone architecture shown in Table 2.1. I also have compared the alkaline stability of the membranes although it was very difficult to compare as researchers used different alkaline conditions and various techniques for stability tests.

Table 2.1. Comparison of hydroxide conductivity, water uptake, ion exchange capacity and alkaline stability of some state-of-art AEMs.

| Membrane [Ref. no.] | Backbone type | $IEC_{exp}$ (mmol $g^{-1}$) | WU (%) | $\sigma_{OH^-}$ (mS $cm^{-1}$) | Alkaline Stability (1 M NaOH, 80 ºC) | Configuration |
|---|---|---|---|---|---|---|
| AI-PES-12 [49] | poly (arylene ether sulfone) | 1.02 | 11.5 | [a]140 | 13 days (2 M NaOH, 60 ºC) [c](no degradation) | 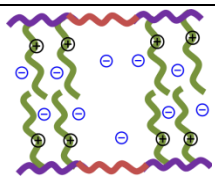 |
| AI-PES-16 [49] | | 0.92 | 11.2 | [a]120 | | |
| XE-Imd60 [50] | poly (arylene ether sulfone) | 2.43 | 92.4 | [b]97 | 21 days (remaining conductivity 69%) | 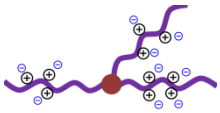 |
| PPO-7Q-1.5 [46] | poly (phenylene oxide) | 1.40 | 46.0 | [a]64 | 8 days [d](no degradation) |  |
| PPO-7Q-1.8 [46] | | 1.60 | 60.0 | [a]85 | | |
| SIPN-60-2 [51] | poly (phenylene oxide) | 1.43 | 124.6 | [a]68 | 30 days (remaining conductivity 74%) | 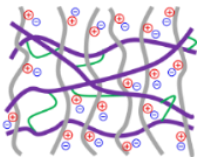 |
| PPO5-4QPip-2.6 [15] | poly (phenylene oxide) | 2.30 | 143.0 | [a]221 | 10 days (1 M NaOH, 90 ºC) [d](no degradation) | 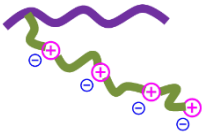 |
| B-g-Q-1.5 [47] | poly (phenylene oxide) | 1.55 | 66.5 (60 ºC) | [a]95 | 12 days (2 M NaOH, 60 ºC) (remaining IEC 63%) | 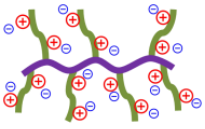 |
| $PFF^+$ [14] | poly (fluorene)s | 2.45 | 26.0 | [a]48 | 30 days [d](no degradation) | 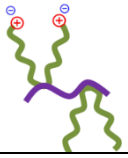 |

[a]in liquid water; [b]at relative humidity (100%); [c]from IEC and conductivity; [d]from $^{1}H$ NMR; ⊕, imidazolium; ⊕, quaternary ammonium; ⊕, piperidinium cationic groups.

From the literature survey, I have found that many research groups have used poly(arylene ether sulfone)s (PAES) and poly(phenylene oxide)s (PPO) as the polymeric material for the synthesis of AEMs however, a few of AEMs are available based on ether free polyfluorenes.

Bae and coworkers [14] reported that ether-bond-free polyfluorene based AEMs with long alkyl substituted QA groups were stable in 1 M NaOH at 80 $^{o}$C for 30 days. No literature is available for imidazolium functionalized AEM with the same fluorene backbone. In this research, I have designed and demonstrated a facile synthetic approach for a similar type of fluorene backbone to have an IEC value of 2.00 mmol/g. For the synthesis of highly conductive and alkaline stable AEM, I have chosen aryl ether-bond-free polyfluorene backbone and newly introduced 1-isopropyl-2-methylimidazolium as cationic groups by flexible alkyl side chains. The properties of the synthesized AEM including the hydroxide conductivity, chemical and thermal stability, water uptake, and swelling ratio were fully investigated.

## 2.2. Experimental

### 2.2.1. Materials

2,7-dibromofluorene, 1,6-dibromohexane, tetrabutylammonium bromide (TBAB), bis(pinacolato)diboron, 2-methylimidazole, 2-bromopropane, 2,7-dibromo-9,9-dioctyl fluorene, tetrakis(triphenylphosphine)palladium(0) $Pd(PPh_3)_4$ were received from Tokyo Chemical Industry Co. Ltd., Japan and used without further purification. [1,1-Bis(diphenylphosphino)ferrocene]dichloropalladium(II) ($PdCl_2$)(dppf) from Sigma-Aldrich was used. Dioxane, chloroform, dichloromethane, toluene, ethanol, *N*,*N*-dimethylformamide (DMF), diethyl ether, tetrahydrofuran (THF), hexane, acetonitrile, potassium carbonate, methanol, ethyl acetate, sodium hydroxide, potassium hydroxide, sodium chloride, anhydrous magnesium sulfate, hydrochloric acid, bis(1,5-cyclooctadiene)nickel(0), 2, 2′-bipyridine and potassium acetate (Fujifilm Wako Pure Chemical Corp., Japan) were used as received. For all experimental works, deionized (DI) water was used.

## 2.2.2. Preparation of Monomers and Polymers

A facile synthetic procedure has been presented in this study for the synthesis of imidazolium functionalized fluorene based AEM. The synthetic strategy for polyfluorene (PF) polymers shown in Scheme 2.3.

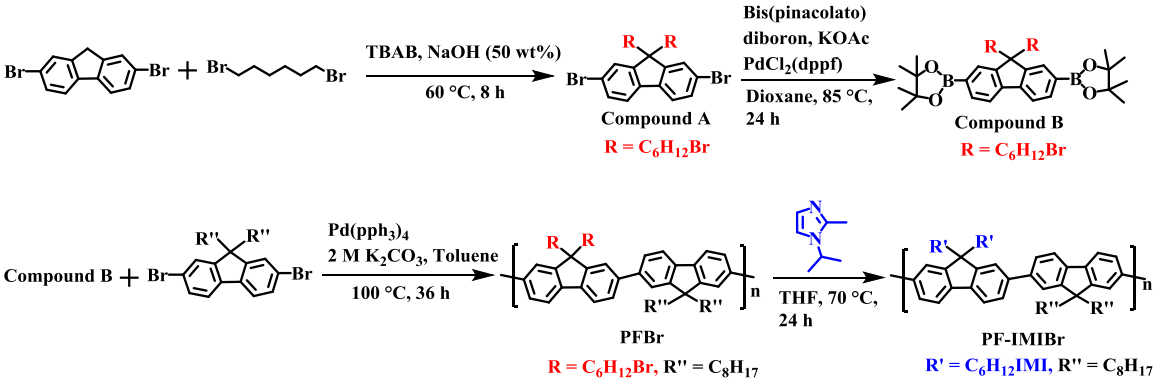


Scheme 2.3. Synthetic route of monomers and imidazolium functionalized fluorene based polymer. Red color means bromine containing alkyl side chains and blue color means imidazolium containing alkyl side chains.

### 2.2.2.1. Synthesis of 2,7-dibromo-9,9-bis(6′-bromohexyl)fluorene (Compound A)

Compound A was synthesized by following the procedure of previous literature [53]. 2,7-Dibromofluorene (5.0 g, 15 mmol) was added to a mixture of 1,6-dibromohexane (30 mL), tetrabutylammonium bromide (TBAB) (0.1 g), and sodium hydroxide (30 mL,

50 wt%) aqueous solution in a 250 mL round-bottom flask at room temperature. The reaction mixture was then stirred for 8 h at 60 °C under argon atmosphere. The mixture was diluted by dichloromethane after cooling down to room temperature. The separated organic layer was washed by using water and brine respectively and dried over anhydrous magnesium sulfate. After evaporation of dichloromethane vacuum distillation was used to remove the unreacted 1, 6-dibromohexane. The crude product was purified by silica gel column chromatography using hexane as eluent and the product obtained as a white crystal (7.57 g, 75%). $^{1}$H NMR ($CHCl_3$-$d_1$, 400 MHz) δ (ppm): 7.54−7.43 (m, 6H, Ar-*H*), 3.29 (t, 4H, C$H_2$-Br), 1.95−1.90 (m, 4H, Ar-*H*), 1.70−1.63 (m, 4H, -C$H_2$-), 1.25−1.04 (m, 8H, -C$H_2$-), 0.62-0.54 (m, 4H, -C$H_2$-).

### 2.2.2.2. Synthesis of 2,7-bis(4,4,5,5-tetramethyl-1,3,2-dioxaborolan-2-yl)-9,9-(6′-dibromohexyl)fluorene (Compound B) [54]

A reaction was set up by mixing Compound A (3.25 g, 5 mmol), bis(pinacolato)diboron (3.0 g, 12 mmol), potassium acetate (3.5 g, 35.5 mmol), $PdCl_2$(dppf) (250 mg), and 50 ml dioxane, in a 200 ml round-bottom flask. After that, freeze–pump–thaw cycles were used three times to degas the reaction mixture under argon. Then let the reaction mixture to reflux for 12 h at 85 ºC under argon. After

cooling down to room temperature, dioxane was distilled off at 45 ºC by using a rotary evaporator. To the reaction flask, water (30 ml) was added and extracted the organic mixture with 60 ml of $CH_2Cl_2$ three times. Then 40 ml of water was used to wash the $CH_2Cl_2$ layer and repeated three times. Brine and $MgSO_4$ were used to dry the $CH_2Cl_2$ layer. The crude product was purified by column chromatography using hexane and ethyl acetate (20:1) to obtain compound B (2.65 g, 71% yield) as a white solid. $^1$H NMR (400 MHz, $CDCl_3$) δ (ppm): 7.81 (d, 2H, Ar-*H*), 7.72 (d, 4H, Ar-*H*), 3.25 (t, 4H, –C*H*$_2$Br), 2.03-1.99 (m, 4H, –C*H*$_2$–), 1.65-1.58 (m, 4H, –C*H*$_2$–), 1.39 (s, 24H, –C*H*$_3$), 1.19-0.99 (m, 8H, –C*H*$_2$–), 0.58-0.51 (m, 4H, –C*H*$_2$–). m/z (SALDI-TOF) 765.25 [M + Na]$^+$.

For the synthesis of compound B, I have chosen $PdCl_2$(dppf) catalyst. The procedure for the synthesis of boronic esters is called the Miyaura borylation reaction which enables the synthesis of boron esters by cross-coupling of aryl halides with bis(pinacolato)diboron ($B_2pin_2$). The $^{11}$B-NMR analysis of the mixture KOAc and the starting material $B_2bin_2$ in DMSO-$d_6$ indicates that there is no coordination of the acetoxy anion to the boron atom [55]. However, after the oxidative addition of aryl halide (acetato)palladium(II) complex is formed which influences the transmetalation reaction rate (Fig. 2.5). The reactivity of the Pd-O bond is more than the Pd-X(X= Br, I).

Furthermore, the driving force of the transmetalation reaction step comes from the high oxophilicity of boron containing an acetato ligand. According to Miyaura *et al.* [55], $PdCl_2$(dppf) gives better results than $Pd(PPh_3)_4$ catalyst.

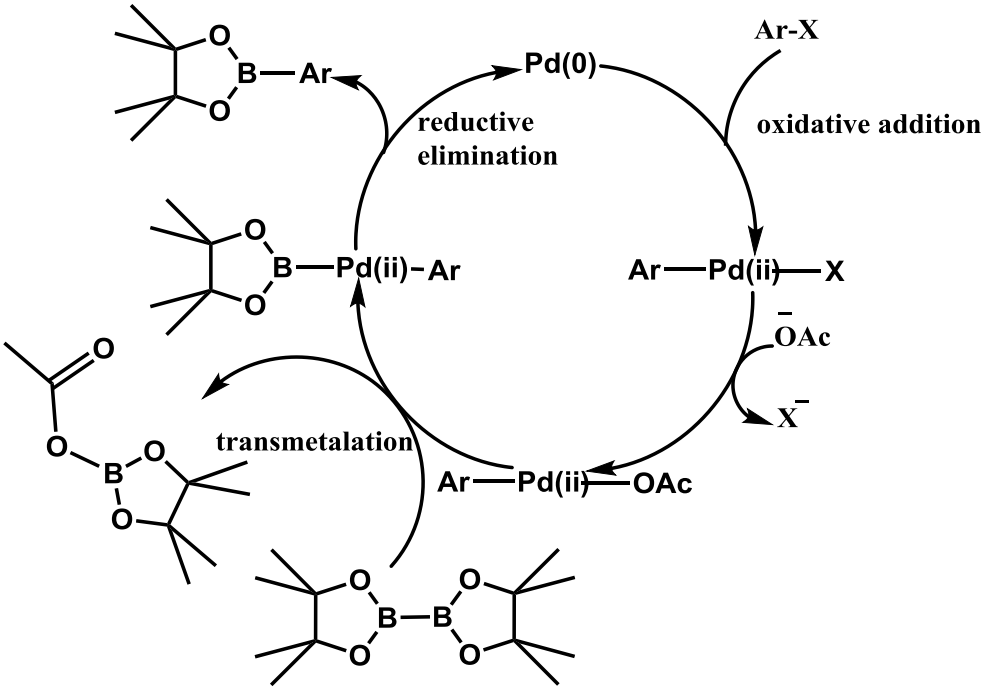


Fig. 2.5. The mechanism of the synthesis of boronic esters.

### 2.2.2.3. Synthesis of poly[(9,9-bis(6′-bromohexyl)fluorene)-co-(9,9-bis (6′-octyl)fluorene)] (PFBr)

The precursor PFBr polymer was synthesized from compound B and 2,7-dibromo-9,9-dioctyl fluorene by using Pd-catalyzed Suzuki cross-coupling reaction [14]. 2,7-Dibromo-9,9-dioctyl fluorene (274 mg, 0.50 mmol) was dissolved in 15 mL of

degassed toluene in a 100 mL three neck-flask then compound B (372 mg, 0.50 mmol) and 5 mL of 2 M $K_2CO_3$ solution was added to the flask. Then the reaction mixture was purged with argon for 30 min, after that in the reaction mixture $Pd(PPh_3)_4$ (32 mg, 0.03 mmol) was added. The reaction mixture was stirred at 100 °C for 36 h. After cooling to room temperature, the polymer was precipitated by adding to an ethanol/HCl (1:1 v/v) solution under stirring condition. A small amount of $CHCl_3$ was added to dissolve the polymer and precipitated by adding methanol and washed by acetone. The polymer was further purified by Soxhlet extraction using a mixture of methanol and hexane (1:1 v/v). Finally, the polymer was dried at room temperature in a vacuum oven and obtained as a yellow solid (400 mg, 91%). $^1$H NMR ($CDCl_3$, 400 MHz): δ (ppm) 7.79-7.30 (m, 12H, Ar-*H*), 3.25-3.20 (m, 4H, -C*H*$_2$Br), 2.06-0.75 (m, 54H, alkyl side chain H).

I also have tried to synthesize the precursor polymer PFBr by using Ni-catalyzed Yamamoto coupling according to the literature [56] (Scheme 2.4). Briefly, a 25 mL three neck round bottomed flask containing Dean–stark trap and a condenser was charged with compound A (325 mg, 0.5 mmol), 2,7-dibromo-9,9-dioctyl fluorene (274 mg, 0.5 mmol) and 2, 2′-bipyridine (364 mg, 2.33 mmol). Then 10 mL of DMAc and 5 mL of toluene were added in the reaction flask. To remove the water the reaction mixture was heated to 170 °C for 2 h under stirring condition. After the removal of

toluene and water, the reaction mixture was cooled down to 80 °C. Then bis(1,5-cyclooctadiene)nickel(0), $Ni(cod)_2$ (600 mg, 2.18 mmol) was added to the mixture. The reaction was stirred at 80 °C for 3 h. After cooled down to room temperature the reaction mixture was poured into a mixture of concentrated hydrochloric acid and methanol (1:1, v/v) solution to precipitate pale yellow powder. The pale yellow crude product was washed with concentrated hydrochloric acid and 0.2 M $K_2CO_3$. Then the product was washed with deionized water and methanol several times. Finally, the pale yellow product (350 mg, 79%) was dried at 60 °C for 12 h in a vacuum oven.

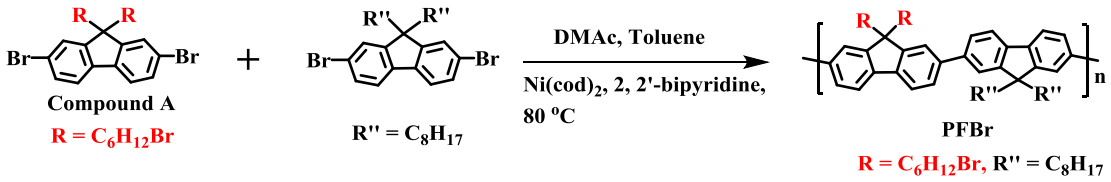


Scheme 2.4. Synthetic route of precursor PFBr polymer by Yamamoto coupling. Red color means bromine containing alkyl side chains.

### 2.2.2.4. Synthesis of 1-isopropyl-2-methylimidazole

1-Isopropyl-2-methylimidazole was synthesized by the following procedure. A mixture of 2-methylimidazole (4 g, 50 mmol), acetonitrile (40 mL) and KOH (5.62 g,

100 mmol) was stirred under argon at room temperature. Then in the reaction mixture, 2-bromopropane (5 mL, 50 mmol) was added dropwise under stirring condition. During this process, the mixture was cooled by using an ice-water bath. Then the reaction mixture was refluxed for 10 hours. When cooled down to room temperature, precipitated KBr was removed by filtration. Acetonitrile was evaporated by using a rotary evaporator. 30 mL of water and 30 mL of $CHCl_3$ were added to the flask. Then the $CHCl_3$ layer was washed by using 30 mL of water three times and dried over anhydrous $MgSO_4$. After evaporating $CHCl_3$, the obtained light yellow oil (5.04 g, 81%) was dried in vacuum for 24 h at room temperature and characterized by $^1$H NMR (400 MHz, $CDCl_3$): δ (ppm) 6.92-6.89 (dd, 2H, Ar-*H*), 4.34-4.24 (m, 1H, -C*H*$(CH_3)_2$, 2.39 (s, 3H, -C*H*$_3$), 1.41 (d, 6H, -CH(C*H*$_3$)$_2$). m/z (ESI-FT-ICR MS) 125.10 $[M + H]^+$.

### 2.2.2.5. Synthesis of new poly[(9,9-bis(6′-(1-isopropyl-2-methy limidazolium)hexyl)fluorene)-co-(9,9-bis(6′-octyl)fluorene)]bromide (PF-IMIBr)

Brominated polymer PFBr (200 mg, 0.2 mmol) was dissolved in THF (10 mL). 1-Isopropyl-2-methylimidazole (2 mL) was added and heated to 70 °C under the stirring condition and let the reaction mixture to reflux for 24 h. The solvents were evaporated

under vacuum. Then the residue was dissolved in 2 mL of MeOH and precipitated by adding in stirred diethyl ether. The resultant polymer (220 mg, 85%) was dried at room temperature under vacuum condition.

### 2.2.3. Membrane Fabrication

The membrane was fabricated by preparing a 4 wt% solution of the polymer in dimethylformamide (DMF) and followed by casting on a leveled PTFE sheet. Then the membranes were slowly dried at 60 °C for 48 h to avoid air bubbles and finally dried at 60 °C for 48 h in vacuum. About 80 μm thick thin films were obtained.

### 2.2.4. Conversion of Polymers to Hydroxide ion form

To convert the membrane in $OH^-$ ion form, the $Br^-$ ion containing membranes were immersed in argon saturated 1M NaOH solution for 48 h. This procedure was followed three times, and during the whole procedure, the NaOH solution was changed three times. After that, the membranes were soaked in argon saturated DI water for 24 h. Finally, the membranes in $OH^-$ form were thoroughly washed by degassed DI water until the pH of water becomes neutral.

## 2.2.5. Characterization and Measurements

The properties of the prepared membrane and the chemical structure of monomers, polymers were investigated using several analytical techniques.

### 2.2.5.1. NMR Spectroscopy

$^{1}H$ and $^{13}C$ NMR spectroscopies have been used to investigate the chemical structure of the synthesized monomers and polymers. The samples were measured on a Bruker Avance III 400 MHz spectrometer (Bruker Analytik GmbH).

### 2.2.5.2. FTIR Spectroscopy

Fourier-transform infrared (FTIR) spectroscopy was used to confirm the synthesis of the precursor polymer and the incorporation of the imidazolium functional group on the polymer backbone. In addition, the alkaline stability of the as-synthesized membrane was also investigated by using FTIR spectroscopy. By using Nicolet 6700 (Thermo Fisher Scientific Inc.) spectrometer the infrared (IR) attenuated total reflection (ATR) spectra were recorded in the range of 400−4000 $cm^{-1}$.

### 2.2.5.3. Mass Spectrometry

The molecular weight of the synthesized monomers was confirmed by using SALDI-TOF/TOF (Bruker) ultrafleXtreme on the $TiO_2$ surface (positive reflector mode) and ESI-FT-ICR MS (Solarix) on the magnetic field strength of 9.4 T (positive mode).

### 2.2.5.4. Gel Permeation Chromatography (GPC)

The number-averaged molecular masses (Mn), weight-average molecular weight (Mw) and the polydispersity indices (PDI, Mw/Mn) of the precursor polymer (PFBr) were evaluated by gel permeation chromatography (GPC) with Shodex KF-803, 804, and 805 columns. THF was applied as an eluent at a flow rate of 1.0 mL $min^{-1}$. Polystyrene (Mn = 1000-3.8 x $10^6$) standards were used for calibration.

### 2.2.5.5. Scanning Electron Microscope and Energy Dispersive X-ray Spectroscopy

The surface morphology and the presence of elements of the polymer were investigated by using scanning electron microscope (SEM) and energy-dispersive X-ray spectroscopy (EDX). The images were taken from TM3030Plus miniscope (Hitachi), and the accelerating voltage was 15 kV.

### 2.2.5.6. Small-angle X-ray Scattering (SAXS)

The SAXS measurement was investigated on an X-ray diffractometer (FR-E; Rigaku Corp.) using Cu Kα radiation of wavelength, λ = 1.54 Å. The beam size was approximately 300 μm × 300 μm. The camera length was 300 mm. In a glass capillary tube, a dry sample was irradiated by using the X-ray beam. For high humidity conditions, in the same glass capillary tube, water droplet and a portion of the dry sample were placed and sealed it. Two days later, the sealed capillary sample was used for SAXS measurements.

### 2.2.5.7. Transmission Electron Microscopy (TEM)

For TEM characterization, $OH^-$ form membranes, PF-IMI were first soaked in a 0.5 M $K_2[PtCl]_4$ aq. solution at 60 °C for 48 h to stain with tetrachloroplatinate ions. After staining, the membranes were rinsed several times with deionized water. The stained membranes were dried in a vacuum oven at 60 °C for 24 h. Then embedded in an epoxy resin, sliced into a 60 nm thick section with a Leica EM UC7 microtome, and placed on copper grids before investigation. A transmission electron microscope (Hitachi H-7650) was used to record the images and the accelerating voltage was 100 kV.

### 2.2.5.8. Thermogravimetric Analyzer

The thermal stability of the membrane was investigated on a thermogravimetric analyzer TG-DTA 2010 SA (NETZSCH) Japan. Under nitrogen flow, a small amount of sample was heated from room temperature to 450 °C, and the heating rate was 10 °C $min^{-1}$.

### 2.2.5.9. Differential Scanning Calorimetry

The glass transition temperature ($T_g$) was investigated by using differential scanning calorimetry on DSC 6200 (Seiko instruments) at a heating rate of 10 ºC $min^{-1}$ under $N_2$ flow from room temperature to 300 ºC.

### 2.2.5.10. Mechanical Properties

The mechanical properties of $Br^-$ ion form membrane were determined by using Autograph (Shimadzu Co., Ltd., Kyoto, Japan) with a crosshead speed of 0.5 mm $min^{-1}$ at 25 °C in water. Before measurement, membranes were immersed under ultrapure water for 24 h. Prior to the test, the membranes were cut into a dumbbell shape.

### 2.2.5.11. Water Uptake and Swelling Ratio

The membrane samples were dried in a vacuum oven at 60 ºC for 24 h and then immersed in the argon-saturated deionized water at 20 ºC, 40 ºC, 60 ºC and 80 $^{o}$C for 24 h, respectively. After taken out of the hydrated membranes from water, the surface water was wiped by a tissue paper and taken the weight immediately. The wet polymer membranes were dried at 60 °C for 24 h under vacuum. The water uptake (%) of the membranes was obtained with the following equation,

$$\text{Water uptake } (\%) = (W_{Wet} - W_{dry})/W_{dry} \times 100\% \quad (1)$$

where, $W_{wet}$ and $W_{dry}$ represent the weight of the wet and dry membranes, respectively.

The swelling ratio (%) of the membranes (1 cm in length and 0.5 cm in width) was investigated by using the linear expansion ratio (LER), determined by calculating the difference between wet and dry dimensions of a sample. The swelling ratio was calculated using the following equation,

$$\text{Swelling ratio } (\%) = (l_{wet} - l_{dry})/l_{dry} \times 100\% \quad (2)$$

where, $l_{wet}$ and $l_{dry}$ are the lengths of wet and dry membranes, respectively.

To measure the thickness change I have soaked the membranes from 20 to 80 °C for 24 h.

## 2.2.5.12. Ion Exchange Capacity (IEC)

The ion-exchange capacities (IEC) of the $OH^-$ containing membranes were measured by using the back-titration method. Samples were soaked in 50 mL of 0.01 M HCl solution for 48 h. Then the unreacted HCl was determined by titrating with a standardized 0.01 M NaOH solution in the presence of phenolphthalein indicator. The IEC value of the membranes was calculated using the following expression,

$$\text{IEC (mmol g}^{-1}) = (V_{0,NaOH}C_{NaOH} - V_{x,NaOH}C_{NaOH})/W_{dry} \qquad (3)$$

here, $V_{x,NaOH}$ and $V_{0,NaOH}$ represents the required volume of NaOH during the titration with and without membranes respectively, $C_{NaOH}$ represents the molar concentration of the NaOH, which was titrated by the standard oxalic acid solution, and $W_{dry}$ is the mass of the dry membranes. Two samples were used for determining the IEC and for each sample, three replicates were conducted.

## 2.2.5.13. Hydroxide Ion Conductivity

The in-plane hydroxide conductivity of the membranes (approximate size: 2 cm x 1.2 cm) was measured by using an impedance analyzer and dielectric interface system (SI1260 and SI1296; Solartron Analytical). The frequency range between 10 MHz and 1 Hz with an amplitude of 50 mV was used to collect the impedance data of membranes

and a four-point probe alternating current (ac) system was used. To control the temperature in the range of 20 – 80 °C, a chamber (SH-221; Espec Corp.) was used. The conductivity of the membrane was measured in a homemade chamber, which was filled with argon-saturated deionized water. During the measurement, all the membranes were equilibrated for 30 min at a given temperature. The hydroxide conductivity σ of a membrane was calculated from the following equation,

$$\sigma(S\ cm^{-1}) = L/(RA) \qquad (4)$$

where L is the inner distance (1 cm) between two Pt electrodes, A is the cross-sectional area ($cm^2$) (membrane thickness x width) (80 μm x 1.2 cm) and R (Ω) is the resistance value of the membrane.

## 2.2.5.14. Alkaline Stability of the Membrane

To investigate the alkaline stability of the polymer membranes, the membranes were soaked in argon-saturated 1 M NaOH (aq.) solution at both room temperature (RT) and 80 °C. The degradation of polymer samples was examined by the changes of FT-IR spectra and by using reported degradation mechanism [57]. I could not measure the degradation of polymers by using $^1$H NMR as the $OH^-$ containing polymers were not soluble in NMR solvents such as DMSO, $CH_3OH$, $H_2O$, and $CHCl_3$. To convert $Cl^-$ ion

form AEMs, the membranes were immersed in 1 M NaCl solution at 60 $^{o}$C under stirring for 48 h. During this time the NaCl solution was exchanged three times with fresh solution. To remove the residual NaCl salt the membranes were washed several times and stored in DI water for 24 h under stirring condition. Then the membranes were dried at 60 $^{o}$C for 24 h.

## 2.3. Results and Discussion

### 2.3.1. Synthesis and Characterization of Monomers and Polymers

Compound A was successfully synthesized by the reaction between 2,7-dibromofluorene and 1,6-dibromohexane shown in Scheme 2.3. The chemical structure was investigated by $^{1}H$ and $^{13}C$ NMR spectra (Fig. 2.6 and 2.7). The triplet peak at 3.29 ppm indicated the presence of bromine-containing terminal methylene groups. The five multiplets from 1.95 to 0.54 ppm confirmed the grafting of long hexyl chain on the C9 position of fluorene ring. The peaks from 7.54 to 7.43 ppm corresponded to the aromatic protons of the fluorenyl group. The $^{13}C$ NMR spectrum also confirmed the structure of compound A.

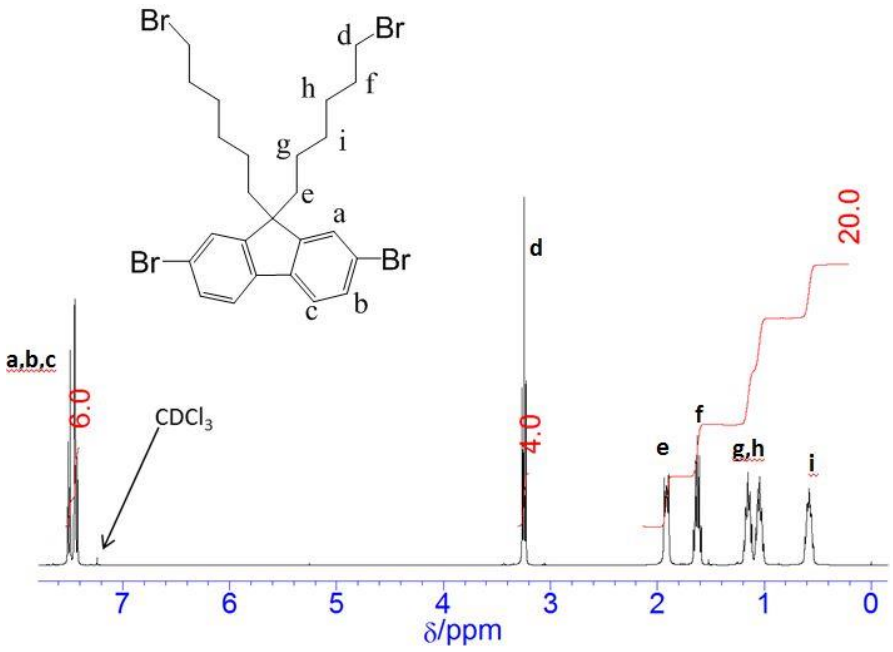


Fig. 2.6. $^{1}$H NMR spectrum of 2,7-dibromo-9,9-bis(6′-bromohexyl) fluorene (Compound A).

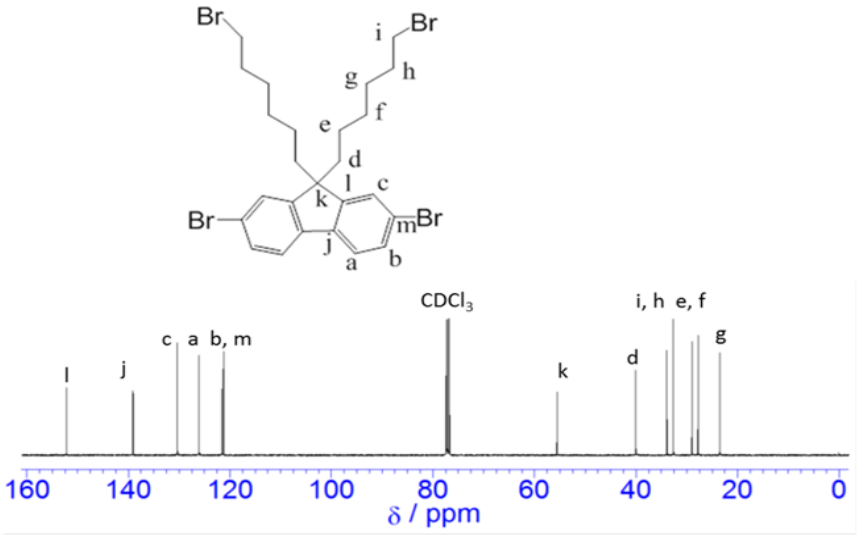


Fig. 2.7. $^{13}$C NMR of 2,7-dibromo-9,9-bis(6′-bromohexyl)fluorene (Compound A).

By using $^{1}H$ NMR spectroscopy the chemical structure of Compound B was characterized (Fig. 2.8). The appearance of a peak at 1.39 ppm confirmed the successful incorporation of 4,4,5,5-tetramethyl-1,3,2-dioxaborolane group. The product was further confirmed by SALDI-TOF mass spectrum shown in Fig. 2.9. The calculated m/z of $[M+Na]^{+}$ is 765.25 and I found 765.56. However, after investigation of the mass spectrum, I observed the product contains compound B and boronic acid form of compound B.

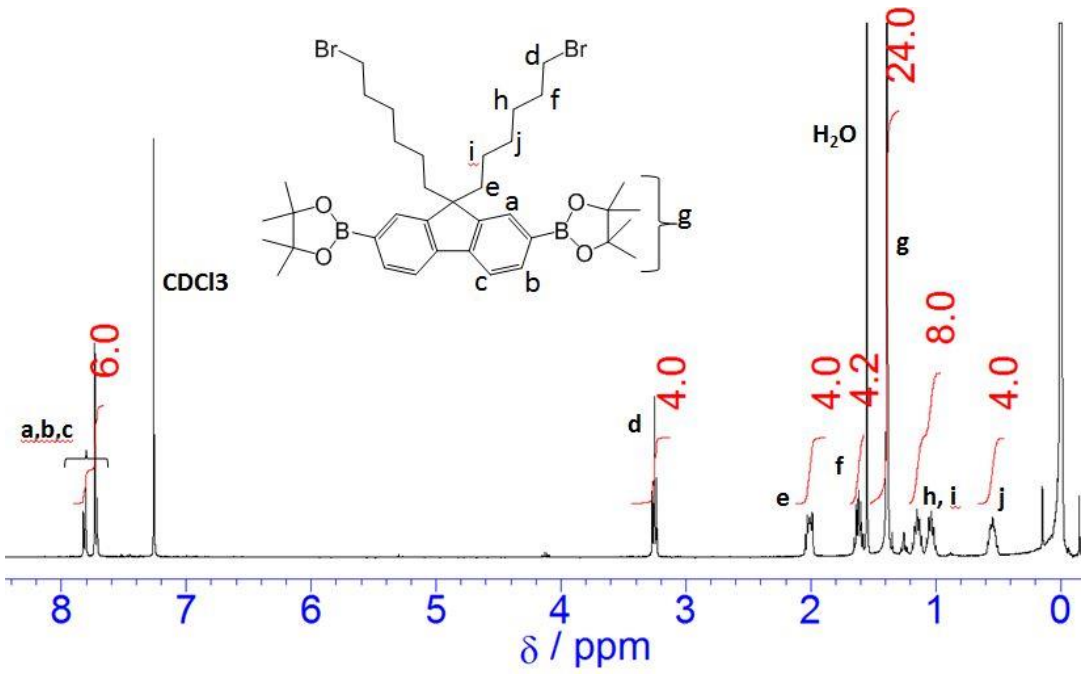


Fig. 2.8. $^{1}H$ NMR spectrum of 2,7-bis(4,4,5,5-tetramethyl-1,3,2-dioxaborolan-2-yl) -9,9-bis(6′-bromohexyl)fluorene (Compound B).

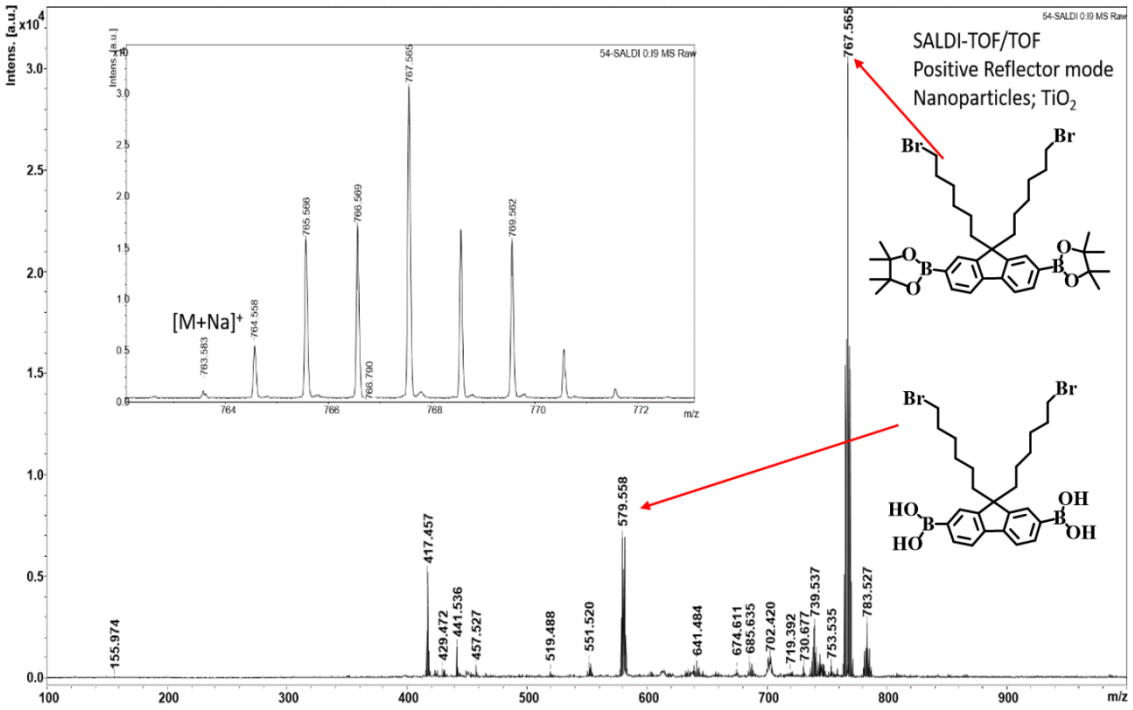


Fig. 2.9. Mass spectrum of 2,7-bis(4,4,5,5-tetramethyl-1,3,2-dioxaborolan-2-yl) -9,9-bis(6′-bromohexyl)fluorene (Compound B).

To use 1-isopropyl-2-methylimidazolium as a functional group in the polymer, I have synthesized this group from 2-methylimidazole and 2-bromopropane. In the $^{1}H$ NMR spectrum, two doublet peaks appeared at 6.92 and 6.89 ppm (Fig. 2.10) for aromatic hydrogens. The septet peak located at 4.34-4.24 ppm confirmed the attachment of the isopropyl group. The methyl protons of the C2 position showed a peak at 2.39 ppm. The $^{13}C$ NMR spectrum also confirmed the chemical structure of 1-isopropyl-2-methylimidazole (Fig. 2.11). The structure further confirmed by

ESI-FT-ICRMS mass spectrum, where m/Z found 125.10 for $(M+H)^+$.

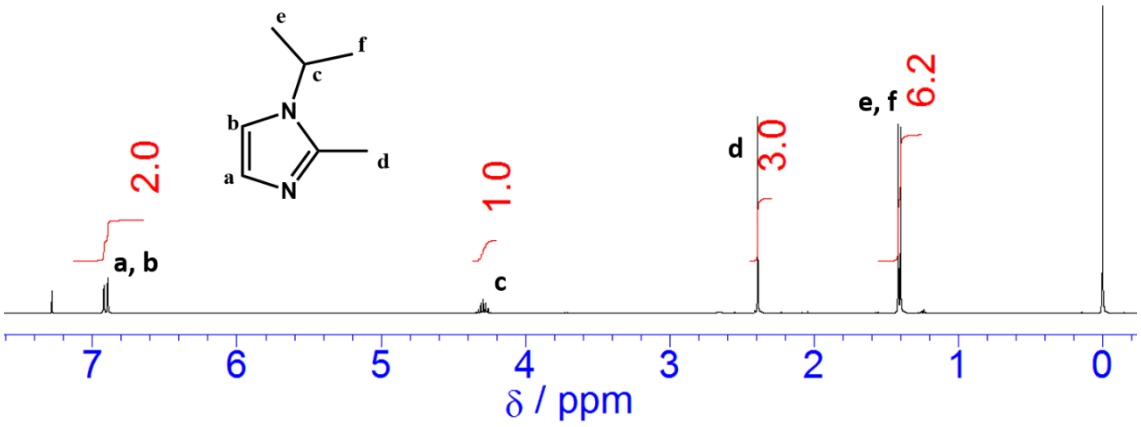


Fig. 2.10. $^{1}$H NMR spectrum of 1-isopropyl-2-methylimidazole.

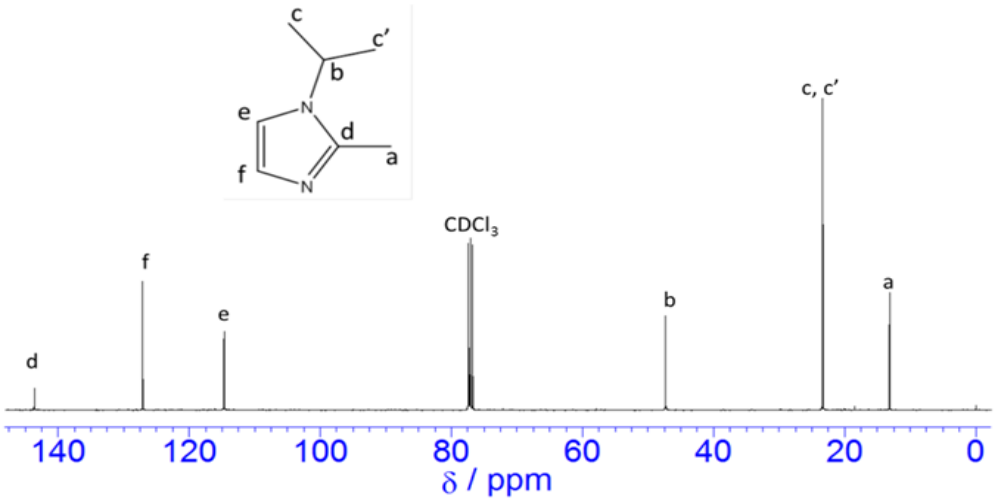


Fig. 2.11. $^{13}$C NMR spectrum of 1-isopropyl-2-methylimidazole.

The chemical structure of the synthesized precursor PFBr was analyzed by $^{1}$H NMR spectroscopy (Fig. 2.12A). The aromatic peaks appeared at 7.79-7.30 ppm, and the multiplet from 3.25 to 3.20 ppm corresponds to methylene protons containing the bromine group. The peaks at 2.06-0.75 ppm can be assigned to alkyl side chain protons. The integral ratio and peak position confirm that the polymerization reaction was successful. The precursor PFBr polymer was soluble in tetrahydrofuran (THF) and chloroform. The weight average molecular weight ($M_w$), number average molecular weight (Mn) and polydispersity index (PDI) of PFBr were determined with GPC using THF eluent and found to be $2.4 \times 10^4$ g mol$^{-1}$, $9.0 \times 10^3$ g mol$^{-1}$ and 2.8 respectively.

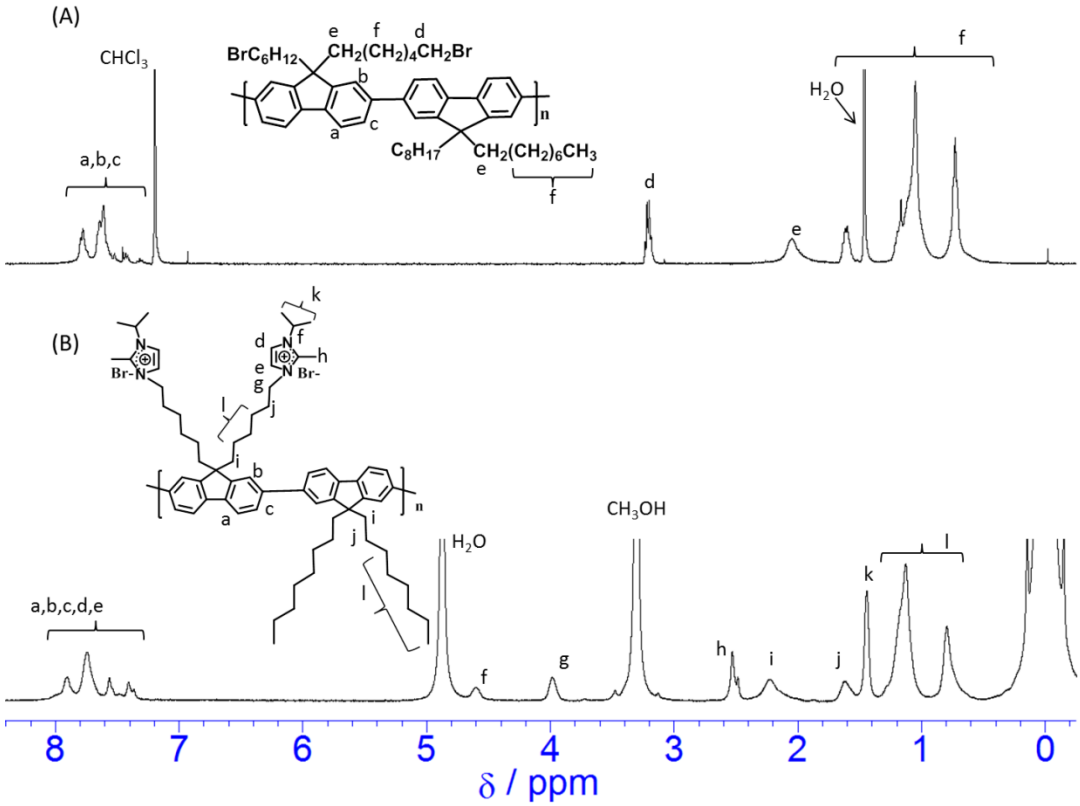


Fig. 2.12. $^{1}$H NMR spectra of (A) PFBr and (B) PF-IMIBr.

By using Ni catalyzed Yamamoto coupling reaction I did not get the expected precursor polymer, PFBr. The peak position, peak shape, and integral ratio did not match with the synthesized polymer by using the Suzuki coupling reaction. The appearance of new peaks at 7.00 ppm, 5.60 ppm, 4.80 ppm, 2.50 ppm and the absence of a peak at 3.20 ppm due to -C*H*$_2$Br indicates aryl–aryl bond was not formed successfully (Fig. 2.13). I think to synthesize PFBr, Pd catalyzed Suzuki coupling reaction is better than Ni catalyzed Yamamoto coupling.

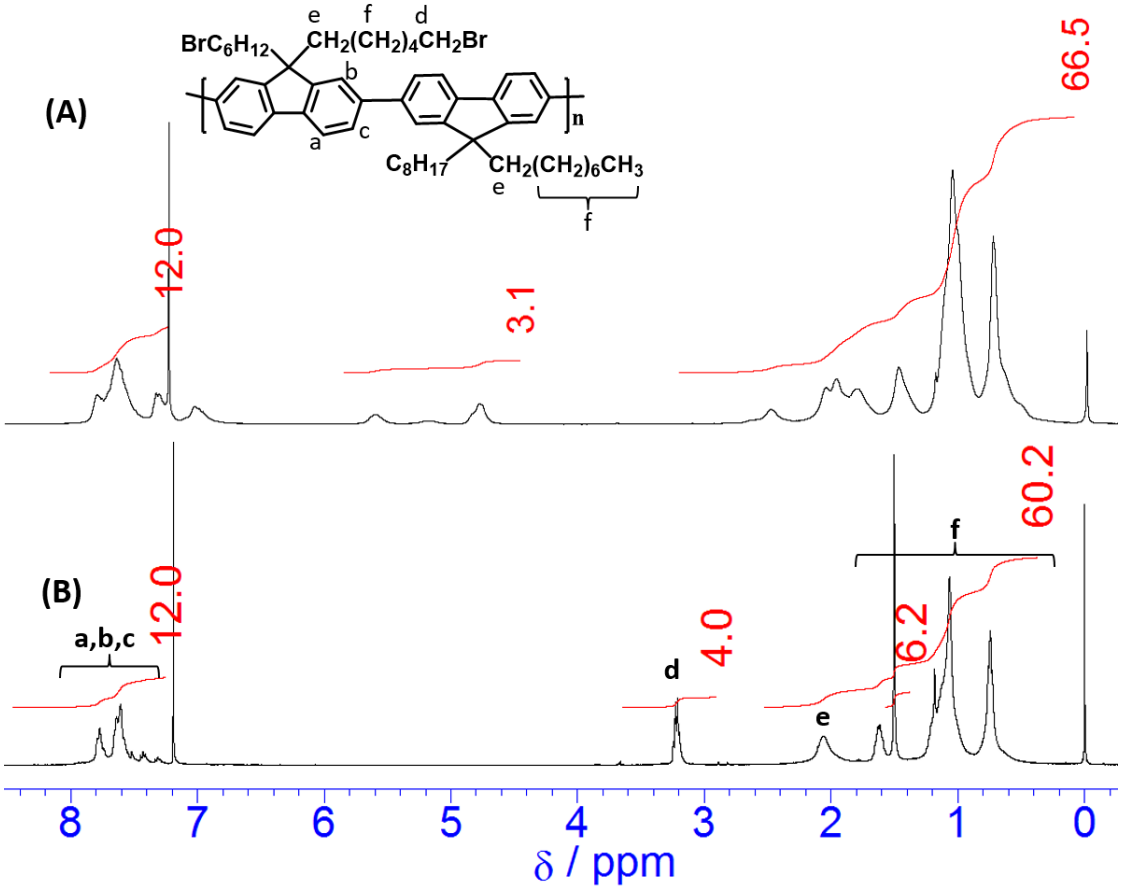


Fig. 2.13. $^{1}$H NMR spectra of PFBr polymer synthesized by (A) Yamamoto coupling and (B) Suzuki coupling.

I have newly synthesized PF-IMIBr, a fluorene based polymer, which has imidazolium groups on the long alkyl side chains by the reaction between PFBr and 1-isopropyl-2-methylimidazole (Scheme 2.3). Fig. 2.12B shows the $^{1}H$ NMR spectrum of imidazolium functionalized $Br^-$ form polymer, PF-IMIBr. The new peaks at 7.55 ppm and 7.39 ppm belong to two aryl protons of the imidazolium group, the peaks at 4.6 ppm, 2.53 ppm, and 1.45 ppm attribute the isopropyl and methyl protons of imidazolium cationic group. All the new peaks indicate the successful incorporation of imidazolium groups. The polymer PF-IMIBr was soluble in organic solvents, for example, DMF, $CH_3OH$, and DMSO but was not soluble in $H_2O$.

The chemical structure of copolymer was further studied by using the FT-IR spectrum. The FT-IR spectra of the resultant polyfluorene copolymer PFBr and PF-IMIBr are shown in Fig. 2.14. The C-H absorption bands of both polymers for methylene ($-CH_2$) were observed at 2853 and 2927 $cm^{-1}$ for symmetric and asymmetric vibrations respectively. The presence of polyphenylene was confirmed by the absorption bands at 1603 and 1458 $cm^{-1}$. The peaks around 1578 $cm^{-1}$ and 1522 $cm^{-1}$ in PF-IMIBr polymer were attributed to the stretching vibration of C=N, and an absorption band at 1181 $cm^{-1}$ was observed for the C-N bond of imidazolium group. The results confirmed that the incorporation of imidazolium cation onto the polymer was successful. Furthermore, a

strong and broad band at 3400 $cm^{-1}$ appeared in imidazolium functionalized polymer which was attributed as the stretching vibration of O-H bonds of water. The improved hydrophilic property of PF-IMIBr polymer also confirmed the successful attachment of imidazolium groups on the polymer.

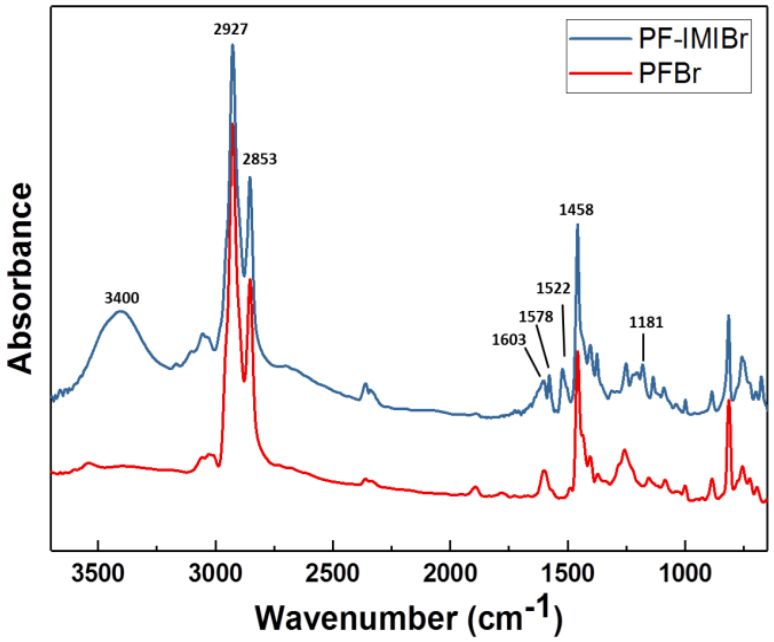


Fig. 2.14. FT-IR spectra of PFBr and PF-IMIBr.

The EDX spectra before and after ion exchange of $Br^-$ form to $OH^-$ form as shown in Fig. 2.15A to Fig. 2.15B confirms that more than 91% $Br^-$ ions have been exchanged by $OH^-$. The remaining Br may be comes from the terminal group of the polymer. Zhuo *et al.* [58] also found bromine elements of AEMs were declined or almost disappeared after alkalization by using KOH aqueous solution from EDX spectra. The EDX spectra

further confirmed the sufficient conversion of alkyl Br groups and successful alkalization.

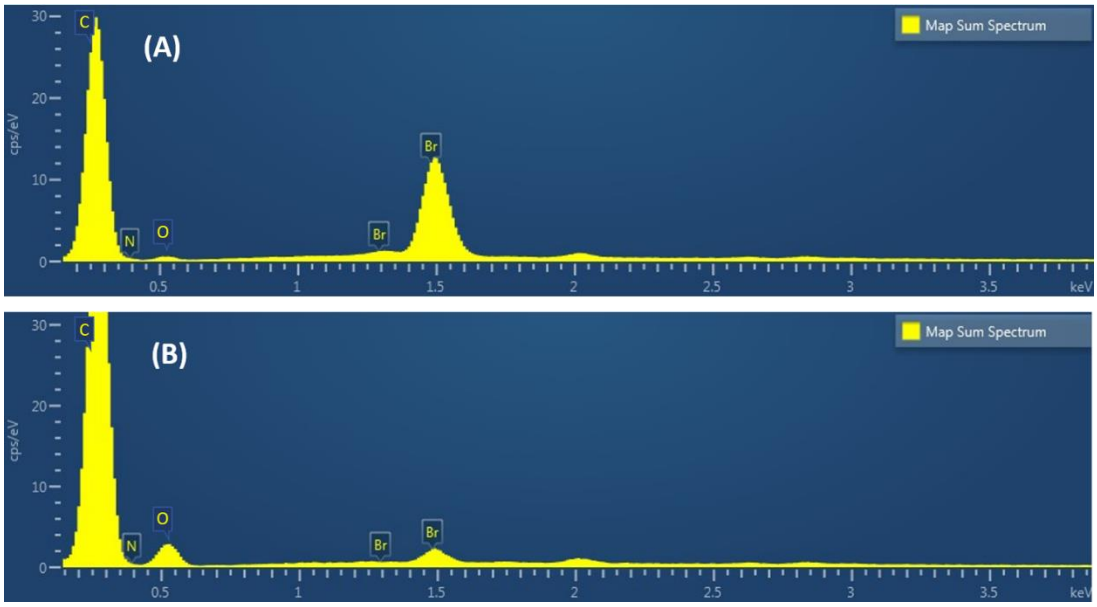


Fig. 2.15. EDX spectra for (A) PF-IMIBr and (B) PF-IMI membranes.

## 2.3.2. Membrane Morphology

Membranes were fabricated from 4 wt% solutions in DMF and casted on a flat PTFE sheet. After removing the solvent, the resultant membranes become transparent as shown in Fig. 2.16A. By using SEM, the morphology of the PF-IMIBr membrane was investigated. As shown in Fig. 2.16B and 2.16C, the SEM images showed that the surface and cross-section of the resultant polymer membranes are uniform, tight and dense and no pores are visible on this scale.

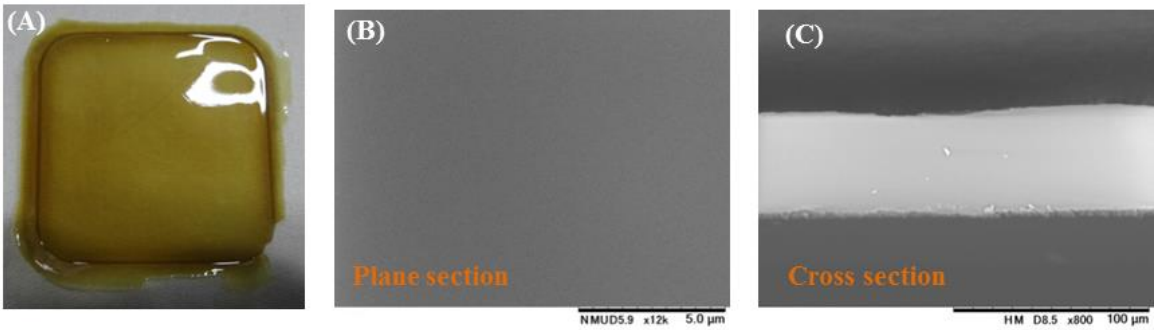


Fig. 2.16. (A) Photograph of the membrane, SEM images of the PF-IMIBr: (B) plane section and (C) cross section of the polymer.

I have tried small angle X-ray scattering (SAXS) measurements to clarify the surface morphology of the membrane in the dry condition. I also checked the SAXS profiles in both humidified, in-water and humidified at 80 °C conditions. Unfortunately, I could not observe any scattering peak for the ionic domain in PF-IMIBr AEM as shown in Fig. 2.17. Other literature suggests that imidazolium containing membranes sometimes show no apparent (or very weak, if any) scattering peak [59, 60].

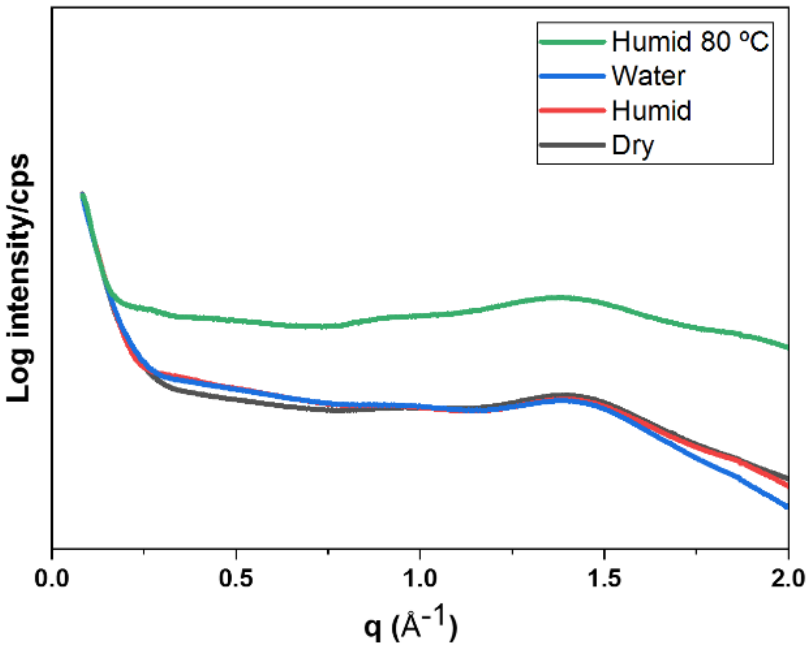


Fig. 2.17. The SAXS profile of PF-IMIBr.

The cross-sectional TEM image of PF-IMI was observed after stained with tetrachloroplatinate ion as shown in Fig. 2.18. The hydrophilic domains are represented by the dark areas whereas the hydrophobic domains are represented by bright areas. In PF-IMI, the domain size of hydrophilic groups is not clear (< 1 nm) which is compatible with the SAXS result as no scattering peak was observed.

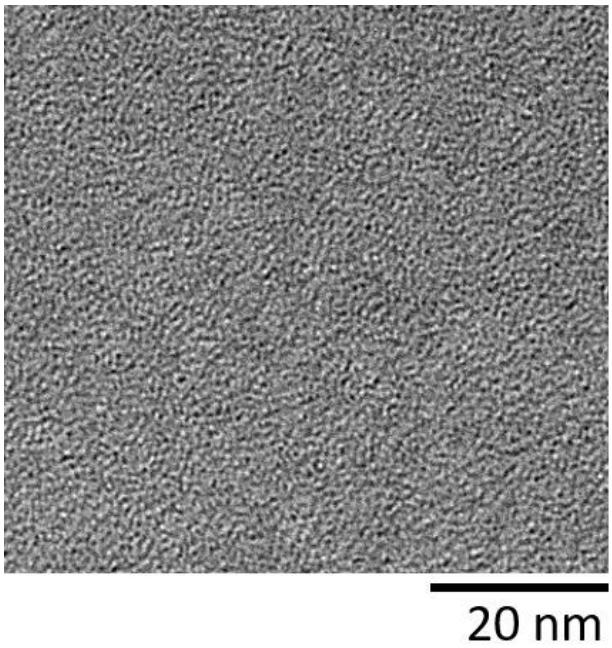


Fig. 2.18. The cross-sectional TEM image of the PF-IMI membrane.

### 2.3.3. Thermal Stability

The thermal stability is a primary concern for AEMs since some AEMs containing benzyl quaternary ammonium cationic groups usually show the instability of cationic groups above 120 ºC [61]. As aromatic polymers have outstanding thermal stability, therefore aromatic backbones are the preferred candidates for application in high temperature AEMFCs. Fig. 2.19 shows the result of the thermogravimetric analysis. The first weight loss below 200 $^{o}$C has less than 4 wt%. This weight loss originates from the evaporation of adsorbed water in the membrane. From the calculation of weight percentage, the second weight loss around 10% between 200 °C and 300 °C is due to

the degradation of the isopropyl groups of the imidazolium cations. The third degradation at temperatures above 390 °C might be due to the decomposition of the polyfluorene backbones. The thermal stability of long alkyl tethered imidazolium cationic groups in this study is much higher than that of the benzyl substituted quaternary ammonium groups. The result showed that the thermal stability of the synthesized AEM is comparable to the reported imidazolium containing AEM [53] and long alkyl-tethered QA containing polyfluorene backbone [14].

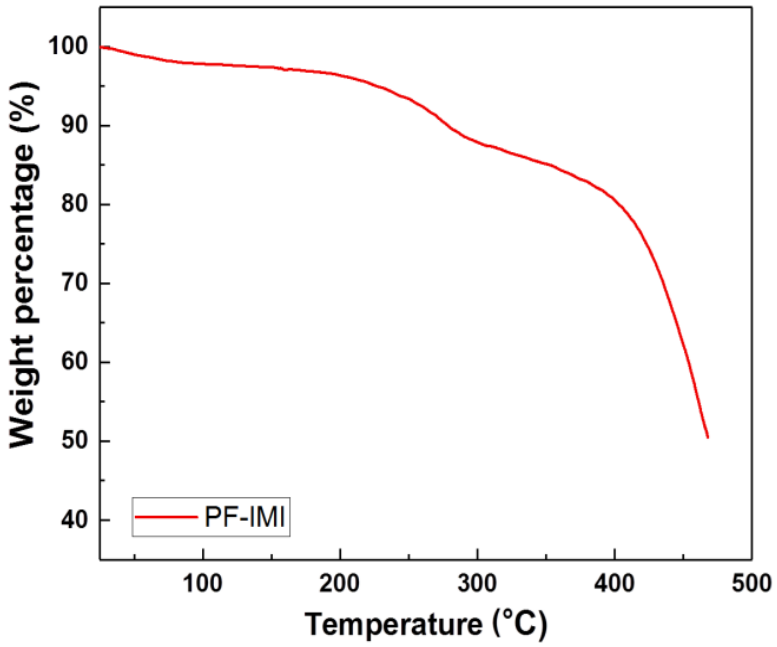


Fig. 2.19. TGA graph of PF-IMI under $N_2$ flow. Heating rate: 10 $^oC$ $min^{-1}$.

The overall result of thermal analysis implies that the resultant polyfluorene polymer maintains high thermal stability up to 200 $^oC$, which is far beyond the desired

temperature range for fuel cell applications.

## 2.3.4. DSC Result of PF-IMI Polymer

To understand the thermal behavior of $OH^-$ containing polymer (PF-IMI), DSC was also tried as shown in Fig. 2.20. The DSC curve analysis showed that glass transition temperature (Tg) of the polymer found near about 250 ºC. And no clear thermal change was observed until 220 ºC. This thermal stability may be due to the rigid backbone of the polymer, and molecular segments hindered movement.

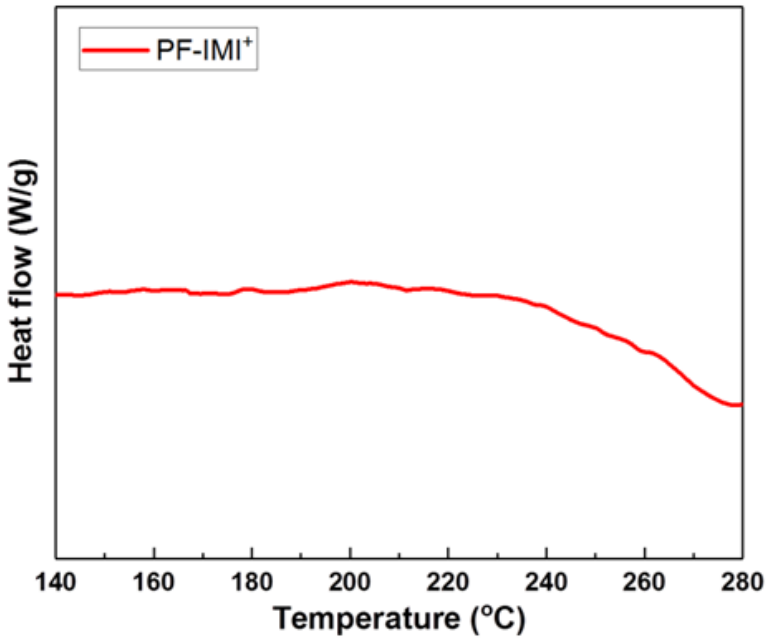


Fig. 2.20. DSC result of PF-IMI polymer under $N_2$ flow at a heating rate of 10 ºC $min^{-1}$.

## 2.3.5. Mechanical properties

In a fully hydrated state, the tensile strength of PF-IMIBr polymer was observed as

12.3 MPa with an elongation at break of 4.2%. The Young′s modulus was found to be 362 MPa.

### 2.3.6. Water Uptake (WU), Swelling Ratio (SR) and Ion Exchange Capacity (IEC)

The water uptake plays an important role in ion conductivity. The swelling behavior of membranes is a critical factor that influences the morphologic stability and mechanical properties of membranes. Excessive WU may lead to mechanical weakness and over swelling. Commonly, with increasing ion exchange capacity (IEC) the WU and swelling ratio also increase. The IEC of membranes is responsible for ion transfer and hence influences the ion conductivity. The IEC of the synthesized membrane was measured by the back titration method and found to be 1.84 mmol/g. The experimental IEC shows good agreement with the calculated value of 1.99 mmol/g. Water uptake of the membranes increased from 19 to 32 wt% with increasing temperature from 20 $^{o}$C to 80 $^{o}$C (Fig. 2.21). This is because at high temperatures, the mobility of the polymer molecules is enhanced and higher free volume as the opening of the micropores increased. As a result, hydrated ion clusters are formed which lead to increase the water adsorption [62, 63]. With increasing the temperature from 20 $^{o}$C to 80 $^{o}$C the swelling ratio of the synthesized membrane increased from 1 to 7%. With increasing the

temperature, the thickness of the wet PF-IMI membranes was not increased.

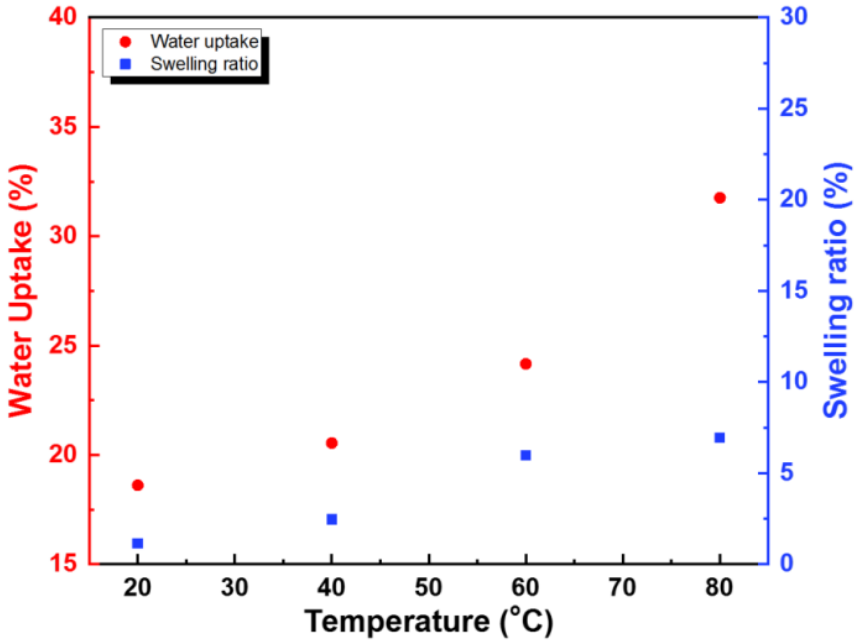


Fig. 2.21. Water uptake and swelling ratio of the PF-IMI membrane.

The water uptake and degrees of swelling of the resultant polymer are lower compared to other reported aromatic AEMs e.g., polyarylene ether sulfones [64] and quaternized polyarylene ether ketones [65] with the similar IEC values. The stiff aromatic backbone of the membrane and the absence of flexible groups (such as thioether or ether bonds) could suppress the water uptake. Therefore, the good dimensional stability of the membrane can be expected as a feasible approach for AEMFCs application.

## 2.3.7. Hydroxide Ion Conductivity and Activation Energy

In the fuel cell performance, the $OH^-$ ion conductivity of the polymeric membranes plays an important role. The IEC values of the AEMs significantly influence the ionic conductivity since IEC expresses the capacity for ion exchangeable functional groups.

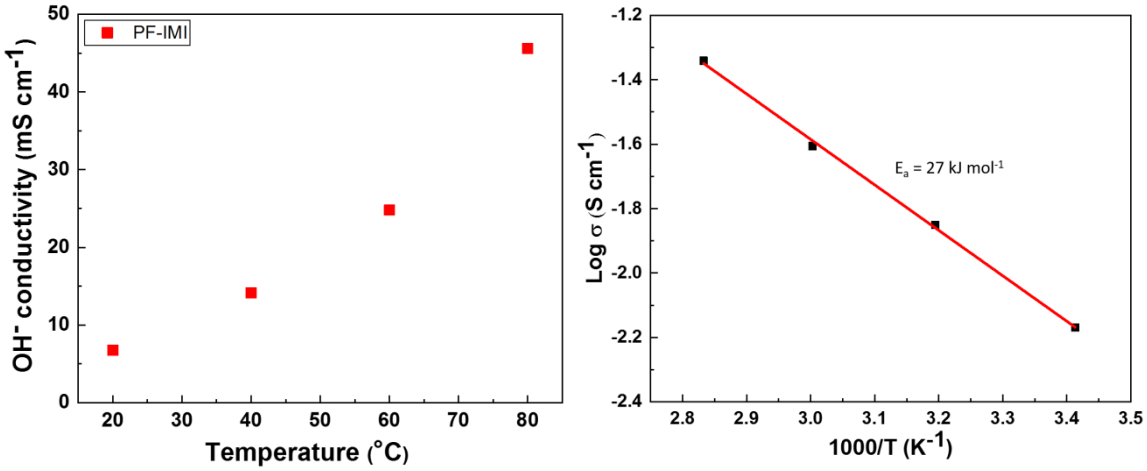


Fig. 2.22. (A) Temperature dependence of the $OH^-$ conductivity and (B) temperature dependence of log (hydroxide conductivity) plots of PF-IMI polymer for estimating activation energy.

The hydrophilic properties are improved with increasing the IEC values of the membranes [15, 66]. As the membranes become more hydrophilic therefore adsorbs more water, which facilitates ionic conduction. The polyfluorene polymeric membrane showed hydroxide conductivity of 7 mS $cm^{-1}$ at 20 $^oC$ and increased to 46 mS $cm^{-1}$ at 80 $^oC$ shown in Fig. 2.22A. The conductivity of AEMs increases with increasing

temperature because of faster ionic migration and higher water molecule diffusion. Simultaneously, at the higher temperature, the flexibility of the polymer chains increases and membrane adsorbs more water, resulting in more water swollen membranes and wider ion-conducting channels, leading to more enhanced ion transfer [34, 38]. The conductivity of the resultant AEM is comparable to the hydroxide conductivity of other membranes with similar IEC values [67, 68].

From the Arrhenius plot of conductivity–temperature relationship, the activation energy ($E_a$) of the hydroxide conduction was determined from Fig. 2.22B. The plots showed that the hydroxide conductivity of the polymer followed the Arrhenius behavior in the temperature range of 20 – 80 $^{o}$C. The activation energy of polyfluorene polymer PF-IMI is 27 kJ mol$^{-1}$ which is comparable with some reported AEMs [69, 70].

For more understanding of the performance of the polyfluorene polymer, the IEC, WU, and hydroxide conductivity are summarized with some reported imidazolium functionalized AEMs such as polyarylene ether ketones (MIPAEKs) [67, 68], polyarylene ether sulfones [60, 71-73], polyarylene ethers [74], PPO [75], and cross linked [38, 69] AEMs with similar IEC values, shown in Table 2.2. The presence of water in AEMs is critical for hydroxide conductivity, but dimensional instability may cause by excessive water uptake. Due to the rigid backbone of the polyfluorene polymer

of this study and without flexible thioether or ether bonds, the water uptake is low compared to other AEMs. The hydroxide conductivity of the synthesized AEM is comparable with the presented AEMs but less than ImPES-0.45 and trimPES-0.4 with multiimidazolium, PP-60, [PVMIm][OH]$_{40}$-DVB$_4$ and ANM-22-100 with higher water uptake.

Table 2.2. Comparison of IEC, WU, and hydroxide conductivity of PF-IMI with some representative AEMs at 80 $^{o}$C.

| Membrane (Ref) | IEC (mmol g$^{-1}$) Cal.[a] | Exp.[b] | WU (wt%) | $\sigma_{OH^-}$ (mS cm$^{-1}$) |
|---|---|---|---|---|
| PF-IMI (This work) | 1.99 | 1.84 | 32.0 | 46 |
| MIPAEK-b [67] | | 1.97 | 70.5 | 35 |
| MIPAEK-c [67] | | 2.57 | 84.0 | 39 |
| MIPAEK-SF-c [67] | | 1.81 | 73.7 | 30 |
| MIPAEK-SF-d [67] | | 1.89 | 82.8 | 33 |
| CL-8C/PAEK/UnIm0.2MeIm0.8 [68] | 2.82 | 1.91 | 51.7 | 40 |
| PP-60 [69] | 2.63 | 1.98 | 36.6 (60 °C) | 60 |
| C-FPAEO-75-MIM [74] | | 1.80 | 76 (60 °C) | 36 |
| ImPES-0.45 [71] | 1.95 | 1.84 | 57.3 (60 °C) | 112 |
| trimPES-0.4 [60] | 2.34 | 2.03 | 62.0 (60 °C) | 120 |
| [PVMIm][OH]$_{40}$-DVB$_4$ [38] | 1.60 | 1.47 | 157[c] | 53.5 (60 °C) |
| [PUVBIm][OH] [72] | 1.80 | 1.65 | | 40 |
| PSf-ImmOH-70 [73] | 2.06 | 1.94 | 129 (60 °C) | 26 (60 °C) |
| ANM-22-100 [75] | 1.82 | 1.67 | 22 (30 °C) | 78 (60 °C) |

[a]Calculated from chemical structure. [b]Experimental value obtained by titration.

## 2.3.8. Alkaline Stability

### 2.3.8.1. Alkaline Stability at 80 °C

One of the major challenges of AEMs for practical application is the thermochemical stability, particularly in the high-temperature operation of alkaline fuel cells. The $OH^-$ form membranes were soaked in 1M NaOH solution at 80 $^oC$ for 168 h and 360 h to examine the chemical stability. The changes in the chemical structure of AEMs were investigated by FT-IR spectra. I also have tried to analyze the degradation of polymer membranes by using the $^1H$ NMR spectrum. Unfortunately, the $OH^-$ containing polymers were not soluble in $^1H$ NMR solvents such as DMSO, $CH_3OH$, $H_2O$, and $CHCl_3$. To investigate the $^1H$ NMR spectrum I also have converted the membranes in $Cl^-$ form but I could not dissolve the membranes in NMR solvents even under heating. The tested membranes retained the membrane shape and there were no visible changes after alkaline treatment. Bae *et al.* [14] reported a similar type of polyfluorene backbone where they didn′t observe any degradation of the main chain from the $^1H$ NMR spectra after the alkaline test for 30 days at 80 °C. Fig. 2.23 shows the time dependence of the FT-IR spectra of the PF-IMI ($OH^-$ form) membrane after the alkaline treatment at 80 °C. After the alkaline test, the absorbance of the conjugated C=N band at 1576 and 1518 $cm^{-1}$ significantly reduced with the treatment time. This indicates that imidazolium

cation degraded by the attack of $OH^-$ at the C2 position of the imidazolium ring as shown in Scheme 2.5. By the addition of $OH^-$ on the imidazolium ring, a nonaromatic intermediate structure is generated. As this produced transition state structure is unstable, finally aldehyde/keto group containing product is irreversibly formed and hence stimulates the decomposition of imidazolium containing AEMs [76]. Ye *et al.* [77] observed an aldehyde group in their $^1H$ NMR results due to the degradation of imidazolium cation. The possible mechanism of degradation for the imidazolium group is shown in Scheme 2.5.

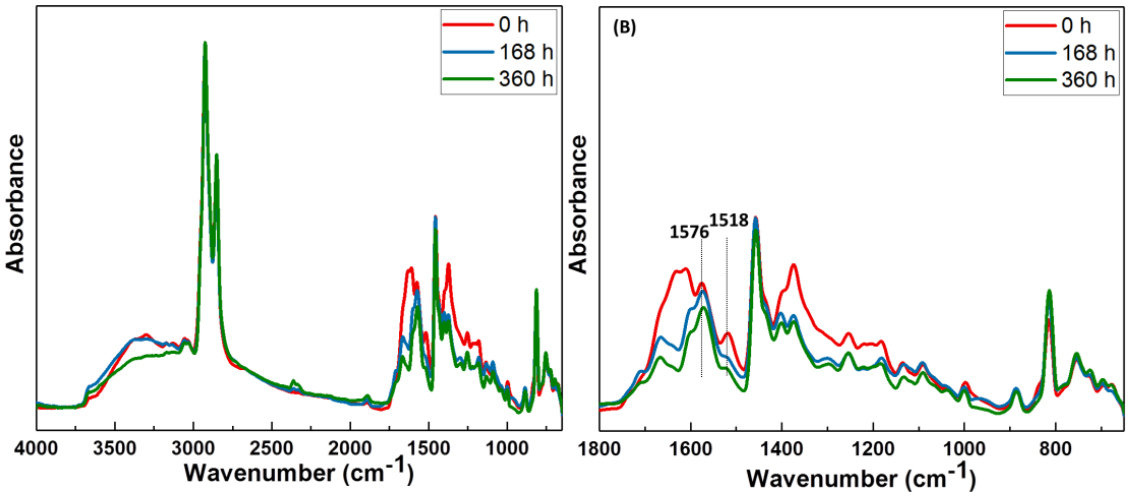


Fig. 2.23. (A) FT-IR spectra of PF-IMI ($OH^-$ form) membrane and $OH^-$ form after alkaline stability test. (B) close-up of the region from 1800 to 650 $cm^{-1}$ to show the changes in peak intensity.

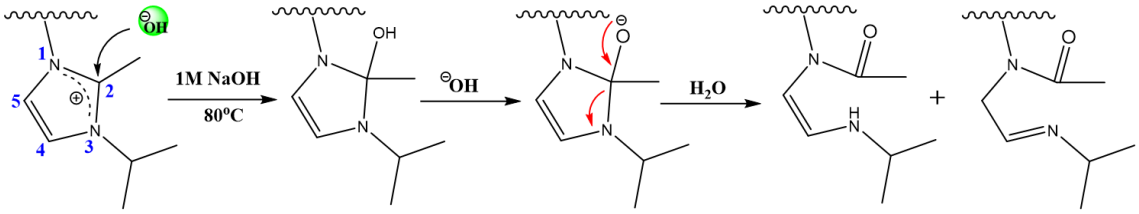


Scheme 2.5. Possible degradation mechanism of the 1-isopropyl-2-methylimidazolium cation in high alkaline condition.

The absorption band of O-H stretching vibrations of water at 3400 $cm^{-1}$ reduced after alkaline treatment. This can be related to the decrease of hydrophilic imidazolium cationic groups. As I have observed the degradation of imidazolium groups at 80 °C, I also investigated the degradation at room temperature (RT). Moreover, surprisingly I have found imidazolium cationic groups also degraded at RT.

### 2.3.8.2. Alkaline Stability at Room Temperature (RT)

Imidazolium containing membranes are proposed to degrade by the ring opening reaction of cationic groups by the attack of $OH^-$ ions in alkaline medium [77, 78]. To investigate the RT alkaline stability, I have soaked the $Br^-$ ion containing membranes (PF-IMIBr) in 1 M NaOH solution for 144 h, 192 h, 240 h, 288 h, and 360 h. During this process, I have exchanged the NaOH solution every two days with fresh solution. I investigated the time dependent changes of chemical structure by FT-IR spectra. Fig.

2.24A shows the time dependence of FT-IR spectra. I have observed that the peak intensity at 1518 and 1576 $cm^{-1}$ for conjugated C=N bond significantly reduced with time, as shown in Fig. 2.24B. This reduced intensity indicates the imidazolium cationic group was degraded at room temperature by the attack of $OH^-$ ion. The reduction of absorption band with time in alkaline solutions at 3400 $cm^{-1}$ due to O-H stretching vibrations of water may be related to the degradation of hydrophilic imidazolium cationic groups.

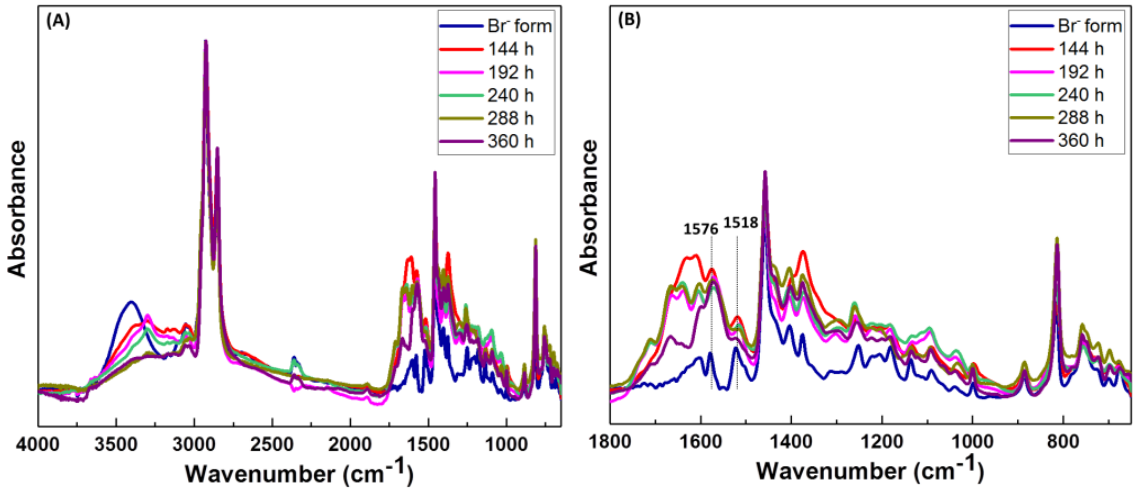


Fig. 2.24. Comparison of FT-IR spectra of PF-IMI polymer (A) before and after soaking in 1 M NaOH solution at room temperature (B) close-up of the region from 1800 to 650 $cm^{-1}$ to show the changes of peak intensity.

Although some literature [37, 45, 53, 79] has suggested the high chemical stability of imidazolium cationic groups; however, some other reports [13, 16, 80] have revealed

that in high alkaline conditions, the imidazolium cations are less stable. I also observed the degradation of the imidazolium cationic group even at room temperature. Despite high LUMO energies imidazolium groups degraded in alkaline condition. According to Yamaguchi *et al.* [81], the LUMO orbital of the imidazolium group is π-type and the HOMO orbital of $OH^-$ ion is also π-type. The interaction and overlapping of imidazolium and $OH^-$ ion π-π orbitals is larger than σ-π orbitals. As a result, the imidazolium cationic groups with high LUMO energies degrades quickly in basic condition. From this observation, the discrepancy of imidazolium alkaline stability can be concluded.

## 2.4. Conclusion

In summary, fluorene based alkyl 1-isopropyl-2-methylimidazolium functionalized AEM was newly synthesized, and fuel cell membrane properties were analyzed. The polyfluorene polymer was prepared by the Suzuki cross-coupling reaction and casted from DMF solvent, followed by ion exchange with $OH^-$ anions. The prepared membrane showed high thermal stability, high anion exchange capacity, low swelling ratio, and moderate water uptake. The AEM membrane exhibited hydroxide conductivity of 46 mS $cm^{-1}$ at 80 $^oC$. I have investigated that the imidazolium cationic group degraded at 80 $^oC$ even at room temperature in alkaline medium. I concluded that the 1-isopropyl-2-methylimidazolium cationic group is not stable in 1 M NaOH solution on the fluorene backbone. This investigation will help researchers for choosing the cationic groups for the synthesis of alkaline stable AEMs for the actual application in AEMFCs.

## References

[1] M.A. Hickner, H. Ghassemi, Y.S. Kim, B.R. Einsla, J.E. McGrath, Alternative polymer systems for proton exchange membranes (PEMs), Chemical Reviews 104 (2004) 4587-4612.

[2] M.Z. Jacobson, W. Colella, D. Golden, Cleaning the air and improving health with hydrogen fuel-cell vehicles, Science 308 (2005) 1901-1905.

[3] S. Lu, J. Pan, A. Huang, L. Zhuang, J. Lu, Alkaline polymer electrolyte fuel cells completely free from noble metal catalysts, Proceedings of the National Academy of Sciences 105 (2008) 20611-20614.

[4] K.A. Mauritz, R.B. Moore, State of understanding of Nafion, Chemical Reviews 104 (2004) 4535-4586.

[5] M.A. Hickner, A.M. Herring, E.B. Coughlin, Anion exchange membranes: current status and moving forward, Journal of Polymer Science Part B: Polymer Physics 51 (2013) 1727-1735.

[6] H. Zhang, P.K. Shen, Recent development of polymer electrolyte membranes for fuel cells, Chemical Reviews 112 (2012) 2780-2832.

[7] D.R. Dekel, Review of cell performance in anion exchange membrane fuel cells, Journal of Power Sources 375 (2018) 158-169.

[8] S.A. Nuñez, M.A. Hickner, Quantitative $^{1}$H NMR analysis of chemical stabilities in anion-exchange membranes, ACS Macro Letters 2 (2012) 49-52.

[9] Q. Zhang, S. Li, S. Zhang, A novel guanidinium grafted poly(aryl ether sulfone) for high-performance hydroxide exchange membranes, Chemical Communications 46 (2010) 7495-7497.

[10] J. Ran, L. Wu, Q. Ge, Y. Chen, T. Xu, High performance anion exchange membranes obtained through graft architecture and rational cross-linking, Journal of Membrane Science 470 (2014) 229-236.

[11] N. Li, Q. Zhang, C. Wang, Y.M. Lee, M.D. Guiver, Phenyltrimethylammonium functionalized polysulfone anion exchange membranes, Macromolecules 45 (2012) 2411-2419.

[12] Z. Zhao, J. Wang, S. Li, S. Zhang, Synthesis of multi-block poly(arylene ether sulfone) copolymer membrane with pendant quaternary ammonium groups for alkaline fuel cell, Journal of Power Sources 196 (2011) 4445-4450.

[13] M.R. Hibbs, Alkaline stability of poly(phenylene)‐based anion exchange membranes with various cations, Journal of Polymer Science Part B: Polymer Physics 51 (2013) 1736-1742.

[14] W.-H. Lee, A.D. Mohanty, C. Bae, Fluorene-based hydroxide ion conducting

polymers for chemically stable anion exchange membrane fuel cells, ACS Macro Letters 4 (2015) 453-457.

[15] H.-S. Dang, P. Jannasch, High-performing hydroxide exchange membranes with flexible tetra-piperidinium side chains linked by alkyl spacers, ACS Applied Energy Materials 1 (2018) 2222-2231.

[16] H. Lim, B. Lee, D. Yun, A.Z. Al Munsur, J.E. Chae, S.Y. Lee, H.-J. Kim, S.Y. Nam, C.H. Park, T.-H. Kim, Poly(2,6-dimethyl-1,4-phenylene oxide)s with various head groups: effect of head groups on the properties of anion exchange membranes, ACS Applied Materials & Interfaces 10 (2018) 41279-41292.

[17] X. Ren, S.C. Price, A.C. Jackson, N. Pomerantz, F.L. Beyer, Highly conductive anion exchange membrane for high power density fuel-cell performance, ACS Applied Materials & Interfaces 6 (2014) 13330-13333.

[18] E.N. Hu, C.X. Lin, F.H. Liu, Q. Yang, L. Li, Q.G. Zhang, A.M. Zhu, Q.L. Liu, Cross-linked poly(vinylbenzyl chloride) anion exchange membranes with long flexible multihead for fuel cells, ACS Applied Energy Materials 1 (2018) 3479-3487.

[19] W. Ma, C. Zhao, H. Lin, G. Zhang, H. Na, Poly(aryl ether ketone)s with bromomethyl groups: synthesis and quaternary amination, Journal of Applied Polymer Science 120 (2011) 3477-3483.

[20] A.N. Lai, K. Zhou, Y.Z. Zhuo, Q.G. Zhang, A.M. Zhu, M.L. Ye, Q.L. Liu, Anion exchange membranes based on carbazole-containing polyolefin for direct methanol fuel cells, Journal of Membrane Science 497 (2016) 99-107.

[21] M. Zhang, C. Shan, L. Liu, J. Liao, Q. Chen, M. Zhu, Y. Wang, L. An, N. Li, Facilitating anion transport in polyolefin-based anion exchange membranes via bulky side chains, ACS Applied Materials & Interfaces 8 (2016) 23321-23330.

[22] A.D. Mohanty, S.E. Tignor, J.A. Krause, Y.-K. Choe, C. Bae, Systematic alkaline stability study of polymer backbones for anion exchange membrane applications, Macromolecules 49 (2016) 3361-3372.

[23] J.S. Olsson, T.H. Pham, P. Jannasch, Poly(N,N-diallylazacycloalkane)s for anion-exchange membranes functionalized with n-spirocyclic quaternary ammonium cations, Macromolecules 50 (2017) 2784-2793.

[24] E.J. Park, Y.S. Kim, Quaternized aryl ether-free polyaromatics for alkaline membrane fuel cells: synthesis, properties, and performance–a topical review, Journal of Materials Chemistry A 6 (2018) 15456-15477.

[25] D. Chen, M.A. Hickner, S. Wang, J. Pan, M. Xiao, Y. Meng, Synthesis and characterization of quaternary ammonium functionalized fluorene-containing cardo polymers for potential anion exchange membrane water electrolyzer applications,

International Journal of Hydrogen Energy 37 (2012) 16168-16176.

[26] P.Y. Xu, K. Zhou, G.L. Han, Q.G. Zhang, A.M. Zhu, Q.L. Liu, Fluorene-containing poly(arylene ether sulfone)s as anion exchange membranes for alkaline fuel cells, Journal of Membrane Science 457 (2014) 29-38.

[27] M. Tanaka, K. Fukasawa, E. Nishino, S. Yamaguchi, K. Yamada, H. Tanaka, B. Bae, K. Miyatake, M. Watanabe, Anion conductive block poly(arylene ether)s: synthesis, properties, and application in alkaline fuel cells, Journal of the American Chemical Society 133 (2011) 10646-10654.

[28] C. Wang, N. Li, D.W. Shin, S.Y. Lee, N.R. Kang, Y.M. Lee, M.D. Guiver, Fluorene-based poly(arylene ether sulfone)s containing clustered flexible pendant sulfonic acids as proton exchange membranes, Macromolecules 44 (2011) 7296-7306.

[29] H.-S. Dang, P. Jannasch, A comparative study of anion-exchange membranes tethered with different hetero-cycloaliphatic quaternary ammonium hydroxides, Journal of Materials Chemistry A 5 (2017) 21965-21978.

[30] K.J. Noonan, K.M. Hugar, H.A. Kostalik IV, E.B. Lobkovsky, H.c.D. Abruña, G.W. Coates, Phosphonium-functionalized polyethylene: a new class of base-stable alkaline anion exchange membranes, Journal of the American Chemical Society 134 (2012) 18161-18164.

[31] B. Zhang, S. Gu, J. Wang, Y. Liu, A.M. Herring, Y. Yan, Tertiary sulfonium as a cationic functional group for hydroxide exchange membranes, RSC Advances 2 (2012) 12683-12685.

[32] X. Lin, L. Wu, Y. Liu, A.L. Ong, S.D. Poynton, J.R. Varcoe, T. Xu, Alkali resistant and conductive guanidinium-based anion-exchange membranes for alkaline polymer electrolyte fuel cells, Journal of Power Sources 217 (2012) 373-380.

[33] B. Lin, H. Dong, Y. Li, Z. Si, F. Gu, F. Yan, Alkaline stable C2-substituted imidazolium-based anion-exchange membranes, Chemistry of Materials 25 (2013) 1858-1867.

[34] F. Zhang, H. Zhang, C. Qu, Imidazolium functionalized polysulfone anion exchange membrane for fuel cell application, Journal of Materials Chemistry 21 (2011) 12744-12752.

[35] S. Chempath, J.M. Boncella, L.R. Pratt, N. Henson, B.S. Pivovar, Density functional theory study of degradation of tetraalkylammonium hydroxides, The Journal of Physical Chemistry C 114 (2010) 11977-11983.

[36] S. Chempath, B.R. Einsla, L.R. Pratt, C.S. Macomber, J.M. Boncella, J.A. Rau, B.S. Pivovar, Mechanism of tetraalkylammonium headgroup degradation in alkaline fuel cell membranes, The Journal of Physical Chemistry C 112 (2008) 3179-3182.

[37] B. Qiu, B. Lin, L. Qiu, F. Yan, Alkaline imidazolium-and quaternary ammonium-functionalized anion exchange membranes for alkaline fuel cell applications, Journal of Materials Chemistry 22 (2012) 1040-1045.

[38] B. Lin, L. Qiu, J. Lu, F. Yan, Cross-linked alkaline ionic liquid-based polymer electrolytes for alkaline fuel cell applications, Chemistry of Materials 22 (2010) 6718-6725.

[39] X. Lin, J.R. Varcoe, S.D. Poynton, X. Liang, A.L. Ong, J. Ran, Y. Li, T. Xu, Alkaline polymer electrolytes containing pendant dimethylimidazolium groups for alkaline membrane fuel cells, Journal of Materials Chemistry A 1 (2013) 7262-7269.

[40] Z. Si, L. Qiu, H. Dong, F. Gu, Y. Li, F. Yan, Effects of substituents and substitution positions on alkaline stability of imidazolium cations and their corresponding anion-exchange membranes, ACS Applied Materials & Interfaces 6 (2014) 4346-4355.

[41] F. Gu, H. Dong, Y. Li, Z. Si, F. Yan, Highly stable N3-substituted imidazolium-based alkaline anion exchange membranes: experimental studies and theoretical calculations, Macromolecules 47 (2013) 208-216.

[42] H. Dong, F. Gu, M. Li, B. Lin, Z. Si, T. Hou, F. Yan, S.T. Lee, Y. Li, Improving the alkaline stability of imidazolium cations by substitution, ChemPhysChem 15 (2014) 3006-3014.

[43] J. Wang, S. Gu, R.B. Kaspar, B. Zhang, Y. Yan, Stabilizing the Imidazolium Cation in Hydroxide‐Exchange Membranes for Fuel Cells, ChemSusChem 6 (2013) 2079-2082.

[44] K.M. Hugar, H.A. Kostalik IV, G.W. Coates, Imidazolium cations with exceptional alkaline stability: a systematic study of structure–stability relationships, Journal of the American Chemical Society 137 (2015) 8730-8737.

[45] Z. Sun, B. Lin, F. Yan, Anion‐Exchange Membranes for Alkaline Fuel‐Cell Applications: The Effects of Cations, ChemSusChem 11 (2018) 58-70.

[46] H.-S. Dang, E.A. Weiber, P. Jannasch, Poly(phenylene oxide) functionalized with quaternary ammonium groups via flexible alkyl spacers for high-performance anion exchange membranes, Journal of Materials Chemistry A 3 (2015) 5280-5284.

[47] J. Ran, L. Wu, T. Xu, Enhancement of hydroxide conduction by self-assembly in anion conductive comb-shaped copolymers, Polymer Chemistry 4 (2013) 4612-4620.

[48] L. Wang, M.A. Hickner, Highly ordered ion-conducting block copolymers by hydrophobic block modification, Journal of Materials Chemistry A 4 (2016) 15437-15449.

[49] A.H. Rao, S. Nam, T.-H. Kim, Comb-shaped alkyl imidazolium-functionalized poly(arylene ether sulfone)s as high performance anion-exchange membranes, Journal

of Materials Chemistry A 3 (2015) 8571-8580.

[50] K.H. Lee, D.H. Cho, Y.M. Kim, S.J. Moon, J.G. Seong, D.W. Shin, J.-Y. Sohn, J.F. Kim, Y.M. Lee, Highly conductive and durable poly(arylene ether sulfone) anion exchange membrane with end-group cross-linking, Energy & Environmental Science 10 (2017) 275-285.

[51] J. Pan, L. Zhu, J. Han, M.A. Hickner, Mechanically tough and chemically stable anion exchange membranes from rigid-flexible semi-interpenetrating networks, Chemistry of Materials 27 (2015) 6689-6698.

[52] C.E. Diesendruck, D.R. Dekel, Water–a key parameter in the stability of anion exchange membrane fuel cells, Current Opinion in Electrochemistry 9 (2018) 173-178.

[53] B. Lin, L. Qiu, B. Qiu, Y. Peng, F. Yan, A soluble and conductive polyfluorene ionomer with pendant imidazolium groups for alkaline fuel cell applications, Macromolecules 44 (2011) 9642-9649.

[54] B. Liu, G.C. Bazan, Synthesis of cationic conjugated polymers for use in label-free DNA microarrays, Nature Protocols 1 (2006) 1698.

[55] T. Ishiyama, M. Murata, N. Miyaura, Palladium (0)-catalyzed cross-coupling reaction of alkoxydiboron with haloarenes: a direct procedure for arylboronic esters, The Journal of Organic Chemistry 60 (1995) 7508-7510.

[56] R. Akiyama, N. Yokota, K. Miyatake, Chemically Stable, Highly Anion Conductive Polymers Composed of Quinquephenylene and Pendant Ammonium Groups, Macromolecules 52 (2019) 2131-2138.

[57] S. Gottesfeld, D.R. Dekel, M. Page, C. Bae, Y. Yan, P. Zelenay, Y.S. Kim, Anion exchange membrane fuel cells: Current status and remaining challenges, Journal of Power Sources 375 (2018) 170-184.

[58] Y.Z. Zhuo, A.N. Lai, Q.G. Zhang, A.M. Zhu, M.L. Ye, Q.L. Liu, Highly ionic-conductive crosslinked cardo poly(arylene ether sulfone)s as anion exchange membranes for alkaline fuel cells, Journal of Membrane Science 491 (2015) 138-148.

[59] D. Guo, A.N. Lai, C.X. Lin, Q.G. Zhang, A.M. Zhu, Q.L. Liu, Imidazolium-functionalized poly (arylene ether sulfone) anion-exchange membranes densely grafted with flexible side chains for fuel cells, ACS applied materials & interfaces 8 (2016) 25279-25288.

[60] D. Guo, C.X. Lin, E.N. Hu, L. Shi, F. Soyekwo, Q.G. Zhang, A.M. Zhu, Q.L. Liu, Clustered multi-imidazolium side chains functionalized alkaline anion exchange membranes for fuel cells, Journal of Membrane Science 541 (2017) 214-223.

[61] J. Pan, S. Lu, Y. Li, A. Huang, L. Zhuang, J. Lu, High‐Performance alkaline polymer electrolyte for fuel cell applications, Advanced Functional Materials 20 (2010)

312-319.

[62] F. Bu, C. Zhao, B. Wang, N. Zhang, H. Lu, Z. Cai, Y. Zhang, H. Na, UV irradiation-induced cross-linked bicarbonate anion exchange membranes based on vinylimidazolium-functionalized poly(arylene ether ketone), RSC Advances 5 (2015) 57067-57075.

[63] G. Merle, M. Wessling, K. Nijmeijer, Anion exchange membranes for alkaline fuel cells: A review, Journal of Membrane Science 377 (2011) 1-35.

[64] A.D. Mohanty, Y.-B. Lee, L. Zhu, M.A. Hickner, C. Bae, Anion exchange fuel cell membranes prepared from C–H borylation and Suzuki coupling reactions, Macromolecules 47 (2014) 1973-1980.

[65] D. Chen, M.A. Hickner, Ion clustering in quaternary ammonium functionalized benzylmethyl containing poly(arylene ether ketone)s, Macromolecules 46 (2013) 9270-9278.

[66] C.X. Lin, H.Y. Wu, L. Li, X.Q. Wang, Q.G. Zhang, A.M. Zhu, Q.L. Liu, Anion conductive triblock copolymer membranes with flexible multication side chain, ACS Applied Materials & Interfaces 10 (2018) 18327-18337.

[67] Y. Song, C. Liu, J. Zhao, J. Luo, Imidazolium-functionalized anion exchange polymer containing fluorine group for fuel cell application, International Journal of

Hydrogen Energy 41 (2016) 10446-10457.

[68] Y. Xu, J. Yang, N. Ye, M. Teng, R. He, Modification of poly(aryl ether ketone) using imidazolium groups as both pendants and bridging joints for anion exchange membranes, European Polymer Journal 73 (2015) 116-126.

[69] D. Guo, Y.Z. Zhuo, A.N. Lai, Q.G. Zhang, A.M. Zhu, Q.L. Liu, Interpenetrating anion exchange membranes using poly(1-vinylimidazole) as bifunctional crosslinker for fuel cells, Journal of Membrane Science 518 (2016) 295-304.

[70] X. Li, Q. Liu, Y. Yu, Y. Meng, Quaternized poly(arylene ether) ionomers containing triphenyl methane groups for alkaline anion exchange membranes, Journal of Materials Chemistry A 1 (2013) 4324-4335.

[71] D. Guo, A.N. Lai, C.X. Lin, Q.G. Zhang, A.M. Zhu, Q.L. Liu, Imidazolium-functionalized poly(arylene ether sulfone) anion-exchange membranes densely grafted with flexible side chains for fuel cells, ACS Applied Materials & Interfaces 8 (2016) 25279-25288.

[72] Z. Si, Z. Sun, F. Gu, L. Qiu, F. Yan, Alkaline stable imidazolium-based ionomers containing poly(arylene ether sulfone) side chains for alkaline anion exchange membranes, Journal of Materials Chemistry A 2 (2014) 4413-4421.

[73] Y. Yang, J. Wang, J. Zheng, S. Li, S. Zhang, A stable anion exchange membrane

based on imidazolium salt for alkaline fuel cell, Journal of membrane science 467 (2014) 48-55.

[74] W. Wang, S. Wang, W. Li, X. Xie, Synthesis and characterization of a fluorinated cross-linked anion exchange membrane, International Journal of Hydrogen Energy 38 (2013) 11045-11052.

[75] A.N. Mondal, Y. He, L. Wu, M.I. Khan, K. Emmanuel, M.M. Hossain, L. Ge, T. Xu, Click mediated high-performance anion exchange membranes with improved water uptake, Journal of Materials Chemistry A 5 (2017) 1022-1027.

[76] K.M. Meek, Y.A. Elabd, Alkaline chemical stability of polymerized ionic liquids with various cations, Macromolecules 48 (2015) 7071-7084.

[77] Y. Ye, Y.A. Elabd, Relative chemical stability of imidazolium-based alkaline anion exchange polymerized ionic liquids, Macromolecules 44 (2011) 8494-8503.

[78] W. Wang, S. Wang, X. Xie, V.K. Ramani, Hydroxide-ion induced degradation pathway for dimethylimidazolium groups in anion exchange membranes, Journal of Membrane Science 462 (2014) 112-118.

[79] W. Li, J. Fang, M. Lv, C. Chen, X. Chi, Y. Yang, Y. Zhang, Novel anion exchange membranes based on polymerizable imidazolium salt for alkaline fuel cell applications, Journal of Materials Chemistry 21 (2011) 11340-11346.

[80] O.I. Deavin, S. Murphy, A.L. Ong, S.D. Poynton, R. Zeng, H. Herman, J.R. Varcoe, Anion-exchange membranes for alkaline polymer electrolyte fuel cells: comparison of pendent benzyltrimethylammonium and benzylmethylimidazolium head groups, Energy & Environmental Science 5 (2012) 8584-8597.

[81] K. Matsuyama, H. Ohashi, S. Miyanishi, H. Ushiyama, T. Yamaguchi, Quantum chemical approach for highly durable anion exchange groups in solid-state alkaline fuel cells, RSC Advances 6 (2016) 36269-36272.

# Ether-Bond-Free Anion Exchange Membrane Containing Cycloaliphatic Quaternary Ammonium Groups for Fuel Cells


## Abstract

Quaternary piperidinium cation was incorporated into an aryl-ether-bond-free polyfluorene backbone by flexible alkyl side chains to synthesize a stable hydroxide ion conducting anion exchange membrane (AEM). The membrane of the $OH^-$ form shows good solubility in dimethyl sulfoxide and methanol but not soluble in water. In a fully hydrated state, the $OH^-$ conductivity reached 58 mS $cm^{-1}$ at 80 °C. The results of $^1H$ NMR spectra revealed that only 13% cationic group was degraded after 168 h storage in 1 M NaOH solution at 80 °C.

## 3.1. Introduction

Due to our modern lifestyle, the demand for energy is increasing day by day. In recent years, worldwide attention is growing on the conversion and storage of electricity from renewable energy. Alkaline anion exchange membrane fuel cells (AEMFCs) generate electricity directly from the stored energy in fuels, for example, MeOH and $H_2$. AEMFCs do not rely on the platinum catalyst, and the kinetics of electrode reactions are faster in comparison to the other sorts of fuel cells [1]. So researchers are extensively motivated to develop catalyst materials and membranes for AEMFCs [2-8]. In the AEMFCs, a molecular design is one of the main challenges to synthesize the new AEM with high durability, high ionic conductivity, and long time alkaline stability at 80 $^{o}$C [3].

The polymer backbone of an AEM contains a positively charged anion conducting group which form ion conductive channels [5]. More than 50% of state-of-the-art AEMs have known to main-chain type, which contains anion exchange groups on their backbones. Therefore, the anion conductivity can be increased by only increasing the ion exchange capacity (IEC) [9]. However, higher IEC value of AEMs decrease the mechanical strength because of higher WU, as a result, the cell assembly is failed. This problem can be solved by creating ionic channels, which are well connected and

increase ion conductivity. Highly efficient ion conducting channels can be built either by constructing side chain type AEMs with single cation/multications [10] or synthesize well-ordered block copolymer. AEMs containing side-chain with multication were reported by Hickner and coworkers that enhance the ionic conductivity [11, 12].

In AEMFCs, the attack of nucleophilic $OH^-$ degrades the cationic groups and the polymer backbones of AEMs. For example, if polymer backbones contain electron-withdrawing sulfone and/or ketone groups, these groups stimulate the nucleophilic attack by $OH^-$ groups and resulting in chain scission of backbones [13, 14]. On the other hand, AEMs based on polyphenylene oxide (PPO), are practically stable in the alkaline environment [15]. Polymers without aryl ether links, for instance, polyarylene alkylenes, [14, 16-18] and polyphenylenes [19] are potentially even more stable. Lee *et al.* and Hibbs *et al.* [16, 20-23] synthesized some AEMs without any aryl-ether-bond in the main chain and observed much improved alkaline stability. In this study, I have synthesized ether, sulfone, and ketone free polyfluorene backbone as it can offer high alkaline stability. Fluorenyl group containing aromatic backbones have attracted much attention due to the possibility of diverse chemical modifications. Before the polymerization reaction, alkyl or dialkyl groups are introduced to the C-9 position of the fluorene to increase the solubility of the polymer. Bulky fluorene groups could

enhance free volumes or interchain separations as it forces each polymer chain apart in which water molecules might be confined [24, 25]. AEMs containing fluorenyl groups not only exhibited high thermal and alkaline stability but also have high ionic conductivity [26, 27]. Bae *et al.* [23] reported that aryl-ether-bond free polyfluorene AEMs were stable for 30 days in 1 M NaOH solution at 80 $^{o}$C.

Often the serious problem is the degradation of quaternary ammonium (QA) cations by several different pathways, such as different rearrangement reactions, Hofmann (β) elimination, and nucleophilic substitution [7]. The degradation pathway is dominated by the cationic structure, and how the cationic group is incorporated into the polymer backbone. Therefore, numerous cationic groups including modified tetraalkylammonium, imidazolium, benzimidazolium, guanidinium, and pyridinium have been extensively studied [7, 28-33]. Yan *et al.* have reported two cationic groups with permethyl cobaltocenium and methyl tris(2,4,6- trimethylphenyl)phosphonium [34, 35] show excellent chemical stability in the alkali media. However, their applications are limited in AEMs since the grafting of these cationic groups on the backbone of the polymer is not easy. Even some organometallic cationic groups [36, 37] have not degraded by Hofmann degradation in alkaline condition. However, in these AEMs, there is no report for both good chemical durability and high hydroxide conductivity.

In this circumstance, some heterocycloaliphatic QA cationic groups have reported as predominantly long-lived in alkaline conditions. In a systematic study, Marino and Kreuer found a longer half-life time of piperidinium and pyrrolidinium than the benchmark tetramethylammonium (TMA) in the aqueous solution of 6 M NaOH at 160 °C [38]. The cyclic QA cations that are used in AEMs are shown in Scheme 3.1. Cyclic QAs were identified as particularly more alkaline stable because of the rotationally restricted anti-periplanar β-protons in the ring. The combination of low ring strain and conformational restrictions of the ring increases the transition state energy for both Hofmann β-elimination and ring-opening substitution reactions [38] as shown in Fig. 3.1.

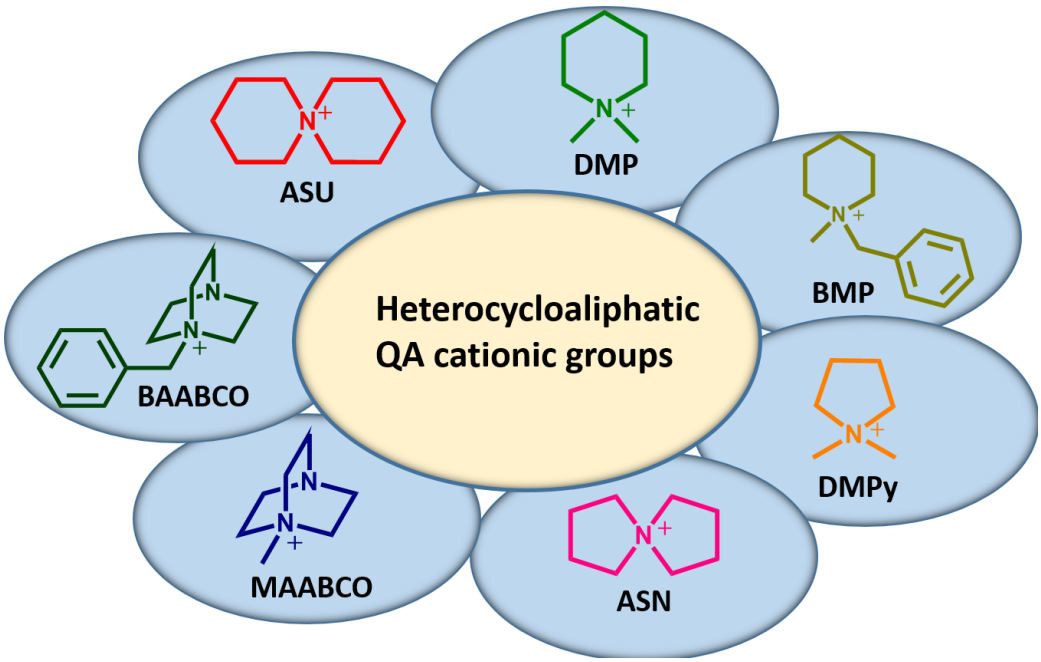


Scheme 3.1 Molecular structures of different cyclic QA cationic groups used in AEMs.

Larger ring sizes such as azepanium (7-membered ring) and additional heteroatoms e.g., morpholinium destabilize the ring structures and have considerably lower chemical stability than the N,N-dimethylpiperidinium cation [39]. N-spirocyclic QA like 6-azonia-spiro[5.5]undecane (ASU) cation is even more stable as shown in Fig. 3.2. However, the attachment of QAs with N-spirocyclic structures into the polymer backbone is rather complicated; as a result, a few reports are available [40-45]. In contrast, the incorporation of aliphatic monocyclic QA cations is relatively straightforward and less expensive.

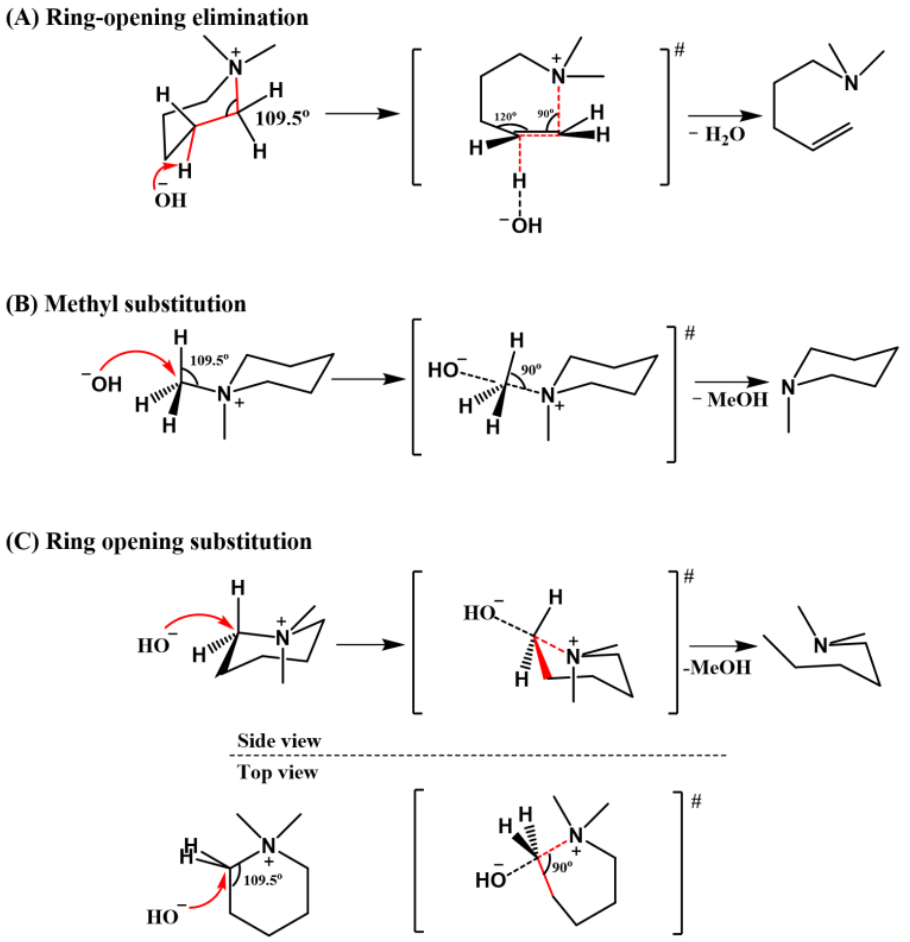


Fig. 3.1 The transition state of (A) ring opening elimination (B) methyl substitution (C) ring opening substitution. All of the transition states require energetically unfavorable bond lengths and angles [38].

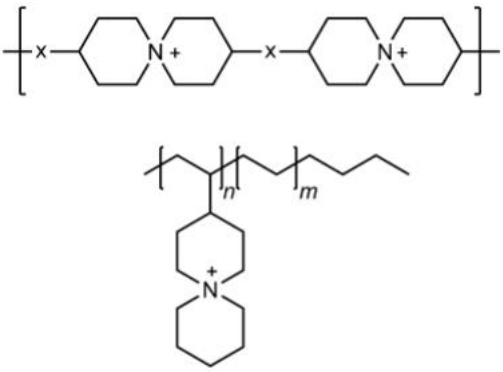


Fig. 3.2 ASU-based polymers. Here x represents any suitable group for linking [38].

The cationic group ASU is more stable than the piperidinium group but the synthesis and incorporation into the polymer are difficult. Zhu *et al.* [45] reported PPO based polymer containing ASU cationic group. They observed little brittleness of ASU-PPO membranes with a high degree of ASU-functionalization, as the ASU rings are rigid. By considering the above reasons, I have chosen piperidinium as a cationic group in this study as piperidine is commercially available and easy to attach to the polymer. Bae *et al.* reported that the most stable cationic group among his studied different QA cationic groups was N-alkyl-tethered quarternary piperidinium [29]. The ether-free AEMs with alkyl piperidinium groups were synthesized by Ren and co-workers and they observed no measurable degradation of the AEM in 1 M NaOH solution at 80 °C for 1200 h [43]. Jannach *et al.* also reported alkali stable PPO based alkyl N-methylpiperidinium

functionalized AEMs [44, 45].

To combine high alkaline stability and high ionic conductivity in this study, I have incorporated N-methyl piperidinium (Pip) cations to the polyfluorene backbone via alkyl side chains and evaluated the properties of ion exchange capacity (IEC), hydroxide conductivity, thermal and chemical stability, and WU.

## 3.2. Experimental

### 3.2.1. Materials

1,6-Dibromohexane, 2,7-dibromofluorene, bis(pinacolato)diboron, tetrabutylammonium bromide (TBAB), 2,7-dibromo-9,9-dioctyl fluorene, tetrakis(triphenylphosphine)palladium(0) denoted as $Pd(PPh_3)_4$ were purchased from Tokyo Chemical Industry Co. Ltd., Japan. [1,1-Bis(diphenylphosphino)ferrocene] dichloropalladium(II) (PdCl2)(dppf) was used from Sigma-Aldrich. N-methylpiperidine, dioxane, dichloromethane, chloroform, toluene, ethanol, tetrahydrofuran (THF), diethyl ether, N,N-dimethylformamide (DMF), potassium carbonate, hexane, acetonitrile, ethyl acetate, methanol, ethanol, sodium chloride, sodium hydroxide, potassium hydroxide, anhydrous magnesium sulfate, potassium acetate, and hydrochloric acid were obtained from Fujifilm Wako Pure Chemical Corp., Japan. For all experimental works, deionized (DI) water was used.

## 3.2.2. Synthesis of Monomers and Polymers

### 3.2.2.1. Synthesis of 2,7-dibromo-9,9-bis(6′-bromohexyl)fluorene (Compound A)

By following the synthetic procedure of previous literature [46] Compound A was prepared. Briefly, 2,7-dibromofluorene (5.0 g, 15 mmol) was added to a mixture of 1,6-dibromohexane (30 mL), tetrabutylammonium bromide (TBAB) (0.1 g), and 30 mL aqueous solution of sodium hydroxide (50 wt%) at room temperature. The resulting solution was stirred at 60 °C for 8 h under argon. Dichloromethane was added to extract the organic layer. Water and brine were used to wash the organic layer and dried over magnesium sulfate. After evaporation of the solvent, vacuum distillation was applied to remove the unreacted 1,6-dibromohexane. The product was separated by column chromatography using pure n-hexane as solvent after adsorption on silica gel, Compound A is a white crystalline powder (7.57 g, 75%). The chemical structure of the resultant product was confirmed by $^{1}$H NMR ($CHCl_3$-$d_1$) and $^{13}$C NMR ($CHCl_3$-$d_1$) spectra. $^{1}$H NMR (400 MHz) δ (ppm): 7.54−7.43 (m, 6H, Ar-*H*), 3.29 (t, 4H, C$H_2$-Br), 1.95−1.90 (m, 4H, Ar-*H*), 1.70−1.63 (m, 4H, -C$H_2$-), 1.25−1.04 (m, 8H, -C$H_2$-), 0.62-0.54 (m, 4H, -C$H_2$-).

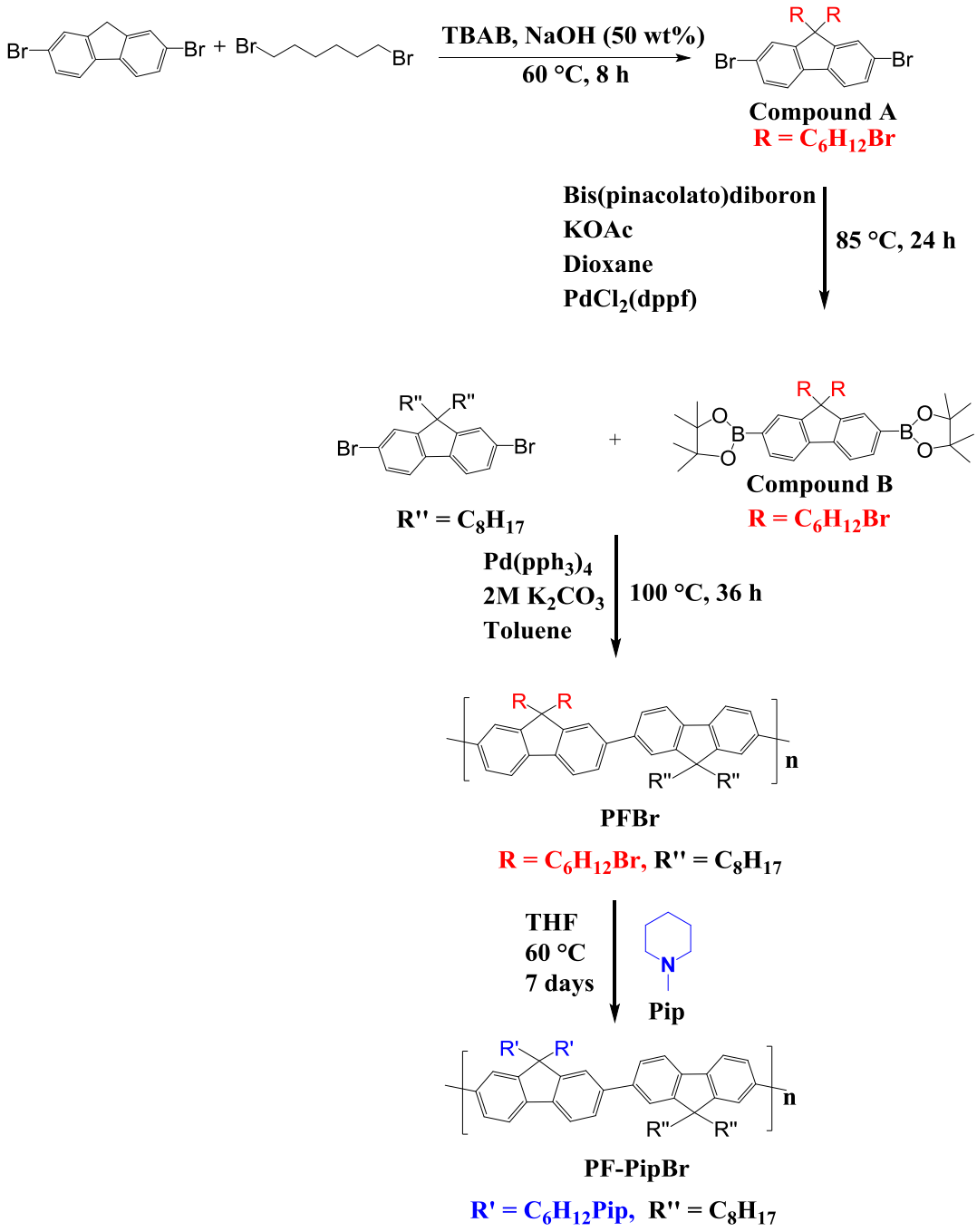


Scheme 3.2. Synthetic route of piperidinium functionalized fluorene based polymer. Red color means bromine atom containing alkyl chains and the blue color stands for piperidinium functionalized alkyl chains.

### 3.2.2.2. Synthesis of 2,7-bis(4,4,5,5-tetramethyl-1,3,2-dioxaborolan-2-yl)-9,9-bis(6′-bromohexyl)fluorene (Compound B)

Compound B was prepared by following the literature [47]: Compound A (3.25 g, 5 mmol), bis(pinacolato)diboron (3.0 g, 12 mmol), potassium acetate (3.5 g, 35.5 mmol), $PdCl_2$(dppf) (250 mg), and 50 ml dioxane were added in a 200 ml round-bottom flask. The reaction mixture was degassed three times by using freeze–pump–thaw cycles. Then the reaction mixture was stirred at 85 ºC for 12 h under argon atmosphere. After the reaction was cooled down to room temperature, dioxane was removed at 45 ºC on a rotary evaporator. The crude product was extracted with $CH_2Cl_2$ (60 mL × 3) and washed with water (40 ml × 3). The $CH_2Cl_2$ layer was dried by using brine and $MgSO_4$. Then the organic layer was concentrated by evaporating the solvent. Compound B was separated by column chromatography after adsorption on silica gel by using hexane and ethyl acetate (20:1). The product was obtained as a white solid (2.65 g, 71% yield). The structure was characterized by the $^1$H NMR spectrum in $CDCl_3$ and the mass spectrum. $^1$H NMR (400 MHz) δ (ppm): 7.81 (d, 2H, Ar-*H*), 7.72 (d, 4H, Ar-*H*), 3.25 (t, 4H, –C*H*$_2$Br), 2.03-1.99 (m, 4H, –C*H*$_2$–), 1.65-1.58 (m, 4H, –C*H*$_2$–), 1.39 (s, 24H, –C*H*$_3$), 1.19-0.99 (m, 8H, –C*H*$_2$–), 0.58-0.51 (m, 4H, –C*H*$_2$–). m/z (SALDI-TOF) 765.25 [M + Na]$^+$.

### 3.2.2.3. Synthesis of poly[(9,9-bis(6′-bromohexyl)-9H-fluorene)-co-(9,9-bis(6′-octyl) fluorene)] (PFBr).

PFBr was prepared as follows according to the literature [23]: in a 100 mL three-neck flask, 2,7-dibromo-9,9-dioctylfluorene (274 mg, 0.50 mmol) was dissolved in 15 mL of degassed toluene then Compound B (372 mg, 0.50 mmol) and 5 mL of 2 M $K_2CO_3$ solution were added to the mixture. The reaction mixture was purged with argon for 30 min, after that in the resulting mixture, $Pd(PPh_3)_4$ (32 mg, 0.03 mmol) was added. The mixture was stirred at 100 °C for 36 h under argon. The mixture was precipitated by pouring to a mixture of ethanol and HCl (1:1 v/v) solution under stirring condition. The polymer was dissolved in a small amount of $CHCl_3$, precipitated in methanol, and washed by acetone. Soxhlet apparatus with a mixture of methanol and hexane (1:1 v/v) was used to further purify the polymer. Finally, the desired PFBr polymer was dried in a vacuum oven at room temperature and obtained as a yellow solid (400 mg, 91%). The chemical structure was confirmed by $^1$H NMR spectrum in $CDCl_3$. $^1$H NMR (400 MHz): δ (ppm) 7.79-7.30 (m, 12H, Ar-*H*), 3.25-3.20 (m, 4H, -C*H*$_2$Br), 2.06-0.75 (m, 54H, alkyl side chain H).

### 3.2.2.4. Synthesis of poly[(9,9-bis(6′-(N-methylpiperidinium)hexyl) fluorene)-co-(9,9-bis(6′-octyl)fluorene)] bromide (PF-PipBr)

A solution was prepared by dissolving brominated polymer PFBr (200 mg, 0.2 mmol) in 5 mL THF. To this, 8 mL N-methylpiperidine was added and the solution was heated at 60 °C for 7 days with the continuous stirring condition under argon. The solvents were evaporated in a vacuum evaporator. The concentrate was dissolved in 2 mL of MeOH, precipitated in THF. The desired PF-PipBr polymer (217 mg, 88%) was dried at 60 °C under vacuum condition. The polymer was characterized by $^{1}$H NMR spectrum in MeOH-$d_4$.

## 3.2.3. Membrane Casting

The PF-PipBr membrane was fabricated by a 4 wt% solution of the polymer in DMF. The solution was poured on a clean PTFE sheet. Then slowly dried for 48 h at 60 ºC to avoid the air bubbles and finally dried the membrane under vacuum for 48 h at 60 ºC. The membrane thickness was 70-80 μm.

### 3.2.4. Ion Exchange of Polymers in Hydroxide Ion form

To obtain the $OH^-$ ion form membranes I have immersed the PF-PipBr membranes in argon saturated 1 M NaOH solution at room temperature for 48 h. Within this time, I have exchanged three times the NaOH solution with fresh solution. Then the membranes were soaked in argon saturated DI water and finally, the $OH^-$ ion form polymeric membranes (PF-Pip) were washed by degassed DI water until the pH becomes neutral.

### 3.2.5. Characterization and Measurements

Several analytical methods have been used to examine the chemical structure of the prepared monomers and polymers and the properties of the polymer as an anion exchange membrane.

#### 3.2.5.1. NMR Spectroscopy

Bruker Avance III (400 MHz) spectrometer (Bruker Analytik GmbH) was used to record $^{1}H$ and $^{13}C$ NMR spectra. NMR spectra were used to study the chemical structure of the synthesized monomers and polymers.

### 3.2.5.2. FTIR Spectroscopy

The synthesis of the monomers and precursor polymer was confirmed by the Fourier-transform infrared (FTIR) spectrometer. The infrared (IR) attenuated total reflection (ATR) spectra were recorded using Nicolet 6700 spectrometer (Thermo Fisher Scientific Inc.) in the wavenumber range of 400−4000 $cm^{-1}$.

### 3.2.5.3. Mass Spectrometry

The molecular weight of the synthesized monomers was confirmed by using SALDI-TOF/TOF (Bruker) ultrafleXtreme on the $TiO_2$ surface (positive reflector mode) and ESI-FT-ICR MS (Solarix) on the magnetic field strength of 9.4 T (positive mode).

### 3.2.5.4. Gel Permeation Chromatography (GPC)

The number-averaged molecular weight (Mn), weight-average molecular masses (Mw) and the polydispersity indices (PDI, Mw/Mn) of the precursor polymer (PFBr) were investigated by gel permeation chromatography (GPC) with Shodex KF-803, 804, and 805 columns. As an eluent, THF was applied at a flow rate of 1.0 mL $min^{-1}$. For calibration polystyrene (Mn = 1000-3.8 x $10^6$) standards were used.

### 3.2.5.5. Scanning Electron Microscope and Energy Dispersive X-ray Spectroscopy

The surface morphology and the presence of elements of the $Br^-$ ion containing polymer was examined by using a scanning electron microscope (SEM) and energy dispersive X-ray spectroscopy (EDX). The images were observed from TM3030Plus miniscope (Hitachi), and the accelerating voltage was 15 kV.

### 3.2.5.6. Small-angle X-ray Scattering (SAXS)

The SAXS measurement was investigated on an X-ray diffractometer (FR-E; Rigaku Corp.) using Cu Kα radiation of wavelength, λ = 1.542 Å where the beam size was approximately 300 μm × 300 μm. The camera length was 300 mm. In a glass capillary tube, a dry sample was irradiated by using the X-ray beam. For high humidity conditions, water droplet and a portion of the dry sample was sealed in the same glass capillary tube. Two days later, the sealed capillary sample was used for SAXS measurements.

### 3.2.5.7. Transmission Electron Microscopy (TEM)

For TEM measurement, membranes were first immersed in a 0.5 M $K_2[PtCl]_4$ aq.

solution at 60 °C for 48 h to stain with tetrachloroplatinate ions. After staining, the membranes were washed several times with deionized water. The stained membranes were dried in a vacuum oven at 60 °C for 24 h. The dried membranes were embedded in an epoxy resin, sliced into a 60 nm thick section with a Leica EM UC7 microtome, and placed on copper grids before investigation. A transmission electron microscope (Hitachi H-7650) was used to record the images with an accelerating voltage of 100 kV.

### 3.2.5.8. Thermal Stability

The thermal stability of the prepared polymer was investigated under nitrogen flow on a thermogravimetric analyzer TG-DTA2010 SA (NETZSCH). Before measurement, the sample was dried for 24 h at 80 ºC. Measurement of the sample was done from room temperature to 500 °C at a heating rate of 10 °C $min^{-1}$.

### 3.2.5.9. Mechanical Properties

The tensile properties of $Br^-$ ion form membrane (PF-PipBr) were investigated by using Autograph (Shimadzu Co., Ltd., Kyoto, Japan) with a tensile speed of 0.5 mm $min^{-1}$ at 25 °C in water. Before measurement, a membrane was soaked into ultrapure water for 24 h. Prior to the test, the membranes were cut into a dumbbell shape.

### 3.2.5.10. Measurements of Water Uptake and Swelling Ratio

First, the samples were dried under vacuum condition at 60 ºC for 24 h and then soaked in DI water (argon-saturated) for 24 h at 20 ºC, 40 ºC, 60 ºC, and 80 ºC. The surface water of the hydrated membranes was wiped by using tissue paper and taken the weight immediately. The wet membranes were dried at 60 °C for 24 h under vacuum. The water uptake (%) of the polymeric membranes was obtained with the following equation,

$$WU(\%) = \frac{W_{Wet} - W_{dry}}{W_{dry}} \times 100\% \quad (1)$$

where, Wdry and Wwet represent the weight of the dry and wet membranes, respectively.

The membranes (1 cm in length x 0.5 cm in width) swelling ratio (%) was calculated from the differences between the lengths of the wet and dry samples. The swelling ratio was calculated by using the following equation,

$$SW(\%) = \frac{l_{Wet} - l_{dry}}{l_{dry}} \times 100\% \quad (2)$$

where $l_{wet}$ and $l_{dry}$ are the lengths of wet and dry membranes, respectively.

For the investigation of thickness change, I have immersed the membranes in deionized water for 24 h from 20 to 80 °C.

### 3.2.5.11. Ion Exchange Capacity (IEC)

The ion-exchange capacity (IEC) of the $OH^-$ containing (PF-Pip) membranes was measured by a back-titration method. Before this measurement, the membranes were soaked for 48 h in 50 mL of HCl (0.01 M) solution. The unreacted HCl was determined by titrating with NaOH (0.01 M) solution in the presence of phenolphthalein indicator. The IEC was calculated by,

$$\text{IEC (mmol g}^{-1}) = \frac{V_{0,NaOH}C_{NaOH} - V_{x,NaOH}C_{NaOH}}{W_{dry}} \quad (3)$$

here, $V_{x,\,NaOH,}$ is the required volume of NaOH solution with membranes and $V_{0,\,NaOH}$ represents the volume of NaOH without membranes respectively during the titration, $C_{NaOH}$ represents the concentration of the NaOH (M), $W_{dry}$ is the mass of the dry membranes. For each sample, three replicates were conducted.

### 3.2.5.12. Hydroxide Ion Conductivity

Impedance analyzer and dielectric interface system (SI1260 and SI1296; Solartron Analytical) were used to measure the in-plane hydroxide conductivity of the membranes. The impedance data of membranes were collected by using a four-point probe alternating current (ac) system within the frequency range of 10 MHz to 1 Hz with an amplitude of 50 mV. The conductivity of the membranes was measured in a homemade chamber, which was filled with argon-saturated deionized water. During the measurement, all the membranes were equilibrated for 30 min at a given temperature. The temperature between 20 and 80 °C was controlled by using a chamber (SH-221; Espec Corp.). The hydroxide conductivity σ of the membrane was calculated from,

$$\sigma(S\ cm^{-1}) = \frac{L}{R \times W \times T} \quad (4)$$

where L is the distance (1.3 cm) between two Pt electrodes, W and T are the width (1.3 cm) and thickness (70 μm) of the membrane, and R (Ω) is the resistance of the membrane.

### 3.2.5.13. Alkaline Stability of the Membrane

The investigation of the alkaline stability was carried out by soaking the PF-Pip membranes in argon-saturated 1M NaOH solution at 80 $^{o}$C. Membranes were taken after 96 h and 168 h storage and thoroughly washed with DI water until the pH becomes neutral. The changes in the molecular structure of the AEMs were investigated by $^{1}$H NMR spectroscopy results.

## 3.3. Results and Discussion

### 3.3.1. Synthesis and Characterization of Monomers and Polymers

A reaction was conducted between 2,7-Dibromofluorene and 1,6-dibromohexane to synthesize Compound A. The chemical structure was confirmed by $^{1}H$ and $^{13}C$ NMR spectra in $CDCl_3$ (Fig. 3.3 and 3.4). The triplet peak appeared at 3.29 ppm indicates the presence of bromine-containing terminal methylene groups. The five multiplets from 1.95 to 0.54 ppm confirmed the grafting of two long hexyl chains on the C9 position of fluorene ring. The peaks from 7.54 to 7.43 ppm corresponded to the aromatic protons of the fluorenyl group. The $^{13}C$ NMR spectrum also confirmed the structure of the synthesized compound A.

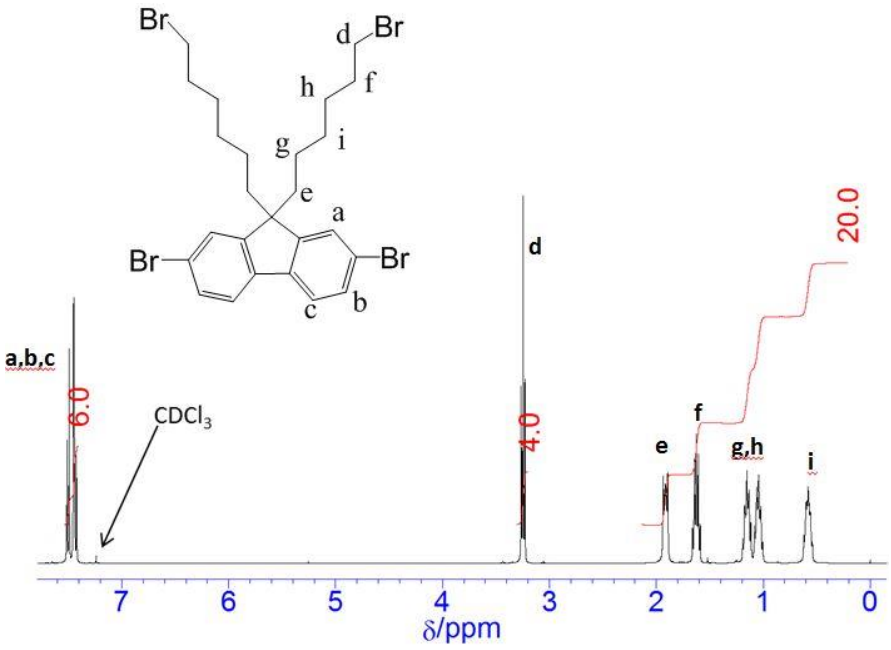


Fig. 3.3. $^{1}$H NMR spectrum of 2,7-dibromo-9,9-bis(6′-bromohexyl)fluorene (compound A)

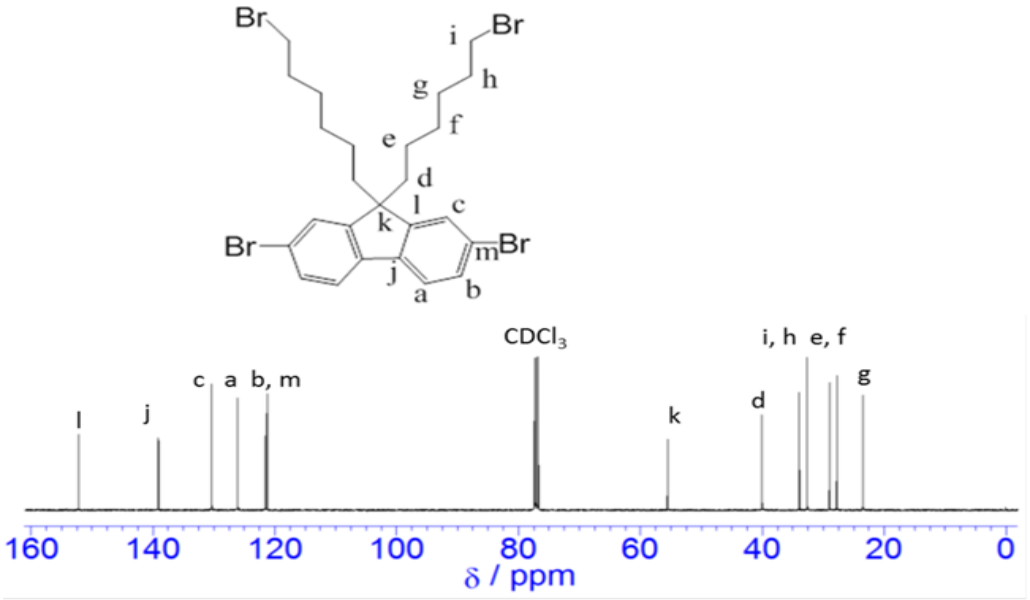


Fig. 3.4. $^{13}$C NMR spectrum of 2,7-dibromo-9,9-bis(6′-bromohexyl)fluorene (Compound A).

By using $^{1}H$ NMR spectroscopy the chemical structure of compound B was characterized as shown in Fig. 3.5. The peak appeared at 1.39 ppm confirmed the successful incorporation of 4,4,5,5-tetramethyl-1,3,2-dioxaborolane. The product was further confirmed by SALDI-TOF mass spectrum as shown in Fig. 3.6. The calculated m/z of $[M+Na]^{+}$ is 765.25 and I found 765.56. However, after investigation of the mass spectrum, I observed the product contains compound B and boronic acid form of compound B.

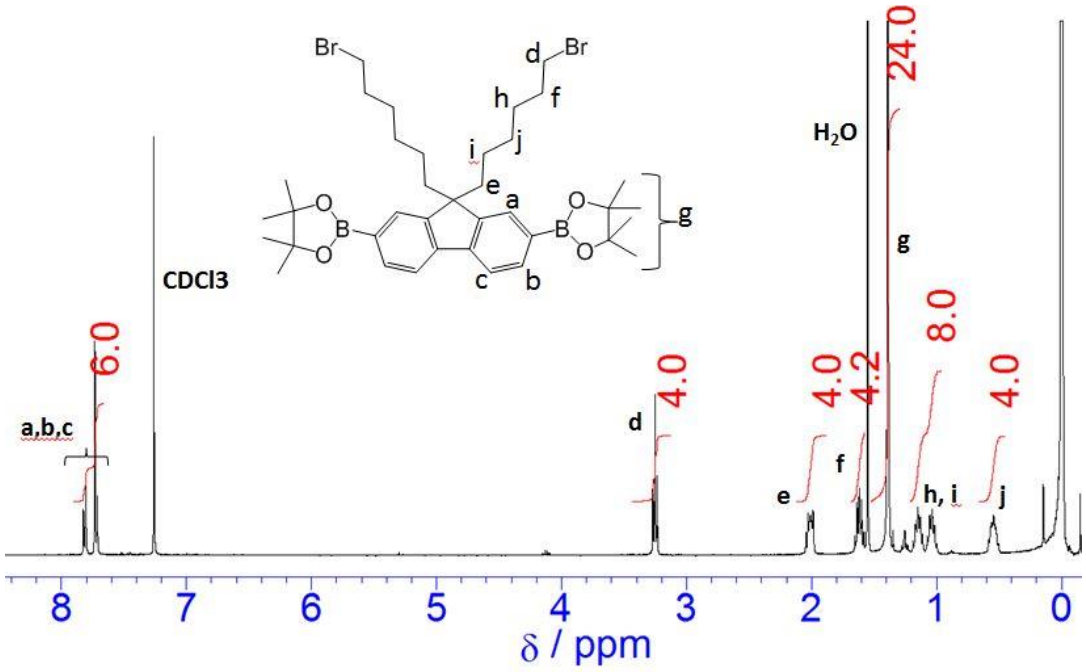


Fig. 3.5. $^{1}H$ NMR spectrum of 2,7-bis(4,4,5,5-tetramethyl-1,3,2–dioxaborolan -2-yl)-9,9-bis(6′-bromohexyl)fluorene (Compound B).

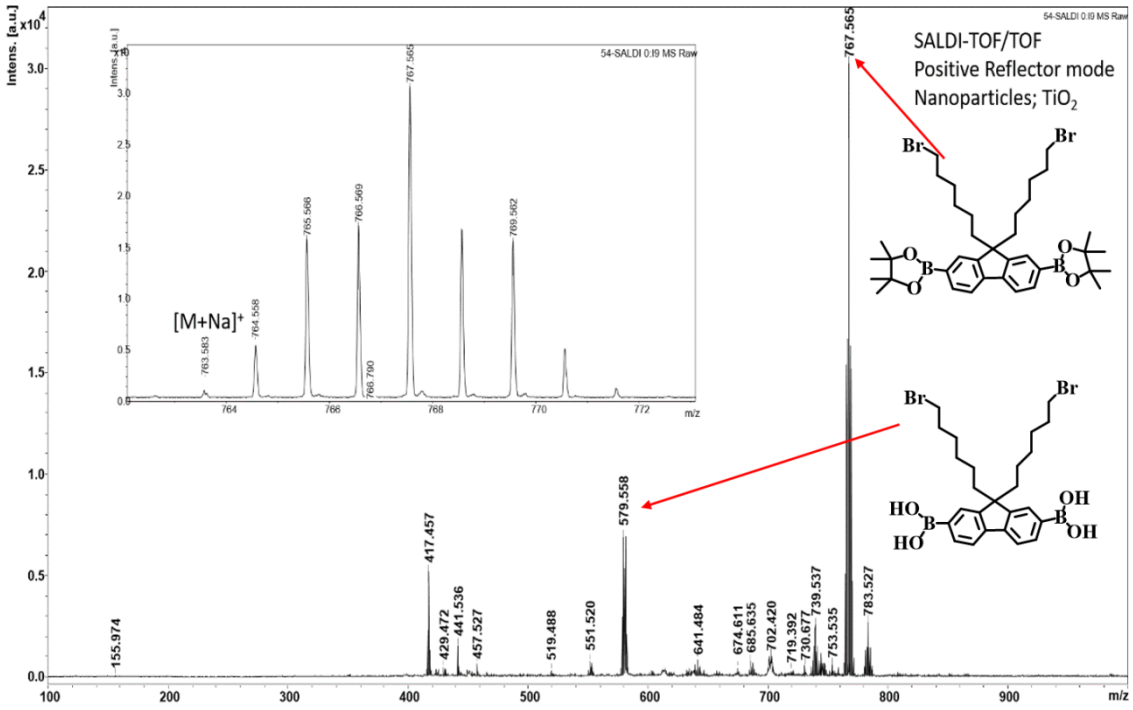


Fig. 3.6. Mass spectrum of Compound B.

The PFBr polymer was characterized by $^{1}$H NMR spectrum as shown in Fig. 3.7A. The aromatic peaks appeared around 7.79 - 7.30 ppm, and the multiplet at 3.25 - 3.20 ppm corresponded to the methylene group containing terminal bromine atoms. The peaks at 2.06 - 0.75 ppm can be assigned to alkyl side chain protons. The integral ratio and peak position confirmed that the polymerization reaction was successful. The PFBr polymer was soluble in THF and chloroform but insoluble in water. The molar masses ($M_w$, $M_n$) and polydispersity index of PFBr were determined with GPC using THF eluent and found to be $2.2 \times 10^4$ g mol$^{-1}$, $1.0 \times 10^4$ g mol$^{-1}$ and 2.2 respectively.

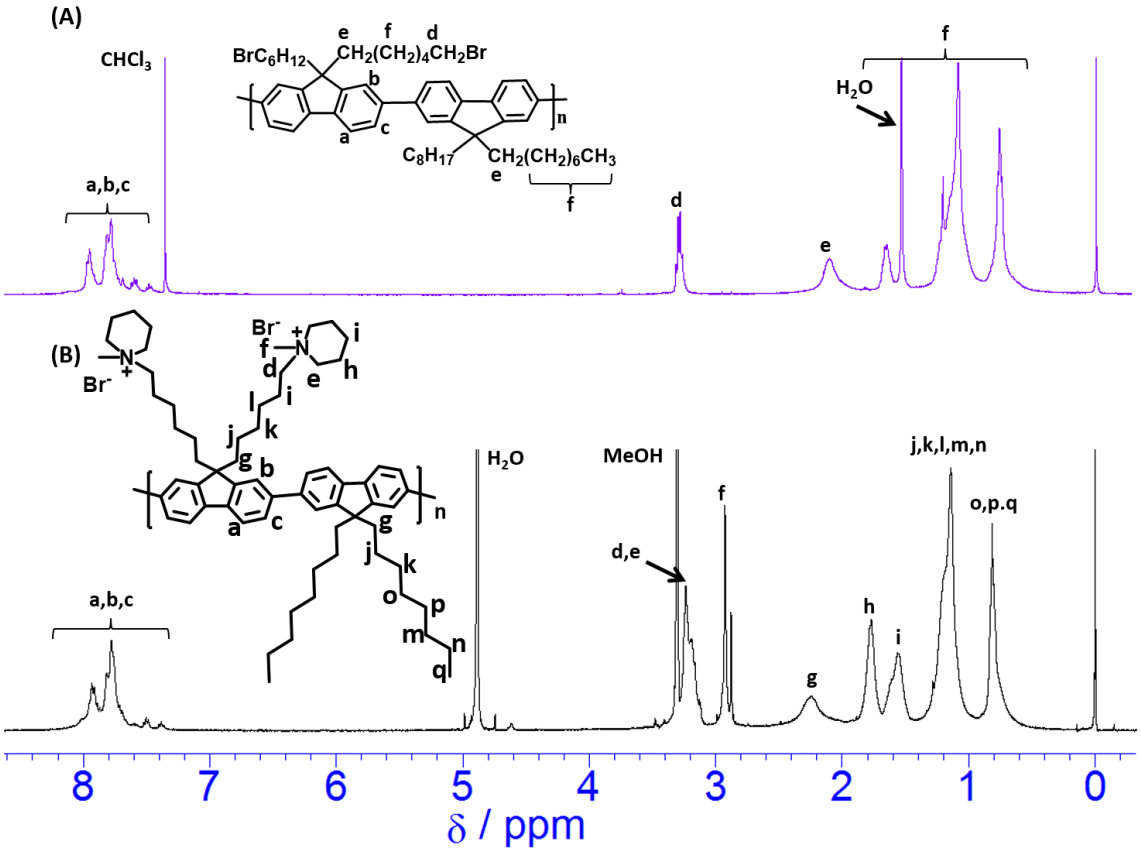


Fig. 3.7. $^{1}$H NMR spectra of PFBr and PF-PipBr.

Fig. 3.7B shows the $^{1}$H NMR spectrum of the PF-PipBr polymer. The new signals appeared at 2.9 ppm and 3.2 ppm due to the protons of $-N^{+}CH_3$ and $-N^{+}CH_2$ of the cyclopiperidinium. The ratio of the peak area between protons of $-N^{+}CH_3$ at 2.9 ppm and the aromatic protons from 7.4 to 8 ppm determined the full substitution of N-methylpiperidine in PFBr polymer. The $Br^{-}$ form polymer, PF-PipBr, was soluble in organic solvents, for example, DMF, $CH_3OH$, and DMSO at room temperature but was not soluble in $H_2O$.

The EDX spectra before and after ion exchange of $Br^-$ form to $OH^-$ form as shown in Fig. 3.8A and 3.8B confirmed that $Br^-$ ions almost exchanged by $OH^-$ in PF-Pip ($OH^-$ form) membrane. The remaining Br elements in Fig. 3.8B may arise from the end groups of the polymer.

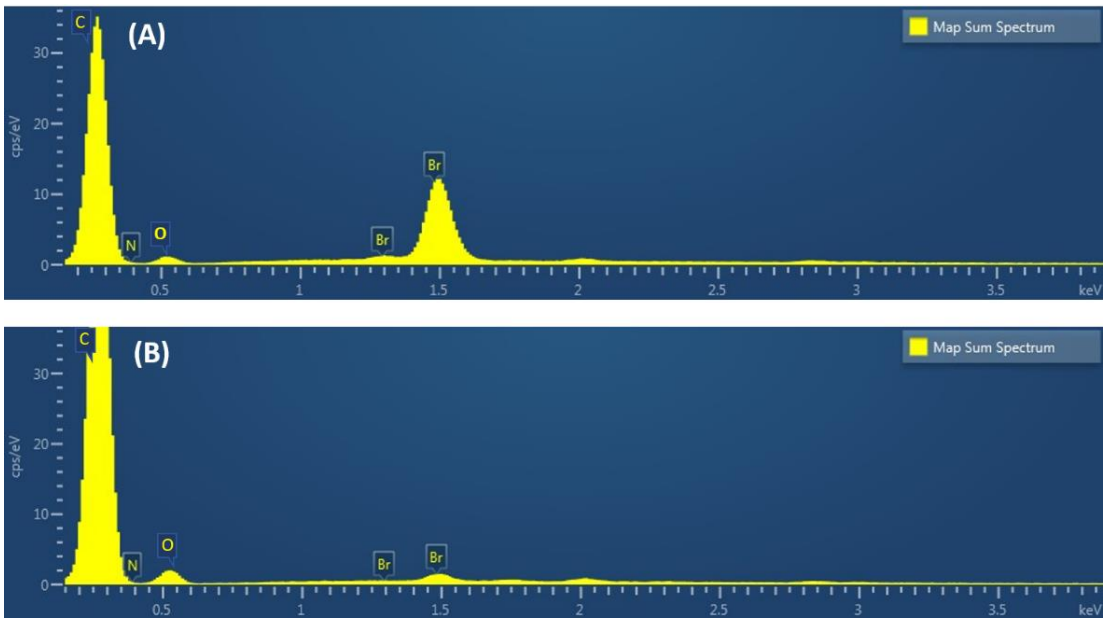


Fig. 3.8. EDX spectra for (A) PF-PipBr and (B) PF-Pip.

## 3.3.2. Membrane Morphology

The PF-PipBr membrane was fabricated from 4 wt% solutions in DMF and casted on a flat PTFE sheet. After removing the solvent, the resultant membranes become transparent as shown in Fig. 3.9A. By using SEM, the morphology of the PF-PipBr membrane was investigated. The SEM images of Fig. 3.9B and 3.9C showed that the membrane surface and cross-section were homogeneous, tight and dense, and no pores

and crack were visible on this scale.

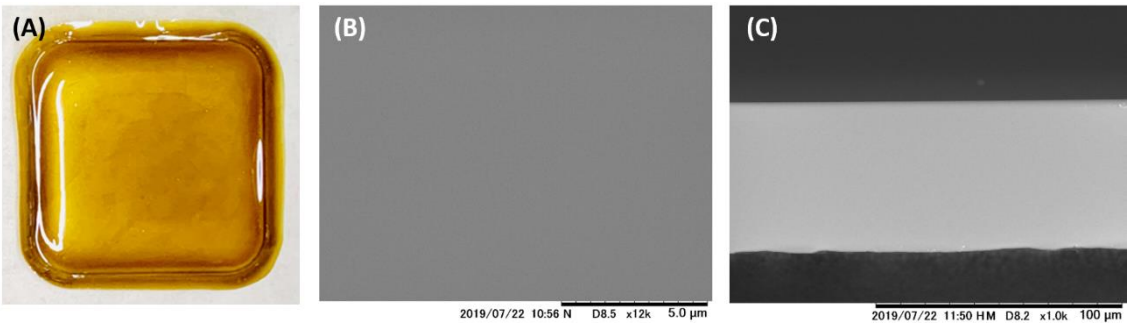


Fig. 3.9. (A) Photograph, SEM images of (B) membrane surface and (C) cross section of the PF-PipBr polymer.

To clarify the surface morphology of the membrane I have tried small angle X-ray scattering (SAXS) measurements in the dry condition. I also investigated the SAXS profiles in both humidified, in-water and humidified at 80 °C conditions. A very weak scattering peak was observed for PF-PipBr AEM at q = 0.21 Å which corresponds to d = 3 nm as shown in Fig. 3.10. This d value represents the distance between the ionic domains. This peak is insensitive to WU indicating molecular ordering is not improved by WU.

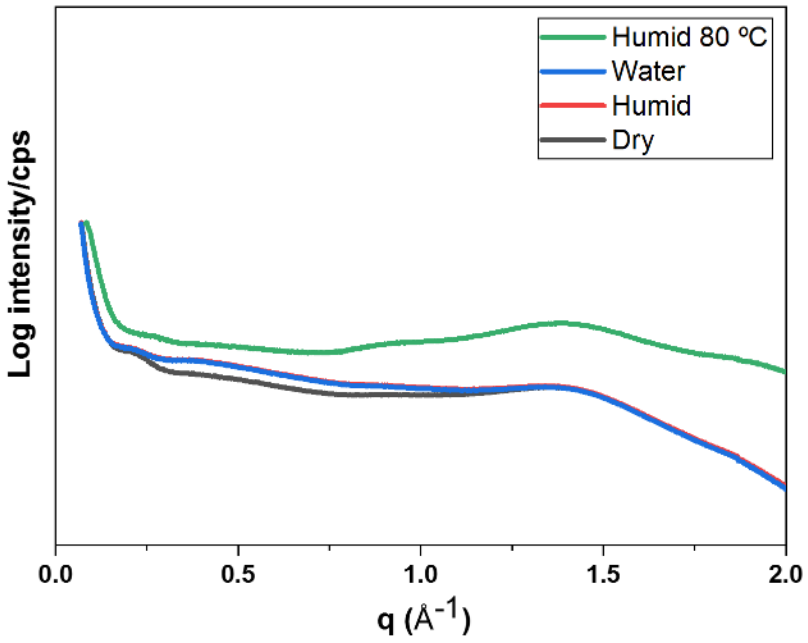


Fig. 3.10. The SAXS profile of PF-PipBr AEM

The cross-sectional TEM images of the PF-Pip membrane were investigated after stained with tetrachloroplatinate ion. The bright regions represent the hydrophobic domains and dark regions correspond to the hydrophilic domains. The domain size of the hydrophilic group was observed as 1 to 2 nm (Fig. 3.11). This morphology is similar to the membranes of literature [48, 49] containing fluorenyl group. The hydrophilic and hydrophobic domains were homogeneously distributed throughout the sight. This microphase-separated morphology influences the hydroxide conductivity of the PF-Pip membrane.

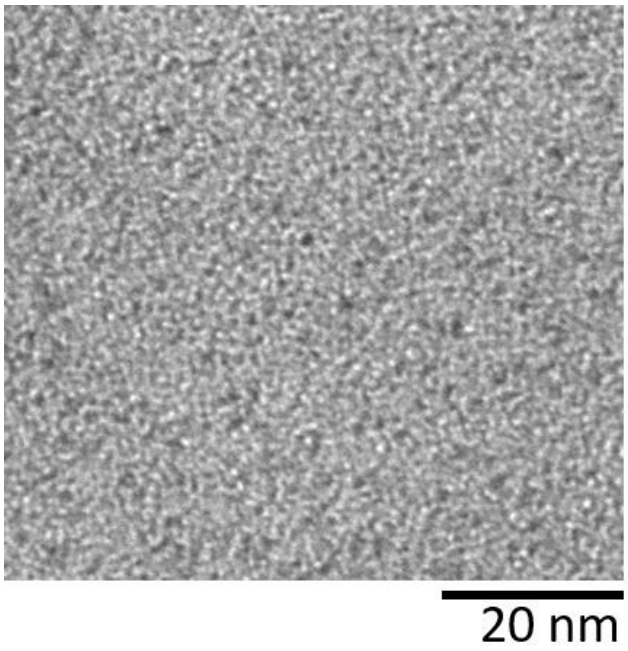


Fig. 3.11. Cross sectional TEM image of PF-Pip.

### 3.3.3. Thermal Stability

The thermal stability is always a concern for the AEMs. Aromatic polymers are the preferred candidates for application in high temperature AEMFCs because of outstanding thermal stability. Fig. 3.12 shows the result of the thermogravimatric analysis. The first weight loss below 150 °C; this weight loss possibly originates from the evaporation of adsorbed water in the membrane. From the calculation of weight percentage, in the second step 5% weight loss occurs between 150 ºC to 190 ºC due to the degradation of the methyl group of the piperidinium cations of the polymer. The

third degradation at temperatures above 390 °C due to the decomposition of the polyfluorene backbones. The overall result of thermal analysis implies that the resultant polymer maintains high thermal stability up to 150 $^{o}$C, which is higher than benzyl quaternary ammonium cationic groups [50]. The thermal stability is clearly well above the desired temperature range for fuel cell applications.

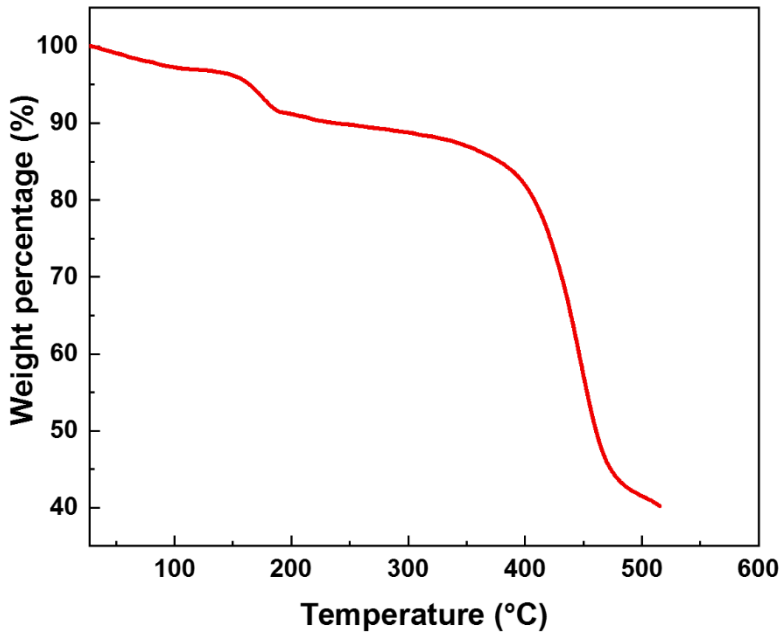


Fig. 3.12. TGA graph of PF-Pip under $N_2$ flow. Heating rate: 10 $^{o}$C min$^{-1}$.

## 3.3.4. Mechanical properties

The tensile strength of PF-PipBr polymer was observed as 10.5 MPa with an elongation at break of 2.5% in water. The Young′s modulus was found to be 354 MPa.

### 3.3.5. Water Uptake (WU), Ion Exchange Capacity (IEC), and Swelling Ratio (SR)

For AEMs, sufficient amounts of WU are essential for the formation of hydrated ionic domain phase and faster migration of ions through the membrane [2, 4, 6]. However, the balanced WU is important since excessive WU may influence undesirable membrane swelling and mechanical properties. Furthermore, the charge carriers e.g., anions are diluted due to high water contents, and conductivity decreases [51]. As anticipated, the WU of polymeric membranes increases with increasing temperature [52]. The WU of the synthesized PF-Pip membrane is shown in Fig. 3.13 as a function of temperature from 20 to 80 °C after soaked in water. I found 35 wt% WU at 20 °C and 81 wt% at 80 °C. The WU of the PF-Pip membrane is higher compared to the imidazolium functionalized PF-IMI membrane (Chapter 2). Kim *et al.* also observed that the WU of piperidinium functionalized PPO based AEM is higher than that of imidazolium containing AEM with the same backbone [53]. To understand the WU behavior, they performed molecular dynamics (MD) simulations and analyzed the cavities or free volumes inside the PPO models. They also calculated the adsorption of water molecules by using Grand Canonical Monte Carlo (GCMC) simulation. From the simulated results, they concluded that the free volume and WU of the piperidinium

containing membrane were higher than imidazolium containing membrane. According to the literature [53] may be the free volume of PF-Pip polymer is higher than PF-IMI polymer so water adsorption of PF-Pip is higher than PF-IMI. The WU of the synthesized PF-Pip membrane is comparable with the literature [18, 39] with the comparable IEC value.

The IEC of the membranes represents the number of exchangeable ions. I have used the back titration technique to determine the IEC of the synthesized membrane and found 1.82 mmol/g. The obtained IEC shows good agreement with the value of 1.89 mmol/g obtained from the $^{1}$H NMR result.

The SR of the synthesized membrane increased with increasing temperature. The SR of the PF-Pip membrane was 11% at 20 °C and 20% at 80 °C as shown in Fig. 3.13. The PF-Pip membrane showed good dimensional stability due to the stiff aromatic backbone and absence of ether linkages. The good dimensional stability of the membrane can be expected as a feasible approach for AEMFCs application.

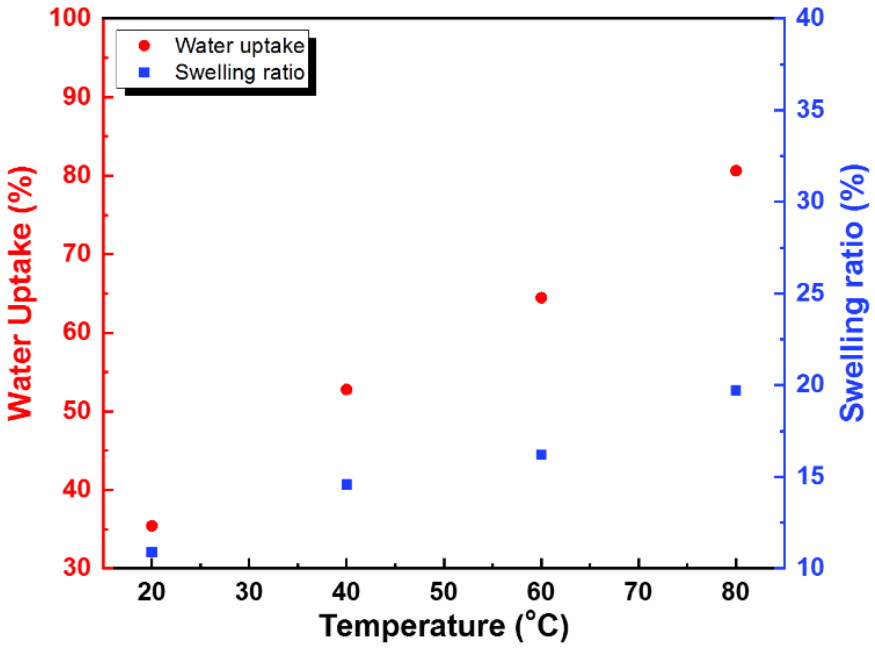


Fig. 3.13. The WU and SR of the PF-Pip membrane.

The thickness of the membranes was not changed after soaked in water at temperatures from 20 to 80 °C.

## 3.3.6. Hydroxide Ion Conductivity and Activation Energy

Hydroxide conductivity is one of the vital performances of AEMs. The hydroxide conductivity of the resultant PF-Pip membrane at different temperatures is shown in Fig. 3.14. The PF-Pip membrane exhibited hydroxide conductivity of 9 mS $cm^{-1}$ at 20 $^{o}$C temperature and increased to 58 mS $cm^{-1}$ at 80 $^{o}$C. The hydroxide conductivity of the AEMs increases with increasing temperature. Higher temperature can cause faster water diffusivity and ionic migrations. The conductivity of the resultant AEMs at elevated

temperature was higher than that of the PF-IMI membrane of chapter 2. The AEMs containing piperidinium cationic groups, have high WU [38, 53] and therefore facilitate the ionic migration through the water clusters.

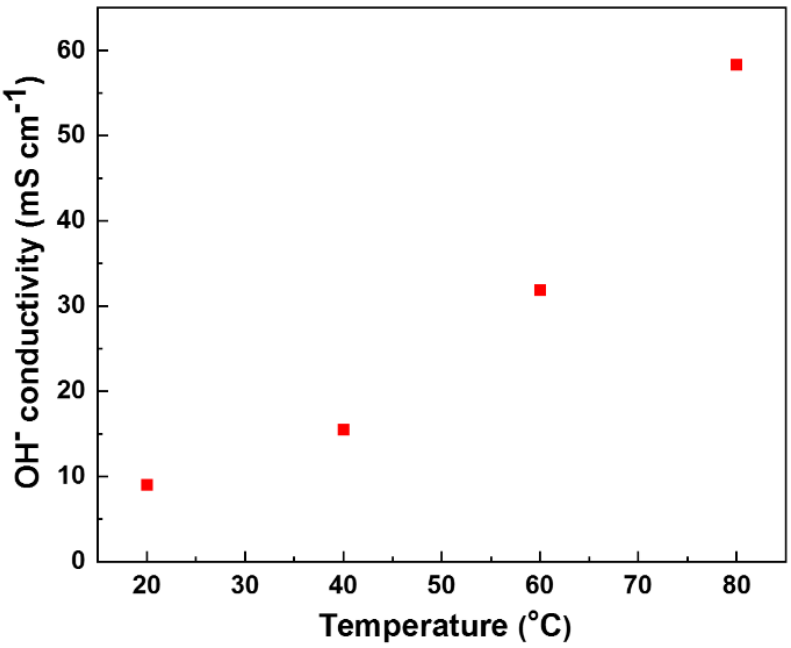


Fig. 3.14. Hydroxide conductivity of the PF-Pip membrane.

The hydroxide conductivity of the PF-Pip membrane follows the Arrhenius behavior from 20 to 80 $^{o}$C as shown in Fig. 3.15. The activation energy of polymer PF-Pip was 27 kJ mol$^{-1}$ which was comparable with some reported AEMs of comparable IEC value [54, 55].

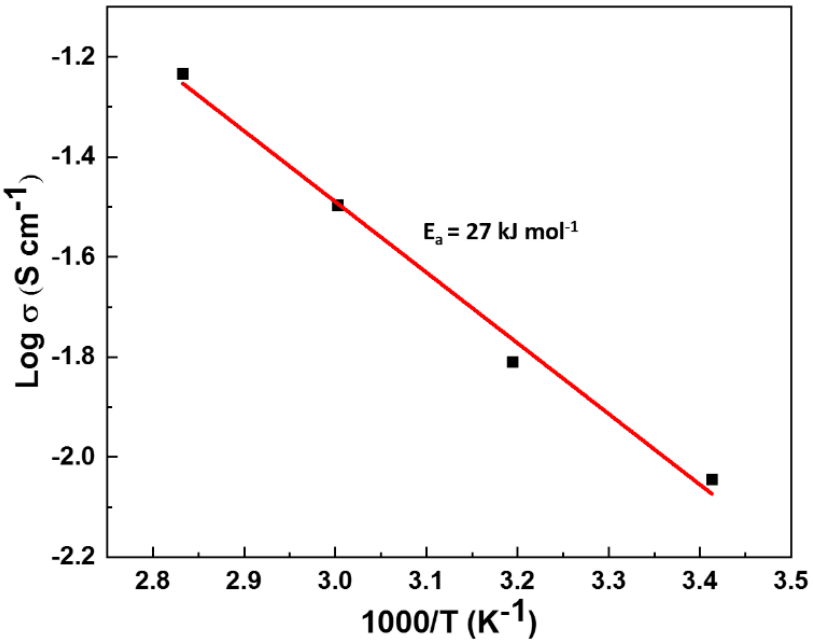


Fig. 3.15. Arrhenius plots of the PF-Pip membrane.

The IEC, WU, SR, hydroxide conductivity, and alkaline stability of the PF-Pip polymer, are summarized with some reported piperidinium functionalized AEMs such as terphenyl based polymer (TP) [18], ether-bond-free polyfluorene (PF) [56], polyphenylene oxides (PPO) [39, 52, 53] of comparable IEC values, shown in Table 3.1. The balanced WU is essential as dimensional instability may be caused by excessive WU. The PF-Pip polymer showed low WU compared to the PPO based AEMs due to the rigid backbone and absence of ether bonds. The WU and hydroxide conductivity is comparable with terphenyl based polymer [18] but lower in comparison to the PPO based polymer due to their high WU.

Table 3.1. Comparison of IEC, WU, SR, hydroxide conductivity, and alkaline stability of PF-Pip with some representative AEMs in liquid water at 80 oC.

| Membrane [Ref. no.] | Backbone type | [a]$IEC_{exp}$ (mmol $g^{-1}$) | [b]WU (%) | [b]SR (%) | [b]$\sigma_{OH^-}$ (mS $cm^{-1}$) | Alkaline Stability (1 M NaOH, 80 °C) |
|---|---|---|---|---|---|---|
| PF-Pip (This work) | PF | 1.82 | 81 | 20.0 | 58 | 168 h [c](13% degradation) |
| PTPipQ8 [18] | TP | 1.98 | 80 | | 61 | 168 h [c](>50% degradation) (2 M NaOH, 90 °C) |
| PBF0.5-OH [56] | | 1.56 | 45 | | 61 | |
| PBF1-OH [56] | PF | 1.94 | 120 | | 69 | 1200 h [c](no degradation) |
| PBF2-OH [56] | | 2.20 | 160 | | 86 | |
| PI-PPO [53] | PPO | 1.95 | 106 | 30.6 | 77 | 500 h (remaining conductivity 80%, IEC 79%) (1 M KOH, 60 °C) |
| PPO5-Pip [39] | PPO | 1.78 | 88 | | 117 | 384 h [c](no degradation) (1 M NaOH, 90 °C) |
| PPO-7bisQPi-1.9 [52] | PPO | 1.90 | 120 | | 186 | 192 h [c](no degradation) (1 M NaOH, 90 °C) |

[a]Experimental value obtained by titration; [b]measured in liquid water at 80 °C;

[c]from $^1$H NMR.

## 3.3.7. Alkaline Stability

The thermochemical stability of AEMs is the most important challenge for practical application, particularly in the high-pH medium of AEMFCs. Fig. 3.16 shows the $^{1}H$ NMR spectra of PF-Pip before and after the alkaline test. After 48 h, 96 h, and 168 h storage in 1 M NaOH solution the peak intensity of the methyl protons for ($-N^{+}CH_3$) at 2.9 ppm and methylene protons linked to N atom at 3.2 ppm was slightly reduced. The peak intensity at 2.9 ppm was reduced due to the substitution of the methyl group and the reduction of peak intensity at 3.2 ppm pointed to the Hofmann β hydrogen elimination reaction of the N-methyl piperidinium cationic group. According to the literature [18, 38], the degradation mechanisms of the piperidinium group can be suggested as in Scheme 3.3. Bae *et al.* reported that the primary route for degradation of piperidinium cation was nucleophilic substitution of methyl groups and degradation by ring opening reaction was not observed [32]. Marino and Kreuer [38] confirmed from the results of $^{1}H$ NMR spectroscopy that the extreme degradation of N,N-methylpiperidinium group was taken by the substitution at the methyl groups in 6 M NaOH solution at 160 °C. In addition, a slight decay comes from the slower ring opening elimination. I observed two new peaks appeared at 5.7 and 5.6 ppm but could not confirm that the peaks appeared from the degradation of cationic groups by a

ring-opening elimination reaction Scheme 3.3 (path B). Jannasch *et al.* also observed new peaks in the region from 5 to 6.5 ppm for vinylic protons due to the degradation of quaternary piperidinium groups [18, 39]. However, in comparison to the peak position, I could not attribute the observed peaks for the vinylic protons. According to the literature [32, 38] I concluded that the degradation of N-methyl piperidinium was methyl substitution by the attack of $OH^-$ ion. The $^1H$ NMR spectra of the PF-Pip membrane revealed that 6% of the initial cationic group was lost after 48 h and 13% degradation occurred after 96 h of storage in 1 M NaOH solution by following the degradation mechanism of Scheme 3.3 (path A). Further, no loss of cationic group was observed after stored for 168 h. I have checked the weight after soaking the membranes for 48 h, 96 h, and 168 h in alkaline condition. After the alkaline tests, the weight was decreased that indicates the degradation of PF-Pip was not occurred by Scheme 3.3 (path C). Some literature reported that the alkyl substituted piperidinium cationic groups were not degradable in alkaline condition [39, 52, 56, 57]. However, I have observed the degradation of N-methyl piperidinium group though it was alkyl tethered. Therefore, from the results of the study, I can conclude that the alkyl substituted N-methyl piperidinium cationic group is also degradable in 1 M NaOH solution at 80 °C on the polyfluorene backbone although degradation is not so significant.

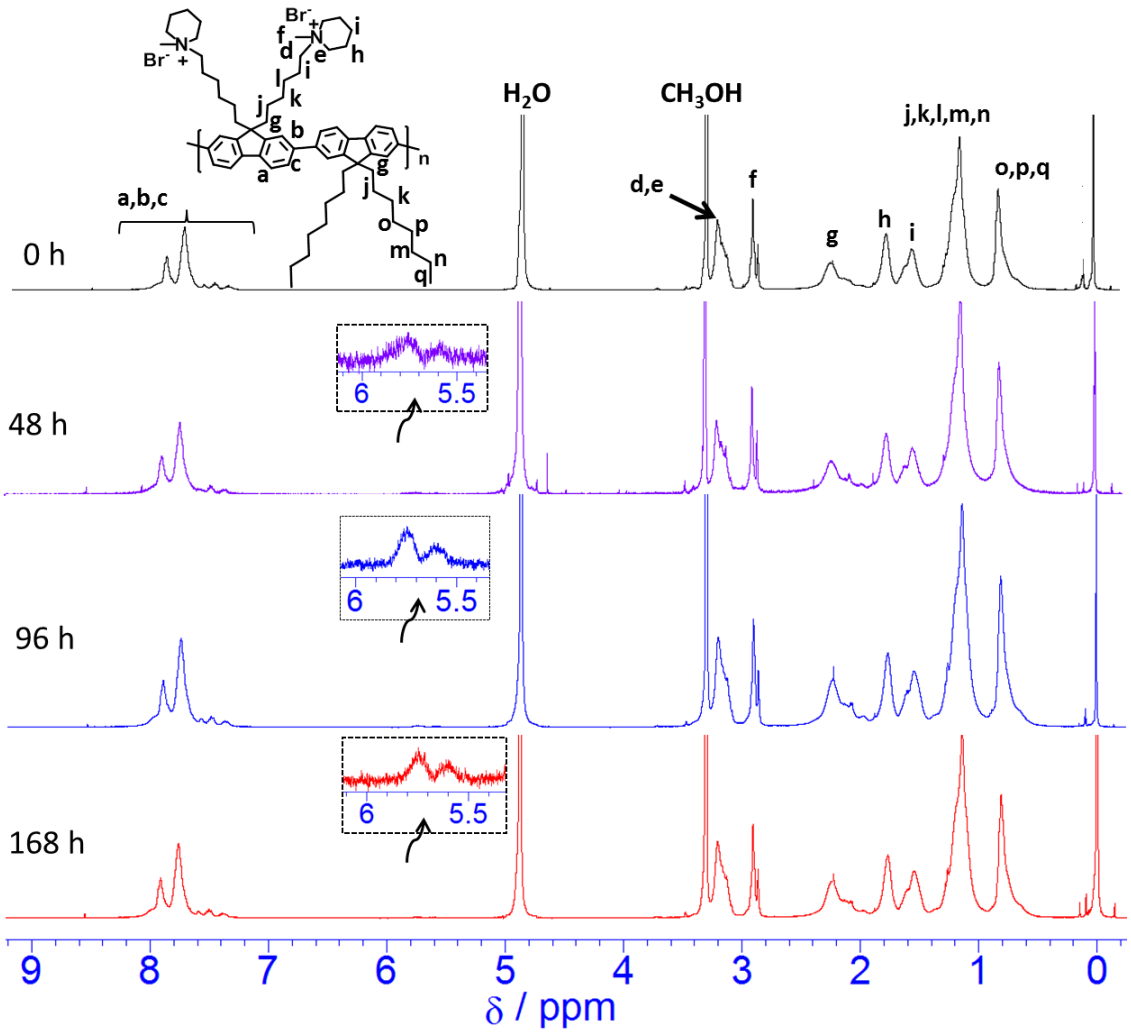


Fig. 3.16. $^{1}$H NMR spectra of PF-Pip in the $OH^-$ form membrane after soaking in 1 M NaOH solution for 80 °C for 48 h, 96 h, and 168 h.

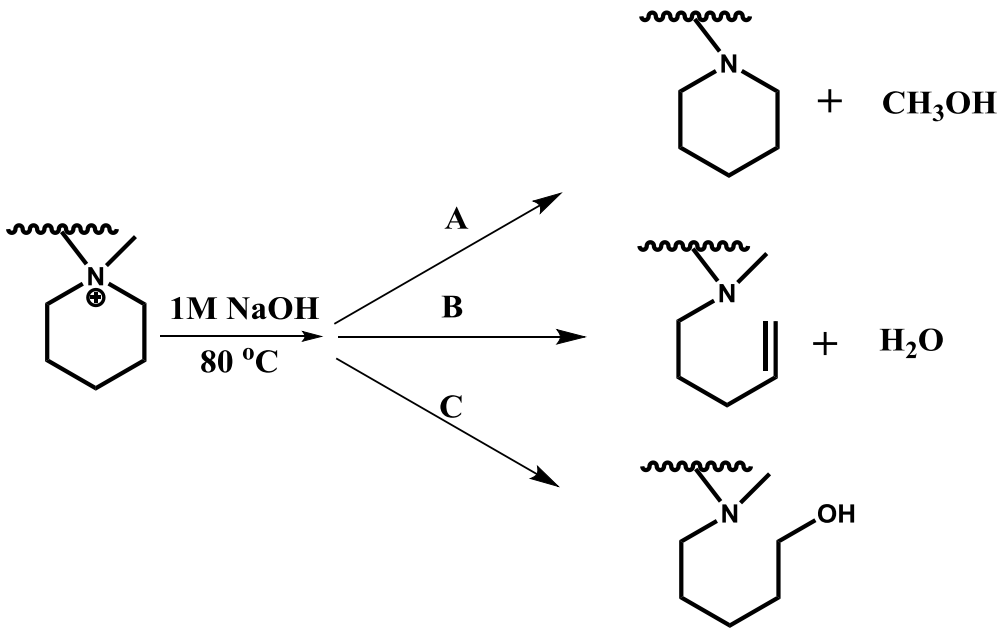


Scheme 3.3. Degradation pathways of N-methylpiperidinium cationic group (A) nucleophilic substitution of the methyl group, (B) Hofmann β elimination, and (C) substitution (ring opening) [38].

## 3.4. Conclusion

In summary, I have synthesized ether-bond-free fluorene based polymer by using Pd catalyzed Suzuki cross-coupling reaction with highly alkaline stable piperidinium cations at the alkyl side chains. The properties of AEM were examined including $OH^-$ conductivity, water uptake and swelling behavior, ion exchange capacity, mechanical properties, thermal and chemical stability. The AEM in $OH^-$ form exhibited excellent thermal and dimensional stability. The hydroxide conductivity reached 58 mS $cm^{-1}$ at 80 °C. The piperidinium cationic group of 13% was lost after storage for 168 h in 1 M NaOH solution at 80 °C. This study suggests that alkyl substituted N-methyl piperidinium cationic group showed sufficient hydroxide conductivity and good alkaline stability.

## References

[1] H. Zhang, P.K. Shen, Recent development of polymer electrolyte membranes for fuel cells, Chemical Reviews 112 (2012) 2780-2832.

[2] G. He, Z. Li, J. Zhao, S. Wang, H. Wu, M.D. Guiver, Z. Jiang, Nanostructured ion‐exchange membranes for fuel cells: recent advances and perspectives, Advanced Materials 27 (2015) 5280-5295.

[3] M.A. Hickner, Strategies for developing new anion exchange membranes and electrode ionomers, The Electrochemical Society Interface 26 (2017) 69-73.

[4] K.-D. Kreuer, Ion conducting membranes for fuel cells and other electrochemical devices, Chemistry of Materials 26 (2013) 361-380.

[5] J. Ran, L. Wu, Y. He, Z. Yang, Y. Wang, C. Jiang, L. Ge, E. Bakangura, T. Xu, Ion exchange membranes: New developments and applications, Journal of Membrane Science 522 (2017) 267-291.

[6] D.W. Shin, M.D. Guiver, Y.M. Lee, Hydrocarbon-based polymer electrolyte membranes: importance of morphology on ion transport and membrane stability, Chemical Reviews 117 (2017) 4759-4805.

[7] J.R. Varcoe, P. Atanassov, D.R. Dekel, A.M. Herring, M.A. Hickner, P.A. Kohl, A.R. Kucernak, W.E. Mustain, K. Nijmeijer, K. Scott, Anion-exchange membranes in

electrochemical energy systems, Energy & Environmental Science 7 (2014) 3135-3191.

[8] A.G. Wright, T. Weissbach, S. Holdcroft, Poly(phenylene) and m‐Terphenyl as Powerful Protecting Groups for the Preparation of Stable Organic Hydroxides, Angewandte Chemie International Edition 55 (2016) 4818-4821.

[9] Y. Liu, J. Zhou, J. Hou, Z. Yang, T. Xu, Hyperbranched Polystyrene Copolymer Makes Superior Anion Exchange Membrane, ACS Applied Polymer Materials 1 (2018) 76-82.

[10] J. Ran, L. Wu, Q. Ge, Y. Chen, T. Xu, High performance anion exchange membranes obtained through graft architecture and rational cross-linking, Journal of Membrane Science 470 (2014) 229-236.

[11] M. Zhang, C. Shan, L. Liu, J. Liao, Q. Chen, M. Zhu, Y. Wang, L. An, N. Li, Facilitating anion transport in polyolefin-based anion exchange membranes via bulky side chains, ACS Applied Materials & Interfaces 8 (2016) 23321-23330.

[12] L. Zhu, X. Yu, M.A. Hickner, Exploring backbone-cation alkyl spacers for multi-cation side chain anion exchange membranes, Journal of Power Sources 375 (2018) 433-441.

[13] C.G. Arges, V. Ramani, Two-dimensional NMR spectroscopy reveals cation-triggered backbone degradation in polysulfone-based anion exchange membranes,

Proceedings of the National Academy of Sciences 110 (2013) 2490-2495.

[14] A.D. Mohanty, S.E. Tignor, J.A. Krause, Y.-K. Choe, C. Bae, Systematic alkaline stability study of polymer backbones for anion exchange membrane applications, Macromolecules 49 (2016) 3361-3372.

[15] L. Liu, X. Chu, J. Liao, Y. Huang, Y. Li, Z. Ge, M.A. Hickner, N. Li, Tuning the properties of poly(2,6-dimethyl-1,4-phenylene oxide) anion exchange membranes and their performance in $H_2/O_2$ fuel cells, Energy & Environmental Science 11 (2018) 435-446.

[16] W.-H. Lee, Y.S. Kim, C. Bae, Robust hydroxide ion conducting poly(biphenyl alkylene)s for alkaline fuel cell membranes, ACS Macro Letters 4 (2015) 814-818.

[17] W.-H. Lee, E.J. Park, J. Han, D.W. Shin, Y.S. Kim, C. Bae, Poly(terphenylene) anion exchange membranes: the effect of backbone structure on morphology and membrane property, ACS Macro Letters 6 (2017) 566-570.

[18] J.S. Olsson, T.H. Pham, P. Jannasch, Poly(arylene piperidinium) hydroxide ion exchange membranes: synthesis, alkaline stability, and conductivity, Advanced Functional Materials 28 (2018) 1702758.

[19] M.R. Hibbs, Alkaline stability of poly(phenylene)‐based anion exchange membranes with various cations, Journal of Polymer Science Part B: Polymer Physics

51 (2013) 1736-1742.

[20] C. Fujimoto, D.-S. Kim, M. Hibbs, D. Wrobleski, Y.S. Kim, Backbone stability of quaternized polyaromatics for alkaline membrane fuel cells, Journal of Membrane Science 423 (2012) 438-449.

[21] C.H. Fujimoto, M.A. Hickner, C.J. Cornelius, D.A. Loy, Ionomeric poly(phenylene) prepared by Diels− Alder polymerization: synthesis and physical properties of a novel polyelectrolyte, Macromolecules 38 (2005) 5010-5016.

[22] M.R. Hibbs, C.H. Fujimoto, C.J. Cornelius, Synthesis and characterization of poly (phenylene)-based anion exchange membranes for alkaline fuel cells, Macromolecules 42 (2009) 8316-8321.

[23] W.-H. Lee, A.D. Mohanty, C. Bae, Fluorene-based hydroxide ion conducting polymers for chemically stable anion exchange membrane fuel cells, ACS Macro Letters 4 (2015) 453-457.

[24] K. Miyatake, B. Bae, M. Watanabe, Fluorene-containing cardo polymers as ion conductive membranes for fuel cells, Polymer Chemistry 2 (2011) 1919-1929.

[25] Y.Z. Zhuo, A.N. Lai, Q.G. Zhang, A.M. Zhu, M.L. Ye, Q.L. Liu, Highly ionic-conductive crosslinked cardo poly(arylene ether sulfone)s as anion exchange membranes for alkaline fuel cells, Journal of Membrane Science 491 (2015) 138-148.

[26] D.W. Seo, M.A. Hossain, D.H. Lee, Y.D. Lim, S.H. Lee, H.C. Lee, T.W. Hong, W.G. Kim, Anion conductive poly(arylene ether sulfone)s containing tetra-quaternary ammonium hydroxide on fluorenyl group for alkaline fuel cell application, Electrochimica Acta 86 (2012) 360-365.

[27] P.Y. Xu, K. Zhou, G.L. Han, Q.G. Zhang, A.M. Zhu, Q.L. Liu, Fluorene-containing poly(arylene ether sulfone)s as anion exchange membranes for alkaline fuel cells, Journal of Membrane Science 457 (2014) 29-38.

[28] D.R. Dekel, S. Willdorf, U. Ash, M. Amar, S. Pusara, S. Dhara, S. Srebnik, C.E. Diesendruck, The critical relation between chemical stability of cations and water in anion exchange membrane fuel cells environment, Journal of Power Sources 375 (2018) 351-360.

[29] K.M. Hugar, H.A. Kostalik IV, G.W. Coates, Imidazolium cations with exceptional alkaline stability: a systematic study of structure–stability relationships, Journal of the American Chemical Society 137 (2015) 8730-8737.

[30] K.-D. Kreuer, P. Jannasch, A practical method for measuring the ion exchange capacity decrease of hydroxide exchange membranes during intrinsic degradation, Journal of Power Sources 375 (2018) 361-366.

[31] A.D. Mohanty, C. Bae, Mechanistic analysis of ammonium cation stability for

alkaline exchange membrane fuel cells, Journal of Materials Chemistry A 2 (2014) 17314-17320.

[32] A.D. Mohanty, S.E. Tignor, M.R. Sturgeon, H. Long, B.S. Pivovar, C. Bae, Thermochemical stability study of alkyl-tethered quaternary ammonium cations for anion exchange membrane fuel cells, Journal of The Electrochemical Society 164 (2017) 1279-1285.

[33] Z. Sun, B. Lin, F. Yan, Anion‐Exchange Membranes for Alkaline Fuel‐Cell Applications: The Effects of Cations, ChemSusChem 11 (2018) 58-70.

[34] S. Gu, J. Wang, R.B. Kaspar, Q. Fang, B. Zhang, E.B. Coughlin, Y. Yan, Permethyl Cobaltocenium (Cp* 2 Co+) as an Ultra-Stable Cation for Polymer Hydroxide-Exchange Membranes, Scientific Reports 5 (2015) No. 11668.

[35] B. Zhang, R.B. Kaspar, S. Gu, J. Wang, Z. Zhuang, Y. Yan, A New Alkali‐Stable Phosphonium Cation Based on Fundamental Understanding of Degradation Mechanisms, ChemSusChem 9 (2016) 2374-2379.

[36] N. Chen, H. Zhu, Y. Chu, R. Li, Y. Liu, F. Wang, Cobaltocenium-containing polybenzimidazole polymers for alkaline anion exchange membrane applications, Polymer Chemistry 8 (2017) 1381-1392.

[37] Y. Zha, M.L. Disabb-Miller, Z.D. Johnson, M.A. Hickner, G.N. Tew,

Metal-cation-based anion exchange membranes, Journal of the American Chemical Society 134 (2012) 4493-4496.

[38] M. Marino, K. Kreuer, Alkaline stability of quaternary ammonium cations for alkaline fuel cell membranes and ionic liquids, ChemSusChem 8 (2015) 513-523.

[39] H.-S. Dang, P. Jannasch, A comparative study of anion-exchange membranes tethered with different hetero-cycloaliphatic quaternary ammonium hydroxides, Journal of Materials Chemistry A 5 (2017) 21965-21978.

[40] L. Gu, H. Dong, Z. Sun, Y. Li, F. Yan, Spirocyclic quaternary ammonium cations for alkaline anion exchange membrane applications: An experimental and theoretical study, RSC Advances 6 (2016) 94387-94398.

[41] J.S. Olsson, T.H. Pham, P. Jannasch, Poly(N,N-diallylazacycloalkane)s for anion-exchange membranes functionalized with n-spirocyclic quaternary ammonium cations, Macromolecules 50 (2017) 2784-2793.

[42] T.H. Pham, P. Jannasch, Aromatic polymers incorporating bis-N-spirocyclic quaternary ammonium moieties for anion-exchange membranes, ACS Macro Letters 4 (2015) 1370-1375.

[43] T.H. Pham, J.S. Olsson, P. Jannasch, N-spirocyclic quaternary ammonium ionenes for anion-exchange membranes, Journal of the American Chemical Society 139 (2017)

2888-2891.

[44] D.J. Strasser, B.J. Graziano, D.M. Knauss, Base stable poly(diallylpiperidinium hydroxide) multiblock copolymers for anion exchange membranes, Journal of Materials Chemistry A 5 (2017) 9627-9640.

[45] N. Chen, C. Long, Y. Li, C. Lu, H. Zhu, Ultrastable and high ion-conducting polyelectrolyte based on six-membered N-spirocyclic ammonium for hydroxide exchange membrane fuel cell applications, ACS Applied Materials & Interfaces 10 (2018) 15720-15732.

[46] B. Lin, L. Qiu, B. Qiu, Y. Peng, F. Yan, A soluble and conductive polyfluorene ionomer with pendant imidazolium groups for alkaline fuel cell applications, Macromolecules 44 (2011) 9642-9649.

[47] B. Liu, G.C. Bazan, Synthesis of cationic conjugated polymers for use in label-free DNA microarrays, Nature Protocols 1 (2006) 1698.

[48] R. Akiyama, N. Yokota, K. Miyatake, Chemically Stable, Highly Anion Conductive Polymers Composed of Quinquephenylene and Pendant Ammonium Groups, Macromolecules 52 (2019) 2131-2138.

[49] H. Ono, T. Kimura, A. Takano, K. Asazawa, J. Miyake, J. Inukai, K. Miyatake, Robust anion conductive polymers containing perfluoroalkylene and pendant

ammonium groups for high performance fuel cells, Journal of Materials Chemistry A 5 (2017) 24804-24812.

[50] J. Pan, S. Lu, Y. Li, A. Huang, L. Zhuang, J. Lu, High‐Performance alkaline polymer electrolyte for fuel cell applications, Advanced Functional Materials 20 (2010) 312-319.

[51] M. Marino, J. Melchior, A. Wohlfarth, K. Kreuer, Hydroxide, halide and water transport in a model anion exchange membrane, Journal of Membrane Science 464 (2014) 61-71.

[52] H.-S. Dang, P. Jannasch, Alkali-stable and highly anion conducting poly(phenylene oxide)s carrying quaternary piperidinium cations, Journal of Materials Chemistry A 4 (2016) 11924-11938.

[53] H. Lim, B. Lee, D. Yun, A.Z. Al Munsur, J.E. Chae, S.Y. Lee, H.-J. Kim, S.Y. Nam, C.H. Park, T.-H. Kim, Poly(2,6-dimethyl-1,4-phenylene oxide)s with various head groups: effect of head groups on the properties of anion exchange membranes, ACS Applied Materials & Interfaces 10 (2018) 41279-41292.

[54] D. Guo, Y.Z. Zhuo, A.N. Lai, Q.G. Zhang, A.M. Zhu, Q.L. Liu, Interpenetrating anion exchange membranes using poly(1-vinylimidazole) as bifunctional crosslinker for fuel cells, Journal of Membrane Science 518 (2016) 295-304.

[55] X. Li, Q. Liu, Y. Yu, Y. Meng, Quaternized poly(arylene ether) ionomers containing triphenyl methane groups for alkaline anion exchange membranes, Journal of Materials Chemistry A 1 (2013) 4324-4335.

[56] R. Ren, S. Zhang, H.A. Miller, F. Vizza, J.R. Varcoe, Q. He, Facile Preparation of an Ether-free Anion Exchange Membrane with Pendant Cyclic Quaternary Ammonium Groups, ACS Applied Energy Materials 2 (2019) 4576-4581.

[57] H.-S. Dang, P. Jannasch, High-performing hydroxide exchange membranes with flexible tetra-piperidinium side chains linked by alkyl spacers, ACS Applied Energy Materials 1 (2018) 2222-2231.

# General Conclusions and Future Prospects

To meet the demand for power storage/conversion devices, it is very urgent to explore durable anion exchange membranes (AEMs) in combination with adequate hydroxide conductivity and alkaline stability for long time use in anion exchange membrane fuel cells (AEMFCs). AEMFCs efficiently generate electricity from the stored energy of fuels such as MeOH and $H_2$ without depending on the precious electrocatalyst, for example, Pt. In addition, exhibits faster kinetics of oxygen reduction reactions in comparison to other sorts of fuel cells. However, the demand for the practical application of AEMs in AEMFCs can hardly meet by the conventional AEMs, in particular, the alkaline stability. Some researchers reported that imidazolium cationic groups are alkaline stable, but some other researchers suggested the less alkaline stability of imidazolium groups. To conclude this discrepancy, I have used 1-isopropyl-2-imidazolium as cationic groups and newly incorporated on a chemically stable ether free polyfluorene backbone. I also have synthesized N-methylpiperidinium cationic group containing polyfluorene AEM.

This present research was conducted to synthesize the new polyfluorene based AEM containing 1-isopropyl-2-methylimidazolium as a cationic group. To confirm the synthesis of monomers and polymers and to measure the membrane properties of the

synthesized polymeric membrane several characteristic techniques have been used. These results revealed that the synthesis of the polymer and incorporation of imidazolium groups were successful (Chapter 2) and the synthesized membrane exhibited adequate hydroxide conductivity, low water uptake, high dimensional stability, and good thermal and physical stability. For example, the ionic conductivity reached up to 46 mS $cm^{-1}$ at 80 °C and the swelling ratio increased only 1 to 7% when the temperature increased from 20 to 80 °C. However, I have observed the degradation of imidazolium groups when I stored the membranes in 1 M NaOH solution at both 80 °C and room temperature though the main chain was chemically stable. I concluded that imidazolium cationic groups are not chemically stable. Since the imidazolium cationic group degraded by the ring-opening reaction of the C2 position because of the attack of nucleophilic hydroxide ion. So the discrepancy state for alkaline stability of imidazolium cationic groups can be concluded from this study.

In contrast, incorporation of piperidinium cationic groups instead of imidazolium groups on the same polyfluorene backbone demonstrated that some fuel cell membrane properties were improved (Chapter 3). For example, the water uptake and ionic conductivity of the synthesized membrane were increased. The hydroxide conductivity of the as-synthesized membrane increased up to 58 mS $cm^{-1}$ at 80 °C. This may be due

to the higher water uptake by the membrane. The alkaline stability results revealed that only 13% piperidinium cationic group was lost after storage for 168 h in 1 M NaOH solution at 80 °C. The degradation happens by the nucleophilic substitution of the methyl group of piperidinium but I did not observe any degradation of the main chain. Some researchers reported that alkyl substituted N-methyl piperidinium group was not degraded in 1 M NaOH solution at 80 °C. However, I have observed the degradation of the N-methyl piperidinium cationic group although it was alkyl substituted. This study suggests that the alkyl substituted piperidinium cationic group also degraded in alkaline condition though the degradation was not so significant.

From the observations, the challenge of chemical stability of imidazolium groups on the polyfluorene backbone are outlined for fuel cell applications. Sufficient hydroxide conductivity and good chemical stability was observed in case of piperidinium containing membrane.

My results of this research may provide an opportunity to synthesize alkaline stable ether-bond-free polyfluorene backbone containing different alkyl tethered cationic groups and the systematic study of membrane properties for fuel cell application. In compared to other synthetic polymerizations, the synthetic strategy of this research was

simple. The major advantage is that the carcinogenic chloromethyl methyl ether could be avoided which is very harmful to human health.

The piperidinium cationic group showed high hydroxide conductivity and good chemical stability. Consequently, it is expected that this study will be encouraged for further investigation to synthesize different types of AEMs containing piperidinium as a cationic group.

Finally, I expect that the investigations of this research will provide significant directions and insights for choosing a cationic group to develop alkaline stable AEMs for the practical application in AEMFCs. I anticipate that the present findings will make a major contribution to a broad audience of fuel cells.

# Acknowledgments

I would like to express my earnest gratitude to my Ph.D. supervisor, Associate Professor Dr. Yuki Nagao for his valuable suggestions, appropriate supervision, kind encouragement, and great support to lead me ahead with my research throughout my doctoral study.

I also deeply acknowledge Prof. Noriyoshi Matsumi for his kind guidance in this study; I learned many helpful things from him for my research. I am also very grateful to him for supporting the glovebox. I express my deepest gratitude to provide me the opportunity to proceed with my minor research project under his supervision. His suggestive encouragement and discussion helped me to widen my knowledge in another research field. I also express my special thanks to Dr. Sai Gourang Patnaik ex-student of Matsumi lab for cordial support in this minor research. I am also grateful to Dr. Rajashekar Badam, Assistant professor of Matsumi lab for his support during the use of glovebox.

I express my thanks to Prof. Tatsuo Kaneko for being my second supervisor and his valuable guidance in this study.

I express my sincere gratitude to Prof. Kazuaki Matsumura for supporting Differential scanning calorimetry (DSC) and mechanical strength measurement. I also like to thank Zhao Yibo student of Matsumura lab for his cordial assistance during mechanical strength measurement.

I would like to sincerely express my appreciation to Associate Prof. Shusaku Nagano at Nagoya University for his kind support for GPC and small-angle X-ray

scattering (SAXS) measurements.

I also deeply express my sincere gratitude to all referees including Prof. Manabu Tanaka of Tokyo Metropolitan University for their valuable suggestions and comments.

I gratefully appreciate the support of Dr. Akio Miyazato (technical staff of mass spectrometry, JAIST) for mass spectra measurements.

I am very grateful to Koichi Higashimine (senior technical specialist, center for nano materials and technology, JAIST) and Shoko Kobayashi (technical staff, center for nano materials and technology, JAIST) for their kind cooperation for transmission electron microscope (TEM) image measurements.

I also gratefully acknowledge Associate Professor Guangtong Wang (Harbin Institute of Technology, China) for his cordial support during the synthesis of the polymer.

I would like to thank the former and present students of Nagao laboratory for their kind support and beneficial discussion with me.

Finally, I profoundly appreciate the support, sacrificing, and encouragement from my family members, all of my friends and colleagues.

Umme Salma

March′2020

# Achievements

## Publications

1. **Umme Salma**, Dishen Zhang and Yuki Nagao "Imidazolium Functionalized Fluorene based Anion Exchange Membrane (AEM) for Fuel Cell Applications." [*ChemistrySelect 2020, 5, 1255-1263*]
2. **Umme Salma** and Yuki Nagao "Alkaline stability of ether bond free fluorene based anion exchange polymer containing cycloaliphatic quaternary ammonium groups." [*Submitted*]

## Conferences

1. Umme Salma and Yuki Nagao "A polyfluorene polymer containing imidazolium cationic groups for anion exchange membrane fuel cells" 68$^{th}$ Polymer Symposium, September 25 -27, 2019, Fukui, Japan.
2. Umme Salma, Dishen Zhang, Yuki Nagao "Hydroxide ion-conducting fluorene based polymers for fuel cell applications" 2019 年度北陸地区講演会と研究発表会, 29 November 2019, Kanazawa, Japan.

## Abstract of Minor Research


# Abstract:

A novel π conjugated fluorene containing copolymer was designed and synthesized by Sonogashira cross-coupling reaction in mild condition. In this research, I co-polymerized fluorene with diethynylbenzene units by a facile one-step reaction to synthesis of the polymer. The structure was confirmed by nuclear magnetic resonance (NMR) spectroscopy and Fourier transform infrared spectroscopy (FTIR). The number average molecular weight (Mn), the weight average molecular weight (Mw) and polydispersity (PDI) were determined by gel permeation chromatography (GPC). The electroactivity of the polymer was measured by cyclic voltammetry. The results of electrochemical performance showed that the polymer will be the proper candidate as a binder for high-performance Li-ion batteries. It also can be used as an organic electrode material.



**Keywords:** Polyfluorene, Copolymer, Conjugation, Binder.